ALMA MATER STUDIORUM · UNIVERSITÀ DI BOLOGNA

Dipartimento di Fisica e Astronomia "Augusto Righi"
Corso di Laurea in Fisica

Diagrammatic Monte Carlo for the Holstein Hamiltonian in the Atomic Limit

Relatore:
Prof. Cesare Franchini

Correlatore:
MSc. Marco Barducci

Presentata da:
Nico Tortorici

Anno Accademico 2024/2025

Abstract

Applichiamo il metodo Diagrammatic Monte Carlo all'Hamiltoniana di Holstein nel limite atomico. Le risultanti proprietà dello stato fondamentale del polarone sono in accordo con la soluzione esatta, confermando la validità della nostra implementazione. Iniziamo questa tesi con uno studio della teoria dei molti corpi, concentrandoci sull'espansione diagrammatica dell'interazione elettrone-fonone. Introduciamo poi il polarone di Holstein nella sua forma in seconda quantizzazione e deriviamo la soluzione esatta per il limite atomico, quando il parametro di hopping è impostato a zero. Gli interessi principali di questo lavoro risiedono nel quadro teorico della teoria dei campi della materia condensata, così come nelle metodologie computazionali sviluppate per il Diagrammatic Monte Carlo nel contesto del problema del polarone. Sviluppi futuri potrebbero includere l'estensione del metodo all'Hamiltoniana di Holstein completa, dove il parametro di hopping è diverso da zero.

Abstract (English)

We apply the Diagrammatic Monte Carlo method to the Holstein Hamiltonian in the atomic limit. The resulting ground-state properties of the polaron are found to be in agreement with the exact solution, confirming the validity of our implementation. We begin this thesis by reviewing many-body theory, with a focus on the diagrammatic expansion of the electron-phonon interaction. We then introduce the Holstein polaron in its second-quantised form and derive the exact solution for the atomic limit, when the hopping parameter is set to zero. Key interests of this work lie in the theoretical framework of condensed matter field theory, as well as in the computational methodologies developed for the Diagrammatic Monte Carlo in the context of the polaron problem. Further developments may include extending the method to the full Holstein Hamiltonian, where the hopping parameter is nonzero.

Acknowledgements

I wish to express my gratitude to all those who have supported me during my degree. First of all, I would like to thank my supervisor, Prof. Cesare Franchini, for his guidance, as well as for giving me the opportunity to work on such an interesting topic. I also thank him for providing me with the *Simple MC* package, developed by Dr. Thomas Hahn. The implementation of the Diagrammatic Monte Carlo was developed on this codebase. I wish to thank MSc. Marco Barducci for his invaluable help during the whole process of this work, from the initial stages of theoretical understanding to the final thesis write-up.

My heartfelt thanks go to my family, especially to my parents, for their continuous support and encouragement throughout my studies. Finally, I wish to thank all my friends and colleagues of the University of Bologna, for making my time here so enjoyable and memorable.

This thesis has been written using the LaTeX template *CleanThesis* by R. Langner, distributed under the LaTeX Project Public License (LPPL). Feynman diagrams have been drawn using the *TikZ-Feynman* package.

Contents

Introduction

The Diagrammatic Monte Carlo (DiagMC) method is a computational technique based on the Markov chain Monte Carlo. It is used to calculate quantities that are expressed in terms of diagrammatic series [1]. In condensed matter physics, the DiagMC method allows one to stochastically sample Feynman diagrams and compute the expectation values of quantities of interest, such as the Green's function. DiagMC was first developed in 1998 by Prokof'ev and Svistunov [2] to study the polaron problem.

The polaron problem itself was first introduced by Landau in 1933 [3]. A polaron is a quasiparticle consisting of an electron with its self-induced polarisation in a ionic crystal. In this thesis, we focus on the Holstein polaron [4], which was developed by its author to describe a one-dimensional molecular crystal. In this model, electron-phonon interactions are taken to be short range, and phonons are assumed to be dispersionless and optical. Here we study the atomic limit, whose second-quantised Holstein Hamiltonian is greatly simplified and has an exact solution. This solution is used to benchmark the implemented DiagMC algorithm to verify its correctness.

In this thesis, a great emphasis is placed in building the theoretical framework that leads to the formulation of Green's functions and Feynman diagrams. After a review of the fundamentals of condensed matter physics in Ch. 1, in Ch. 2 we introduce the Green's functions. In Ch. 3, we make use of Wick's theorem to expand the electron-phonon Green's function in terms of free propagators, and introduce the rules to draw Feynman Diagrams. The Holstein Hamiltonian is then introduced in Ch. 4, and an exact solution is presented for the second-quantised Hamiltonian in the atomic limit. Finally, Ch. 5 is devoted to present the DiagMC method and its implementation in `C++`. The exact solution developed in Ch. 4 serves as a benchmark to verify the correctness of the DiagMC algorithm.

1

Fundamentals of Condensed Matter Physics

The original formalism of Quantum Mechanics was only interested in studying the motion of particles, with the electromagnetic field remaining classical. This approach is called *first quantisation* [5]. Despite its success in describing a diverse set of physical phenomena, first quantisation has built-in limitations when addressing scenarios where the number of particles is not conserved. Later on, the electromagnetic field was quantised, and the particles themselves were represented by quantised fields, leading to a more comprehensive framework known as *second quantisation*. In this approach, each state is represented in the occupation number basis.

Here, we assume the basic principles of Quantum Mechanics as known. However, for the purpose of the present chapter, in Sect. 1.1 we recall the essentials of the first quantisation for many-body problems. In Sect. 1.2, we introduce the second quantisation formalism. In Sect. 1.3, we review the concept of crystal lattice and tight-binding approximation, which is the basis for the Holstein model. Finally, in Sect. 1.4, we introduce the concept of phonons, which are the quantised normal modes of the lattice vibrations.

1.1 Review of First Quantization

We will start our review of first quantisation by considering N-particle systems, i.e. systems containing n identical particles [5]. Two particles are considered *identical* if they share the same quantum numbers. In first quantisation, we denote the N-particle state function as $\psi(\mathbf{r}_1, \mathbf{r}_2, \dots \mathbf{r}_N)$. The fundamental assumption is the *principle of indistinguishability*[1], so that identical particles are considered *indistinguishable in principle*. Suppose now that the positions $\mathbf{r}_i$ and $\mathbf{r}_j$ of two particles are interchanged [5]:

$$\psi(\mathbf{r}_1, \dots, \mathbf{r}_i, \dots, \mathbf{r}_j, \dots, r_N) \longrightarrow \psi(\mathbf{r}_1, \dots, \mathbf{r}_j, \dots, \mathbf{r}_i, \dots, r_N).$$

---

[1] The *principle of indistinguishability* states that identical particles cannot be distinguished from one another by any physical measurement. This implies that exchanging two identical particles does not lead to a new physical state.

From the principle of indistinguishability, this operation must yield the same physical state, which implies that the modified wave function can differ from the original one at most by a prefactor λ:

$$\psi(\mathbf{r}_1, \dots, \mathbf{r}_i, \dots, \mathbf{r}_j, \dots, r_N) = \lambda\psi(\mathbf{r}_1, \dots, \mathbf{r}_j, \dots, \mathbf{r}_k, \dots, r_N).$$

Interchanging again the same two positions:

$$\psi(\mathbf{r}_1, \dots, \mathbf{r}_i, \dots, \mathbf{r}_j, \dots, r_N) = \lambda^2\psi(\mathbf{r}_1, \dots, \mathbf{r}_i, \dots, \mathbf{r}_j, \dots, r_N),$$

we conclude that $\lambda = \pm 1$. We thus identify two possible species of particles, *bosons* and *fermions*:

$$\begin{aligned} \psi(\mathbf{r}_1, \dots, \mathbf{r}_i, \dots, \mathbf{r}_j, \dots, \mathbf{r}_N) &= +\psi(\mathbf{r}_1, \dots, \mathbf{r}_j, \dots, \mathbf{r}_i, \dots, \mathbf{r}_N) \quad \text{(bosons)}, \\ \psi(\mathbf{r}_1, \dots, \mathbf{r}_i, \dots, \mathbf{r}_j, \dots, \mathbf{r}_N) &= -\psi(\mathbf{r}_1, \dots, \mathbf{r}_j, \dots, \mathbf{r}_i, \dots, \mathbf{r}_N) \quad \text{(fermions)}. \end{aligned} \tag{1.1}$$

For fermions, It is immediate to see that if $\mathbf{r}_i = \mathbf{r}_j$ then $\psi = 0$. This is the *Pauli exclusion principle*, stating that two fermions cannot occupy the same state.

Let us now consider the orthonormal single-particle basis $\{\psi_\nu(\mathbf{r})\}$, where ν is a set of quantum numbers. By using the completeness relation, it is easy to show that the N-Particle state function can be written as a linear superposition of the product of the single-particle basis states:

$$\psi(\mathbf{r}_1, \mathbf{r}_2, \dots, \mathbf{r}_N) = \sum_{\nu_1, \dots, \nu_N} A_{\nu_1, \nu_2, \dots, \nu_N} \psi_{\nu_1}(\mathbf{r}_1)\psi_{\nu_2}(\mathbf{r}_2) \dots \psi_{\nu_N}(\mathbf{r}_N).$$

Coefficients $A_{\nu_1, \nu_2, \dots, \nu_N}$ must be chosen according to the type of the particle so that Eq. (1.1) is respected. In particular, it is possible to define the bosonic symmetrisation operator $\hat{S}_+$ and the fermionic antisymmetrisation operator $\hat{S}_-$ acting on the product of single-particle states in the following way:

$$\hat{S}_\pm \prod_{j=1}^{N} \psi_{\nu_j}(\mathbf{r}_j) = A \begin{vmatrix} \psi_{\nu_1}(\mathbf{r}_1) & \psi_{\nu_1}(\mathbf{r}_2) & \dots & \psi_{\nu_1}(\mathbf{r}_N) \\ \psi_{\nu_2}(\mathbf{r}_1) & \psi_{\nu_2}(\mathbf{r}_2) & \dots & \psi_{\nu_2}(\mathbf{r}_N) \\ \vdots & \vdots & \ddots & \vdots \\ \psi_{\nu_N}(\mathbf{r}_1) & \psi_{\nu_N}(\mathbf{r}_2) & \dots & \psi_{\nu_N}(\mathbf{r}_N) \end{vmatrix}_\pm .$$

For the fermionic operator $\hat{S}_{-}$, the *Slater determinant* [6] is used. The Slater determinant is simply the ordinary determinant:

$$\begin{vmatrix} \psi_{\nu_1}(\mathbf{r}_1) & \psi_{\nu_1}(\mathbf{r}_2) & \dots & \psi_{\nu_1}(\mathbf{r}_N) \\ \psi_{\nu_2}(\mathbf{r}_1) & \psi_{\nu_2}(\mathbf{r}_2) & \dots & \psi_{\nu_2}(\mathbf{r}_N) \\ \vdots & \vdots & \ddots & \vdots \\ \psi_{\nu_N}(\mathbf{r}_1) & \psi_{\nu_N}(\mathbf{r}_2) & \dots & \psi_{\nu_N}(\mathbf{r}_N) \end{vmatrix}_{-} = \sum_{p \in S_N} \left(\prod_{j=1}^{N} \psi_{\nu_j}(\mathbf{r}_{p(j)}) \right) \operatorname{sign}(\mathbf{p}).$$

Exchanging two columns of the Slater determinant changes its sign, thereby fulfilling the fermionic antisymmetrisation requirement in Eq. (1.1). As for the bosons, we use the permanent (the sign-less analogue of the determinant),

$$\begin{vmatrix} \psi_{\nu_1}(\mathbf{r}_1) & \psi_{\nu_1}(\mathbf{r}_2) & \dots & \psi_{\nu_1}(\mathbf{r}_N) \\ \psi_{\nu_2}(\mathbf{r}_1) & \psi_{\nu_2}(\mathbf{r}_2) & \dots & \psi_{\nu_2}(\mathbf{r}_N) \\ \vdots & \vdots & \ddots & \vdots \\ \psi_{\nu_N}(\mathbf{r}_1) & \psi_{\nu_N}(\mathbf{r}_2) & \dots & \psi_{\nu_N}(\mathbf{r}_N) \end{vmatrix}_{+} = \sum_{p \in S_N} \left(\prod_{j=1}^{N} \psi_{\nu_j}(\mathbf{r}_{p(j)}) \right).$$

Here, S_N denotes the symmetric group of all $N!$ permutations p, with $\operatorname{sign}(p)$ representing the sign of the permutation. The normalisation factor A is found to be $\frac{1}{\prod_{\nu'} \sqrt{n_{\nu'}!}} \frac{1}{\sqrt{N!}}$, where $n_{\nu'}$ is the occupation number of state ν'.

In summary, any wave function in the Hilbert space may be expressed as

$$\psi(\mathbf{r}_1, \mathbf{r}_2, \dots, \mathbf{r}_N) = \sum_{\nu_1, \dots, \nu_N} C_{\nu_1, \nu_2, \dots, \nu_N} \hat{S}_{\pm} \psi_{\nu_1}(\mathbf{r}_1) \psi_{\nu_2}(\mathbf{r}_2) \dots \psi_{\nu_N}(\mathbf{r}_N).$$

1.2 Second Quantisation

In the *second quantisation* representation, each state is represented by the occupation numbers of the single-particle states [5]. Let us denote n_{ν_j} as the occupation number of the state ν_j (i.e. the number of particles in the state ν_j), then the basis states for the N-particle system are simply defined as

$$|n_{\nu_1}, n_{\nu_2}, n_{\nu_3}, \dots\rangle, \quad \text{with} \quad \sum_j n_{\nu_j} = N.$$

The writing $|n_{\nu_1}, n_{\nu_2}, \dots\rangle$ is a shorthand notation for the state with n_{ν_1} particles in the state ν_1, n_{ν_2} particles in the state ν_2, and so on. The *Fock space* is formed by those states that are a linear superposition of the basis defined above. The occupation numbers n_{ν_j} are of course non-negative integers, i.e. $n_{\nu_j} \in \mathbb{N}_0$. It is natural to introduce the *occupation number operator* $\hat{n}_{\nu_j}$, which is defined as the operator that acts on the previous basis states and counts the number of particles in the state ν_j:

$$\hat{n}_{\nu_j} |n_{\nu_1}, \ldots, n_{\nu_j}, \ldots\rangle = n_{\nu_j} |n_{\nu_1}, \ldots, n_{\nu_j}, \ldots\rangle \,. \tag{1.2}$$

Notation. Let us make an important remark about the operator notation. In this thesis we will follow Mahan's approach [7]. An operator will be generally denoted in its Schrödinger representation by O, while its interaction representation will be denoted by $\hat{O}(t)$. Representations are discussed in detail in Sect. 2.1. When ambiguity between an operator and its eigenstate arises, we will use the hat like in Eq. (1.2).

1.2.1 Boson Creation and Annihilation Operators

Let us now suppose that the particles with quantum numbers ν_j are bosons. The next step is to introduce the *boson creation operator* $b^\dagger_{\nu_j}$, which is defined as the operator that increments the occupation number of the state $|\nu_j\rangle$:

$$b^\dagger_{\nu_j} \mid \ldots, n_{\nu_{j-1}}, n_{\nu_j}, n_{\nu_{j+1}}, \ldots\rangle \equiv B_+(n_{\nu_j}) \mid \ldots, n_{\nu_{j-1}}, n_{\nu_j}+1, n_{\nu_{j+1}}, \ldots\rangle, \tag{1.3}$$

with $B_+(n_{\nu_j})$ to be determined. Now, it is clear that the only nonzero matrix elements of $b^\dagger_{\nu_j}$ are $\langle n_{\nu_j}+1|b^\dagger_{\nu_j}|n_{\nu_j}\rangle$. It follows immediately that the complex conjugation

$$\left(\langle n_{\nu_j}+1|b^\dagger_{\nu_j}|n_{\nu_j}\rangle\right)^* = \langle n_{\nu_j}|b_{\nu_j}|n_{\nu_j}+1\rangle \tag{1.4}$$

is also nonzero. Therefore, the operator $b_{\nu_j} \equiv \left(b^\dagger_{\nu_j}\right)^\dagger$ acts to decrease the occupation number n_{ν_j}. We thus define the *boson annihilation operator* b_{ν_j} in direct analogy with Eq. (1.3):

$$b_{\nu_j} \mid \ldots, n_{\nu_{j-1}}, n_{\nu_j}, n_{\nu_{j+1}}, \ldots.\rangle = B_-(n_{\nu_j}) \mid \ldots, n_{\nu_{j-1}}, n_{\nu_j}-1, n_{\nu_{j+1}}, \ldots\rangle.$$

Let us consider the vacuum state $|n_{\nu_j}=0\rangle$. By definition, the annihilation operator must satisfy $b_{\nu_j}|n_{\nu_j}=0\rangle = 0$, which implies $B_-(0)=0$. To fix the normalization, we require $b^\dagger_{\nu_j}|n_{\nu_j}=0\rangle = |n_{\nu_j}=1\rangle$, so we set $B_+(0)=1$. Applying Eq. (1.4), we then find $B_-(1)=1$.

Recall that bosonic states are symmetric under particle exchange. This means that the order in which creation operators are applied does not matter:

$$b^\dagger_{\nu_i} b^\dagger_{\nu_j} |\phi\rangle = b^\dagger_{\nu_j} b^\dagger_{\nu_i} |\phi\rangle \,,$$

which leads to the commutation relations[2]

$$\left[b^\dagger_{\nu_i}, b^\dagger_{\nu_j}\right] = 0, \qquad \left[b_{\nu_i}, b_{\nu_j}\right] = 0.$$

It is clear that $b^\dagger_{\nu_j}$ and b_{ν_k} commute if $j \neq k$. However, if $j = k$ we see that

$$b_{\nu_j} b^\dagger_{\nu_j} \left|0\right\rangle - b^\dagger_{\nu_j} b_{\nu_j} \left|0\right\rangle = \left|0\right\rangle - 0 = \left|0\right\rangle,$$

hence, we require $\left[b_{\nu_j}, b^\dagger_{\nu_j}\right] = 1$. In conclusion, we have found the three commutation relations for the bosonic operator:

$$\left[b_{\nu_j}, b^\dagger_{\nu_k}\right] = \delta_{\nu_j,\nu_k}, \qquad \left[b^\dagger_{\nu_j}, b^\dagger_{\nu_k}\right] = 0, \qquad \left[b_{\nu_j}, b_{\nu_k}\right] = 0, \tag{1.5}$$

Now consider the following commutation relations:

$$[b^\dagger_\nu b_\nu, b_\nu] = -b_\nu \qquad [b^\dagger_\nu b_\nu, b^\dagger_\nu] = b^\dagger_\nu, \tag{1.6}$$

Now, let us analyse the Hermitian operator $b_\nu b^\dagger_\nu$. For any nonzero state $\left|\phi\right\rangle$, we have $\langle\phi|b^\dagger_\nu b_\nu|\phi\rangle \geq 0$, so for any real eigenvalue λ such that $b^\dagger_\nu b_\nu \left|\phi_\lambda\right\rangle = \lambda \left|\phi_\lambda\right\rangle$, it follows that $\lambda \geq 0$. Using Eq. (1.6), we find that

$$(b^\dagger_\nu b_\nu) b_\nu |\phi_{\lambda_0}\rangle = (b_\nu b^\dagger_\nu - 1) b_\nu |\phi_{\lambda_0}\rangle = b_\nu (b^\dagger_\nu b_\nu - 1)|\phi_{\lambda_0}\rangle = b_\nu(\lambda_0 - 1)|\phi_{\lambda_0}\rangle, \tag{1.7}$$

which means that the operator b_ν has decreased the eigenvalue λ_0 by 1. This process can be repeated until a negative eigenvalue is encountered, when the above condition for λ is violated. When $\lambda = 0$, we are applying the operator b_ν on the empty state $\left|\nu = 0\right\rangle$. By denoting $\left|\phi_\lambda\right\rangle = \left|n_\nu\right\rangle$, with $\lambda = n = 0, 1, \ldots$, we immediately conclude that $b^\dagger_\nu b_\nu$ is the number operator in Eq. (1.2):

$$b^\dagger_\nu b_\nu \left|n_\nu\right\rangle = n_\nu \left|n_\nu\right\rangle.$$

and that $b_\nu \left|n_\nu\right\rangle \propto \left|n_\nu - 1\right\rangle$. The value $B_-(n_\nu)$ is immediately found to be

$$\langle n_\nu|b^\dagger_\nu b_\nu|n_\nu\rangle = n_\nu, \qquad \langle n_\nu|b^\dagger_\nu b_\nu|n_\nu\rangle = |B_-(n_\nu)|^2 \implies B_-(n_\nu) = \sqrt{n_\nu}.$$

We can write Eq. (1.7) for the creation operator:

$$(b^\dagger_\nu b_\nu) b^\dagger_\nu |n_\nu\rangle = (n+1) b^\dagger_\nu |n_\nu\rangle,$$

---

[2] The second follows immediately by Hermitian conjugation of the first.

from which we conclude that the creation operator increases the number by one, i.e. $b_\nu^\dagger |n_\nu\rangle \propto |n_\nu + 1\rangle$. Now calculate

$$|B_+(n_\nu)|^2 = \langle n_\nu | b_\nu b_\nu^\dagger | n_\nu\rangle = \langle n_\nu | b_\nu^\dagger b_\nu | n_\nu\rangle + \langle n_\nu | n_\nu\rangle = n_\nu + 1$$

In summary, we have found that

$$b_\nu |n_\nu\rangle = \sqrt{n_\nu}\,|n_\nu - 1\rangle\,, \qquad b_\nu^\dagger = \sqrt{n_\nu + 1}\,|n_\nu + 1\rangle\,.$$

Most importantly, we conclude that it is possible to write any N-particle system of bosonic particles by using the operators we have just introduced:

$$\hat{S}_+ \left|\psi_{\nu_{n_1}}(\tilde{\mathbf{r}}_1)\right\rangle \left|\psi_{\nu_{n_2}}(\tilde{\mathbf{r}}_2)\right\rangle \ldots \left|\psi_{\nu_{n_N}}(\tilde{\mathbf{r}}_N)\right\rangle = b_{\nu_{n_1}}^\dagger b_{\nu_{n_2}}^\dagger \ldots b_{\nu_{n_N}}^\dagger |0\rangle.$$

1.2.2 Fermion Creation and Annihilation Operators

We introduce the *fermion creation* and *annihilation operators* $c_{\nu_j}^\dagger$ and c_{ν_j}, respectively. In analogy with the boson operators:

$$\begin{aligned} c_{\nu_j}^\dagger \left|\ldots, n_{\nu_{j-1}}, n_{\nu_j}, n_{\nu_{j+1}}, \ldots\right\rangle &= C_+\left(n_{\nu_j}\right) \left|\ldots, n_{\nu_{j-1}}, n_{\nu_j} + 1, n_{\nu_{j+1}}, \ldots\right\rangle, \\ c_{\nu_j} \left|\ldots, n_{\nu_{j-1}}, n_{\nu_j}, n_{\nu_{j+1}}, \ldots\right\rangle &= C_-\left(n_{\nu_j}\right) \left|\ldots, n_{\nu_{j-1}}, n_{\nu_j} - 1, n_{\nu_{j+1}}, \ldots\right\rangle. \end{aligned}$$

In order to make the state antisymmetric for particle interchange, one must account for the order of the occupation numbers. We require that, if $j \neq k$:

$$\left|\ldots, n_{\nu_j} = 1, \ldots, n_{\nu_k} = 1, \ldots\right\rangle = -\left|\ldots, n_{\nu_k} = 1, \ldots, n_{\nu_j} = 1, \ldots\right\rangle,$$

which implies:

$$c_{\nu_j}^\dagger c_{\nu_k} |\phi\rangle = -c_{\nu_k} c_{\nu_j}^\dagger |\phi\rangle\,,$$

i.e. the operators c_{ν_j} and $c_{\nu_k}^\dagger$ must anticommute if $j \neq k$. However, $c_{\nu_j}^\dagger$ and c_{ν_j} do not:

$$\left\{c_{\nu_j}^\dagger, c_{\nu_j}\right\} |0\rangle = \left(c_{\nu_j}^\dagger c_\nu + c_{\nu_j} c_{\nu_j}^\dagger\right) |0\rangle = |0\rangle\,,$$

from which we conclude

$$\left\{c_{\nu_j}, c_{\nu_k}^\dagger\right\} = \delta_{\nu_j,\nu_k}, \qquad \left\{c_{\nu_j}^\dagger, c_{\nu_k}^\dagger\right\} = 0, \qquad \left\{c_{\nu_j}, c_{\nu_k}\right\} = 0. \tag{1.8}$$

It is immediate to observe that

$$\left(c_{\nu_j}^+\right)^2 = 0, \qquad \left(c_{\nu_j}\right)^2 = 0.$$

We see that $c^\dagger_\nu$ and c_ν raises or lowers the eigenvalue of $c^\dagger_\nu c_\nu$ respectively

$$\left(c^\dagger_\nu c_\nu\right) c^\dagger_\nu \left|\phi\right\rangle = c^\dagger_\nu \left(c^\dagger_\nu c_\nu\right) \left|\phi\right\rangle - c^\dagger_\nu \left|\phi\right\rangle = \left(n_\nu + 1\right) c^\dagger_\nu \left|\phi\right\rangle$$

and

$$\left(c^\dagger_\nu c_\nu\right) c_\nu \left|\phi\right\rangle = \left(n_\nu - 1\right) c_\nu \left|\phi\right\rangle .$$

We now evaluate

$$\left(c^\dagger_\nu c_\nu\right)^2 = c^\dagger_\nu \left(c_\nu c^\dagger_\nu\right) c_\nu = c^\dagger_\nu \left(1 - c^\dagger_\nu c_\nu\right) c_\nu = c^\dagger_\nu c_\nu - \left(c^\dagger_\nu\right)^2 \left(c_\nu\right)^2 = c^\dagger_\nu c_\nu$$

and find that

$$c^\dagger_\nu c_\nu \left(c^\dagger_\nu c_\nu - 1\right) = 0$$

which implies that $c^\dagger_\nu c_\nu \left|n\right\rangle = n \left|n\right\rangle$ with $n = 0, 1$, as expected for the fermions due to Pauli exclusion principle. We identify $\hat{n}_\nu \equiv c^\dagger_\nu c_\nu$ as the fermion number operators. In summary:

$$c_\nu|0\rangle = 0, \quad c^\dagger_\nu|0\rangle = |1\rangle, \quad c_\nu|1\rangle = |0\rangle, \quad c^\dagger_\nu|1\rangle = 0.$$

As we did for the bosons, we conclude that it is possible write any N-particle system of fermionic particles by using the fermionic operators:

$$\hat{S}_- \left|\psi_{\nu_{n_1}}\left(\tilde{\mathbf{r}}_1\right)\right\rangle \left|\psi_{\nu_{n_2}}\left(\tilde{\mathbf{r}}_2\right)\right\rangle \dots \left|\psi_{\nu_{n_N}}\left(\tilde{\mathbf{r}}_N\right)\right\rangle = c^\dagger_{\nu_{n_1}} c^\dagger_{\nu_{n_2}} \dots c^\dagger_{\nu_{n_N}} |0\rangle.$$

1.2.3 Operators

One-particle operators

Let us first consider the one-particle operator $T_j = T(\mathbf{r_j}, \nabla_{\mathbf{r}_j})$. In first quantisation, we write it as [5]

$$T_j = \sum_{\nu_a,\nu_b} T_{\nu_a\nu_b} \left|\psi_{\nu_b}(\mathbf{r}_j)\right\rangle \left\langle\psi_{\nu_a}(\mathbf{r}_j)\right| ,$$

with

$$T_{\nu_b\nu_a} = \int d\mathbf{r}_j \ \psi^*_{\nu_b}(\mathbf{r}_j) T(\mathbf{r}_j, \nabla_{\mathbf{r}_j}) \psi_{\nu_a}(\mathbf{r}_j).$$

In an N-particle system, we often consider the operator given by the sum of all the identical operators acting on each particle, i.e. $T_{\text{tot}} = \sum_{j=1}^N T_j$. An immediate example of this kind is the kinetic operator, which is given by the sum of the kinetic operators for each particle. The action on the product state is

$$\begin{aligned}
&T_{\text{tot}}\,|\psi_{\nu_{n_1}}(\mathbf{r}_1)\rangle\,|\psi_{\nu_{n_2}}(\mathbf{r}_2)\rangle\ldots|\psi_{\nu_{n_N}}(\mathbf{r}_N)\rangle = \\
&\quad= \sum_{j=1}^{N}\sum_{\nu_b\nu_a} T_{\nu_b\nu_a}\,|\psi_{\nu_{n_1}}(\mathbf{r}_1)\rangle\ldots|\psi_{\nu_b}(\mathbf{r}_j)\rangle\,\langle\psi_{\nu_a}(\mathbf{r}_j)|\psi_{\nu_{n_j}}(\mathbf{r}_j)\rangle\ldots|\psi_{\nu_{n_N}}(\mathbf{r}_N)\rangle \\
&\quad= \sum_{j=1}^{N}\sum_{\nu_b\nu_a} T_{\nu_b\nu_a}\delta_{\nu_b\nu_{n_j}}\,|\psi_{\nu_{n_1}}(\mathbf{r}_1)\rangle\ldots|\psi_{\nu_b}(\mathbf{r}_j)\rangle\ldots|\psi_{\nu_{n_N}}(\mathbf{r}_N)\rangle
\end{aligned} \tag{1.9}$$

In second quantisation, one simply inserts the operator $b^\dagger_{\nu_b}$ at site n_j in Eq. (1.9), obtaining the following representation:

$$T_{\text{tot}}b^\dagger_{\nu_{n_1}}\ldots b^\dagger_{\nu_{n_N}}\,|0\rangle = \sum_{\nu_a\nu_b} T_{\nu_b\nu_a}\sum_{j=1}^{N}\delta_{\nu_a,\nu_{n_j}}b^\dagger_{\nu_{n_1}}\ldots b^\dagger_{\nu_b}\ldots b^\dagger_{n_N}.$$

In order to find an optimal representation for the operator, one wants to have the same operators on the left and right hand side of the equation. Thus, let us consider $\nu \equiv \nu_{n_j}$. Suppose that ν appears $p > 0$ times in the left hand side with a contribution $\left(b^\dagger_\nu\right)^p|0\rangle$. In the RHS, the contribution is

$$b^\dagger_{\nu_b}\left(b^\dagger_\nu\right)^{p-1}|0\rangle = b^\dagger_{\nu_b}\left(\frac{1}{p}b_\nu b^\dagger_\nu\right)\left(b^\dagger_\nu\right)^{p-1}|0\rangle = \left(\frac{1}{p}b^\dagger_{\nu_b}b_\nu\right)\left(b^\dagger_\nu\right)^{p}|0\rangle.$$

Summing over j, the factor $\delta_{\nu_a,\nu_{n_j}}$ yields p identical contributions cancelling the factor $1/p$, hence

$$T_{\text{tot}}\left[b^\dagger_{\nu_{n_1}}\ldots b^\dagger_{\nu_{n_N}}|0\rangle\right] = \sum_{a,b} T_{\nu_b\nu_a}b^\dagger_{\nu_b}b_{\nu_a}\left[b^\dagger_{\nu_{n_1}}\ldots b^\dagger_{\nu_{n_N}}|0\rangle\right],$$

leading to the the operator identity:

$$T_{\text{tot}} = \sum_{a,b} T_{\nu_a\nu_b}b^\dagger_{\nu_a}b_{\nu_b}.$$

The same procedure can be followed for the case of fermions, where the operator is given by

$$T_{\text{tot}} = \sum_{a,b} T_{\nu_a\nu_b}c^\dagger_{\nu_a}c_{\nu_b}.$$

If we take the quantum numbers to be the wavevectors, then the matrix for the electron kinetic operator is diagonal [8]:

$$\langle \mathbf{k}'\sigma' | T | \mathbf{k}\sigma\rangle = \frac{\hbar^2 k^2}{2m}\delta_{\mathbf{k}',\mathbf{k}}\delta_{\sigma',\sigma}.$$

Thus, second quantisation representation of the kinetic operator is

$$T = \sum_{\mathbf{k},\sigma} \frac{\hbar^2 k^2}{2m} c^\dagger_{\mathbf{k},\sigma} c_{\mathbf{k}\sigma}, \tag{1.10}$$

The free-electron Hamiltonian in second quantisation is

$$H_{\text{free}} = \sum_{\mathbf{k},\sigma} \frac{\hbar^2 k^2}{2m} c^\dagger_{\mathbf{k}\sigma} c_{\mathbf{k}\sigma} = \sum_{k,\sigma} \frac{\hbar^2 k^2}{2m} n_{\mathbf{k}\sigma},$$

where we introduced the occupation number operator $n_{\mathbf{k}\sigma}$.

Two-particle operators

We shall now consider two-particle operators, e.g. the Coulomb interaction

$$V(\mathbf{r}_i - \mathbf{r}_j) = \frac{e^2}{4\pi\varepsilon_0}\frac{1}{|\mathbf{r}_i - \mathbf{r}_j|}.$$

The operator V can be decomposed as

$$V(\mathbf{r}_i, \mathbf{r}_j) = \sum_{\substack{\nu_a\nu_b \\ \nu_c\nu_d}} V_{\nu_c\nu_d,\nu_a\nu_b} |\psi_{\nu_c}(\mathbf{r}_i)\rangle |\psi_{\nu_d}(\mathbf{r}_j)\rangle \langle\psi_{\nu_a}(\mathbf{r}_i)| \langle\psi_{\nu_b}(\mathbf{r}_j)|,$$

with

$$V_{\nu_c\nu_d,\nu_a\nu_b} = \int d\mathbf{r}_i d\mathbf{r}_j\, \psi^*_{\nu_c}(\mathbf{r}_i)\psi^*_{\nu_d}(\mathbf{r}_j) V(\mathbf{r}_i - \mathbf{r}_j)\psi_{\nu_a}(\mathbf{r}_i)\psi_{\nu_b}(\mathbf{r}_j).$$

In a N-particle system, we are often interested in considering all possible interactions between the particles:

$$V_{\text{tot}}(\mathbf{r}_1, \ldots, \mathbf{r}_N) = \sum_{i>j}^{N} V(\mathbf{r}_i, \mathbf{r}_j) = \frac{1}{2}\sum_{i,j\neq i}^{N} V(\mathbf{r}_i, \mathbf{r}_j).$$

The operator acts on a product state as follows:

$$V_{\text{tot}} |\nu_{n_1}\rangle |\nu_{n_2}\rangle \dots |\nu_{n_N}\rangle$$
$$= \frac{1}{2} \sum_{j \neq k}^{N} \sum_{\substack{\nu_a \nu_b \\ \nu_c \nu_d}} V_{\nu_c \nu_d, \nu_a \nu_b} \delta_{\nu_a, \nu_{n_j}} \delta_{\nu_b, \nu_{n_k}} |\nu_{n_1}\rangle \dots |\nu_c\rangle_j \dots |\nu_d\rangle_k \dots |\nu_{n_N}\rangle . \quad (1.11)$$

In second quantisation, we follow a similar procedure to what was described in the previous section and gets the following operator identity:

$$V_{tot} = \frac{1}{2} \sum_{\substack{\nu_i \nu_j \\ \nu_k \nu_l}} V_{\nu_i \nu_j \nu_k \nu_l} a^{\dagger}_{\nu_i} a^{\dagger}_{\nu_j} a_{\nu_l} a_{\nu_k}.$$

1.2.4 Harmonic Oscillator

The harmonic oscillator is a particularly important example in many-body theory, so we shall study the second-quantised form [5]. The one-dimensional harmonic oscillator's Hamiltonian is

$$H = \frac{1}{2m} p^2 + \frac{1}{2} m \omega^2 x^2,$$

with x and p being the position and the momentum operators, respectively. The important aspect is that they are conjugate variables:

$$[x, p] = i\hbar.$$

It is possible to introduce the operators

$$\begin{aligned} a_{\omega} &= \frac{1}{\sqrt{2}} \left(\frac{x}{\sqrt{\hbar / m\omega}} + i \frac{p}{\hbar} \sqrt{\hbar / m\omega} \right), \\ a^{\dagger}_{\omega} &= \frac{1}{\sqrt{2}} \left(\frac{x}{\sqrt{\hbar / m\omega}} - i \frac{p}{\hbar} \sqrt{\hbar / m\omega} \right). \end{aligned} \quad (1.12)$$

These operators allow us to express the position and momentum operators as:

$$\begin{aligned} x &= \frac{\sqrt{\hbar / m\omega}}{\sqrt{2}} \left(a^{\dagger}_{\omega} + a_{\omega} \right), \\ p &= \hbar \frac{i}{\sqrt{2} \sqrt{\hbar / m\omega}} \left(a^{\dagger}_{\omega} - a_{\omega} \right), \end{aligned}$$

and the Hamiltonian is rewritten in terms of a_ω and $a_\omega^\dagger$ as:

$$H = \hbar\omega\left(a_\omega^\dagger a_\omega + \frac{1}{2}\right).$$

It is straightforward to verify that the operators defined in Eq. (1.12) obey the same bosonic commutation relations as in Eq. (1.5). The corresponding eigenstates $|n\rangle$ are given by:

$$|n\rangle = \frac{\left(a^\dagger\right)^n}{\sqrt{n!}}|0\rangle, \qquad H|n\rangle = \hbar\omega\left(n + \frac{1}{2}\right)|n\rangle.$$

By similarity with the boson creation operators, $a^\dagger$ operator, increases the number of quanta in the harmonic oscillator by one. We shall see its usefulness when describing phonon fields, which are the quantised excitations of the harmonic oscillator in a solid.

1.3 Crystal Lattice

It is known that in solid systems the fundamental structure is called *lattice*, which consists of a regular arrangement of ions. At zero temperature, the ions remain fixed in their equilibrium position. In this case, the electrons interact only with the static lattice potential, giving rise to a term $V_{\text{el-lat}}$. At finite temperature, the ions vibrate around their equilibrium positions; such vibrations can be described in terms of quantised normal modes of the lattice, known as *phonons*. The interaction between phonons and electrons is indicated as $V_{\text{el-ph}}$. Before studying the phonons, in this section we see how to formalise the lattice structure and state the *Bloch's theorem*.

1.3.1 Bloch's Theorem

The equilibrium positions $\mathbf{R}$ of each ion in a three-dimensional lattice can be represented through the lattice basis vectors $\{\mathbf{a}_1, \mathbf{a}_2, \mathbf{a}_3\}$ as

$$\mathbf{R} = n_1\mathbf{a}_1 + n_2\mathbf{a}_2 + n_3\mathbf{a}_3, \qquad n_1, n_2, n_3 \in \mathbb{Z}.$$

We define the reciprocal lattice as the Fourier transform of the equilibrium positions from the real space to the wavevector space, referred to as *reciprocal space* (RS). The *reciprocal lattice* (RL) is defined as [5]

$$\text{RL} \equiv \left\{\mathbf{G} \in \text{RS} : e^{i\mathbf{G}\cdot\mathbf{R}} = 1\right\},$$

and any vector $\mathbf{G}$ of the RL can be written through some basis $\{\mathbf{c}_1, \mathbf{c}_2, \mathbf{c}_3\}$

$$\mathbf{G} = n'_1\mathbf{c}_1 + n'_2\mathbf{c}_2 + n'_3\mathbf{c}_3, \qquad n'_1, n'_2, n'_3 \in \mathbb{Z}.$$

It can be shown that the following definition of the RL basis is consistent with the definition of the RL given above:

$$\mathbf{c}_1 = 2\pi\frac{\mathbf{a}_2 \times \mathbf{a}_3}{\mathbf{a}_1 \cdot \mathbf{a}_2 \times \mathbf{a}_3}, \quad \mathbf{c}_2 = 2\pi\frac{\mathbf{a}_3 \times \mathbf{a}_1}{\mathbf{a}_2 \cdot \mathbf{a}_3 \times \mathbf{a}_1}, \quad \mathbf{c}_3 = 2\pi\frac{\mathbf{a}_1 \times \mathbf{a}_2}{\mathbf{a}_3 \cdot \mathbf{a}_1 \times \mathbf{a}_2}.$$

Because of the periodicity of the lattice, it is often useful to work in the *First Brillouin Zone*, which is made of all the vectors of the reciprocal space that are closer to $\mathbf{G} = \mathbf{0}$ than to any other vector in the reciprocal lattice. The First Brillouin Zone (FBZ) is thus defined as

$$\text{FBZ} = \{\mathbf{k} \in \text{RS} : |\mathbf{k}| < |\mathbf{k} - \mathbf{M}|,\ \forall\, \mathbf{M} \in \text{RL} \setminus \{\mathbf{0}\}\}$$

Any vector $\mathbf{p} \in \text{RS}$ in the reciprocal space can therefore be represented as the sum of a vector in the reciprocal lattice and a vector in the First Brillouin Zone:

$$\mathbf{p} = \mathbf{G} + \mathbf{k}, \qquad \mathbf{G} \in \text{RL}, \qquad \mathbf{k} \in \text{FBZ}.$$

Let us now consider the Hamiltonian consisting of the kinetic part of the electrons and the static interaction between the lattice and the electrons:

$$H_{\text{Bloch}} = T_{\text{el}} + V_{\text{el-latt}}(\mathbf{r}), \tag{1.13}$$

where the potential is periodic in the lattice:

$$V(\mathbf{r} + \mathbf{R}) = V(\mathbf{r}) \quad \forall \mathbf{R} \in \text{RL}.$$

Any potential periodic in the lattice may be written through a Fourier transform as follows:

$$V(\mathbf{r}) = \sum_{\mathbf{G}} V_{\mathbf{G}} e^{i\mathbf{G}\cdot\mathbf{r}}.$$

We will now state Bloch's theorem [9] without proving it.

Theorem 1.1 (Bloch's theorem)**.** *The wavefunctions of the crystal Hamiltonian H_{Bloch} can be written as the product of a plane wave of vector $\mathbf{k} \in$ FBZ and an appropriate function periodic in the lattice:*

$$H_{Bloch}\psi_{n\mathbf{k}\sigma} = \varepsilon_{n\mathbf{k}}\psi_{n\mathbf{k}\sigma}, \qquad \psi_{n\mathbf{k}\sigma}(\mathbf{r}) = u_{n\mathbf{k}}(\mathbf{r})e^{i\mathbf{k}\cdot\mathbf{r}}\chi_\sigma,$$

where $u_{n\mathbf{k}}(\mathbf{r}+\mathbf{R}) = u_{n\mathbf{k}}(\mathbf{r})$*,* $\mathbf{k} \in$ *FBZ and* $n \in \mathbb{N}$ *is the band index.*

Bloch's theorem classifies energy eigenstates according to the FBZ wavevector $\mathbf{k}$ as well as a *band index* $n \in \mathbb{N}$. This gives rise to the *band structure*. According to the effective-mass approximation [5], one can prove that the eigenstates $\psi_{n\mathbf{k}\sigma}(\mathbf{r})$ may be approximated by plane waves if the electronic mass is changed to a material-dependent effective mass m^*:

$$\psi_{n\mathbf{k}\sigma} = \frac{1}{\sqrt{\mathcal{V}}} e^{i\mathbf{k}\cdot\mathbf{r}} \chi_\sigma,$$

with $\mathbf{k}$ unrestricted, and $\mathcal{V}$ is the volume.

1.3.2 Tight-Binding Approximation

The *tight-binding model* [10] is one of the simplest approaches to describe the electronic structure of solids. In the tight-binding approximation, electrons are considered to be tightly bound to the atom sites. For this reason, they are assumed to occupy atomic-like orbitals and can "hop" between neighbouring sites due to the overlap of these orbitals. This approximation is of great interest for this thesis because it is the basis for the Holstein model.

We consider a crystal lattice made of N identical molecules or atoms, which are located at positions $\mathbf{R}_n$ in the three-dimensional space. Each molecule contributes identically to the potential to which the electrons are subjected. The total potential is given by the sum of the potentials of all the molecules in the crystal lattice:

$$V(\mathbf{r}) = \sum_n U(\mathbf{r} - \mathbf{R}_n).$$

Because of the short-range approximation, one assumes the one-electron wave function of the m-th energy level to have the following form

$$\psi_m(\mathbf{r}) = \frac{1}{\sqrt{N}} \sum_n a_m(\mathbf{R}_n, \mathbf{r}) \phi_m(\mathbf{r} - \mathbf{R}_n), \tag{1.14}$$

where $\phi(\mathbf{r} - \mathbf{R}_n)_m$ are the wave orbitals for the n-th molecule located at position $\mathbf{R}_n$. These orbitals are solution to the stationary Schrödinger equation for a single electron in the potential of the n-th molecule:

$$\left[-\frac{\hbar^2}{2m}\nabla^2 + U(\mathbf{r} - \mathbf{R}_n)\right]\phi(\mathbf{r} - \mathbf{R}_n) = E\,\phi(\mathbf{r} - \mathbf{R}_n).$$

Tight binding in second quantisation

In Eq. (1.10), we have seen how the kinetic operator can be written in second quantisation. In absence of external fields, the Hamiltonian for a single electron would be written as

$$H_{\text{free}} = \sum_{\mathbf{k}\sigma} \varepsilon_{\mathbf{k}\sigma} c^\dagger_{\mathbf{k}} c_{\mathbf{k}}, \qquad \varepsilon_{\mathbf{k}} = \frac{\hbar^2 \mathbf{k}^2}{2m} \tag{1.15}$$

In Eq. (1.14), we can consider the functions ψ_m to be Bloch's wavefunctions:

$$\psi_m(\mathbf{k}, \mathbf{r}) = \frac{1}{\sqrt{N}} \sum_n a_m(\mathbf{R}_n, \mathbf{r}) e^{i\mathbf{k}\cdot\mathbf{R}_n},$$

which leads to the second-quantised Hamiltonian[3]:

$$H_{el} = \sum_{\mathbf{k}} \varepsilon_{\mathbf{k}} c^\dagger_{\mathbf{k}\sigma} c_{\mathbf{k}\sigma}, \qquad \left[-\frac{\hbar^2}{2m}\nabla^2 + V(\mathbf{r}) \right] \psi_{m_0}(\mathbf{k}, \mathbf{r}) = \varepsilon_{\mathbf{k}} \psi_{m_0}(\mathbf{k}, \mathbf{r}),$$

where the dispersion relation for $\varepsilon_{\mathbf{k}}$ is of course different from the free-electron energy in Eq. (1.15). However, it is often the case that, when working with electron wave functions that are tightly bound to their lattice sites, it is more convenient to use the the *Wannier states*, which are the Fourier transform of the Bloch's states [11, 12]:

$$a_{m_0}(\mathbf{R}_n, \mathbf{r}) = \frac{1}{\sqrt{N}} \sum_{\mathbf{k}\in\text{FBZ}} e^{-i\mathbf{k}\cdot\mathbf{R}_n} \psi_{m_0}(\mathbf{k}, \mathbf{r})$$

The Wannier states form a orthonormal basis of the single-particle Hilbert space. The unitary transformation between the Bloch and the Wannier states induces an operator transformation:

$$\begin{aligned} c_{j\sigma} &= \frac{1}{\sqrt{N}} \sum_{\mathbf{k}\in\text{FBZ}} e^{i\mathbf{k}\cdot\mathbf{R}_j} c_{\mathbf{k}\sigma}, \\ c_{\mathbf{k}\sigma} &= \frac{1}{\sqrt{N}} \sum_j e^{-i\mathbf{k}\cdot\mathbf{R}_j} c_{j\sigma}, \end{aligned} \tag{1.16}$$

It is then possible to write the Hamiltonian in the *lattice representation* as

$$H_{el} = \frac{1}{N} \sum_{ij} \sum_{\mathbf{k}} e^{i\mathbf{k}\cdot(\mathbf{R}_i - \mathbf{R}_j)} \varepsilon_{\mathbf{k}} c^\dagger_i c_j = \frac{1}{N} \sum_{ij} t_{ij} c^\dagger_i c_j, \tag{1.17}$$

---

[3] Since we are only interested in one specific electronic band, say m_0, we suppose $m \equiv m_0$, and we suppress the index m from the following operator notations.

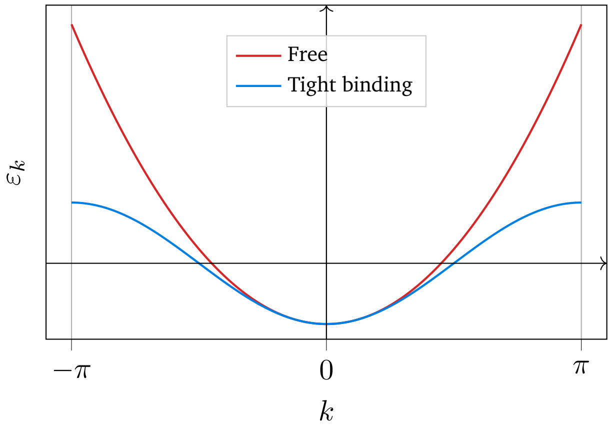

Fig. 1.1: Comparison of the free electron energy dispersion (red) and the tight-binding energy dispersion (blue).

where we have introduced the *hopping matrix* or *hopping term*:

$$t_{ij} \equiv \sum_{\mathbf{k}} e^{i\mathbf{k}\cdot(\mathbf{R}_i-\mathbf{R}_j)}\varepsilon_{\mathbf{k}}. \tag{1.18}$$

The meaning of Eq. (1.17) is quite intuitive. An electron is annihilated at the site $\mathbf{R}_j$ and created at the site $\mathbf{R}_i$. When this happens, we say that the electron *hops* from the j-th site to the i-th site. The hopping term t_{ij} is interpreted as the the energy associated to this process. It is easy to see that the value of t_{ij} will be negligible for large distances between the sites i and j, this effect is even more pronounced given that the potential $U(\mathbf{r})$ is assumed to be short-ranged. Therefore, in the tight-binding approximation the hopping parameter t_{ij} is nonzero only for nearest neighbour sites, and its value is taken to be constant: $-t$. In the nearest-neighbour approximation, the Hamiltonian can be written as

$$H_{tb} = -t\sum_{\langle i,j\rangle}(c_i^\dagger c_j + c_j^\dagger c_i) = -\frac{t}{2}\sum_{i,\delta}\left(c_i^\dagger c_{i+\delta} + c_{i+\delta}^\dagger c_i\right), \tag{1.19}$$

where we have dropped the sum over the same indexes ($i = j$) because it is a constant shift in energy[4]. The symbol $\langle i,j\rangle$ denotes that the sum is over the pairs of sites i, j that are close neighbours. The term δ is used to index the nearest neighbour sites. In case of the extreme *atomic limit*, the energy levels $\varepsilon_{\mathbf{k}}$ are degenerate, and we take $t_{ij} = -t\delta_{ij}$: the hopping is completely suppressed. It is possible to rewrite

---

[4] This is true if we assume that the lattice energies ε_i are the same.

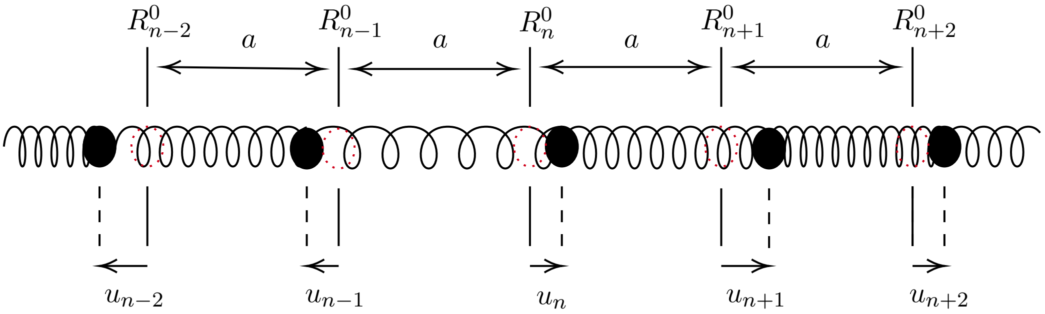

Fig. 1.2: Schematic representation of lattice vibrations in a one-dimensional chain. Each site is at a position $R^0_n = na$, and the corresponding atom is displaced by u_n from its equilibrium position.

the Hamiltonian back in the momentum space:

$$\begin{aligned} H_{tb} &= -\frac{t}{2}\frac{1}{N}\sum_i\sum_\delta\sum_{\mathbf{k},\mathbf{k}'}\left[e^{-i\mathbf{k}\cdot\mathbf{R}_i}e^{i\mathbf{k}'\cdot(\mathbf{R}_i+\mathbf{R}_\delta)}c^\dagger_{\mathbf{k}}c_{\mathbf{k}'} + e^{i\mathbf{k}\cdot\mathbf{R}_i}e^{-i\mathbf{k}'\cdot(\mathbf{R}_i+\mathbf{R}_\delta)}c^\dagger_{\mathbf{k}}c_{\mathbf{k}'}\right] \\ &= \sum_{\mathbf{k}} \varepsilon^{tb}_{\mathbf{k}} c^\dagger_{\mathbf{k}} c_{\mathbf{k}}, \end{aligned} \tag{1.20}$$

with the dispersion relation:

$$\varepsilon^{tb}_{\mathbf{k}} = -t\sum_\delta \cos(\mathbf{k}\cdot\mathbf{R}_\delta). \tag{1.21}$$

The tight-binding dispersion relation is plotted in Fig. 1.1 together with the free electron dispersion relation.

1.4 Phonons

In the previous sections, the concept of lattice vibrations was introduced. To describe vibrations, a simplified model is considered: we take a one-dimensional lattice consisting of N identical atoms of mass m, equally spaced by a lattice constant a. Therefore, in equilibrium each atom occupy the position $R^0_n = na$, where n labels the site index. We denote by u_n the displacement of the n-th atom from its equilibrium position R^0_n. This model is represented in Fig. 1.2.

The ground-state energy of the system is expanded in powers of the displacements [13]:

$$E_0(u_1,\ldots,u_N) \approx E_0(\mathbf{0}) + \sum_n \left[\frac{\partial E_0}{\partial u_n}\right]_{\mathbf{u}=\mathbf{0}} u_n + \frac{1}{2}\sum_{n,m}\left[\frac{\partial^2 E_0}{\partial u_n \partial u_m}\right]_{\mathbf{u}=\mathbf{0}} u_n u_m$$

Where we used $\mathbf{u} \equiv (u_1, u_2, \ldots, u_N)$. Since $u_n = 0$ represents an equilibrium position, the first-derivative term is zero. The *interatomic force constants* are defined as

$$D_{nm} \equiv \left[\frac{\partial^2 E_0}{\partial u_n \partial u_m} \right]_{\mathbf{u}=\mathbf{0}}, \tag{1.22}$$

and thus the total crystal energy is

$$E_0(u_1, \ldots, u_N) = E_0(\mathbf{0}) + \frac{1}{2} \sum_{n,m} D_{nm} u_n u_m.$$

By Eq. (1.22), D_{nm} is real and symmetric: $D_{nm} = D_{mn} \in \mathbb{R}$. Furthermore, when all atomic displacements are equal we require all forces to be zero; this gives rise to the *sum rule*:

$$\sum_m D_{nm} = 0, \quad \forall n.$$

We also require interatomic forces to be relevant only when they occur between neighbouring sites; that is, we impose:

$$D_{nm} \neq 0 \iff |n - m| \leq 1.$$

By applying the symmetry rules stated above, we find:

$$D_{nn} = 2C, \quad D_{n,n+1} = D_{n+1,n} = -C.$$

This leads to the energy[5]

$$\begin{aligned} E_0 &= \frac{1}{2} C \sum_n \left(2u_n^2 - u_n u_{n+1} - u_n u_{n-1} \right) \\ &= \frac{1}{2} C \sum_n \left(u_n^2 + u_{n+1}^2 - u_n u_{n+1} - u_{n+1} u_n \right) \\ &= \frac{1}{2} C \sum_n \left(u_n - u_{n+1} \right)^2. \end{aligned}$$

In Quantum Mechanics, this Hamiltonian is written as

$$H = \sum_n \frac{1}{2\pi} p_n^2 + \frac{1}{2} C \sum_n \left[2u_n^2 - u_n u_{n+1} - u_n u_{n+1} \right]. \tag{1.23}$$

As was done in Sect. 1.3.1, periodic boundary conditions are imposed on the system. With N atom sites forming a linear chain of distance a, then the wavevector k must satisfy

$$kNa = n\pi, \quad n \in \mathbb{Z}$$

---

[5] Ignoring the constant part of the Hamiltonian.

and the wavevectors k in the FBZ are given by

$$k = -\frac{\pi}{a} + \frac{n}{N}\frac{2\pi}{a} \qquad \text{with } n = 1, \dots, N, \tag{1.24}$$

so there are N wavectors in the FBZ.

We can then rewrite Eq. (1.23) using the Fourier transforms of the conjugate variable

$$\begin{aligned} p_n &= \frac{1}{\sqrt{N}} \sum_{k\in\text{FBZ}} p_k e^{ikR_n^0}, & p_k &= \frac{1}{\sqrt{N}} \sum_{j=1}^{N} p_n e^{-ikR_n^0}, \\ u_n &= \frac{1}{\sqrt{N}} \sum_{k\in\text{FBZ}} u_k e^{ikR_n^0}, & u_k &= \frac{1}{\sqrt{N}} \sum_{j=1}^{N} u_n e^{-ikR_n^0}, \end{aligned} \tag{1.25}$$

with the commutation rules:

$$[u_k, p_k] = i\hbar\delta_{k,k'}, \quad [u_k, u_{k'}] = [p_k, p_{k'}] = 0.$$

To compute Eq. (1.23), we use the following relations:

$$\begin{aligned} \sum_n u_n^2 &= \frac{1}{N}\sum_n\sum_{kk'} e^{i(k+k')R_n^0} u_k u_{k'} = \sum_{kk'}\left[\frac{1}{N}\sum_n e^{i(k+k')R_n^0}\right] u_k u_{k'} = \\ &= \sum_{kk'} \delta_{k,-k'} u_k u_{k'} = \sum_k u_k u_{-k}, \\ \sum_n p_n^2 &= \sum_q p_q p_{-q}, \\ \sum_n u_n u_{n+1} &= \frac{1}{N}\sum_n\sum_{kk'} e^{i(k+k')R_n^0 + ik'a} u_k u_{k'} = \sum_k u_k u_{-k} e^{-ika}. \end{aligned}$$

where we used the fact that $R_{n+1}^0 = R_n^0 + a$. These equations are now inserted into Eq. (1.23), yielding

$$\begin{aligned} H &= \sum_k \frac{1}{2M} p_k p_{-k} + \frac{1}{2} C \sum_k u_k u_{-k}\left[2 - e^{-ika} - e^{ika}\right] \\ &= \sum_k \left[\frac{1}{2M} p_k p_{-k} + \frac{1}{2} M\omega_k^2 u_k u_{-k}\right], \end{aligned}$$

with

$$\omega_k^2 = \frac{4C}{M}\sin^2\left(\frac{ka}{2}\right).$$

We now perform a canonical transformation to appropriate creation and annihilation operators. We introduce the operator b_k, which is defined such that

$$u_k = \sqrt{\frac{\hbar}{2M\omega_k}} \left[b_k + b^\dagger_{-k}\right] \tag{1.26}$$

$$p_k = -i\sqrt{\frac{M\hbar\omega_k}{2}} \left[b_{-k} - b^\dagger_k\right] \tag{1.27}$$

It is straightforward to verify that the above definitions of b_k and $b^\dagger_k$ satisfy the bosonic commutation relations, previously introduced in Eq. (1.5):

$$\left[b_k, b^\dagger_{k'}\right] = \delta_{k,k'}, \qquad \left[b_k, b_{k'}\right] = \left[b^\dagger_k, b^\dagger_{k'}\right] = 0.$$

We therefore identify b_k and $b^\dagger_k$ as the annihilation and creation operators for the k-th mode, respectively. Using these operators, the Hamiltonian of the system takes the form

$$H = \sum_k \hbar\omega_k \left[b^\dagger_k b_k + \frac{1}{2}\right].$$

which describes a set of independent quantum harmonic oscillators, one for each mode k. The quantised excitations of these oscillators are known as *phonons*, which represent discrete quanta of lattice vibrations.

Phonon modes: acoustic and optical. In the one-dimensional case [5], when the unit cell contains more than one atom the phonon dispersion relation is no longer a single continuous curve. Instead, the dispersion relation splits into multiple branches, analogous to the formation of the Bloch bands for the electrons. These branches are called *phonon modes* and are indexed by the *branch index* λ. For instance, with two atoms per unit cell the dispersion curve is divided into two branches. Phonons in the lower branch are called *acoustic phonons*; those in the upper branch require high energies to be excited, and are called *optical phonons* because they are excited by optical radiation. In a one-dimensional chain, for s ions per unit cell, there always is 1 acoustic branch and $s-1$ optical branches. Each phonon is indexed by a wavevector k and a branch index λ, and the phonon frequency is denoted by $\omega_{k\lambda}$.

Three-dimensional case. The three-dimensional case can be analysed in a manner analogous to the one-dimensional case; here we summarize the main results. For each value of $\mathbf{k}$ in the single-atom unit cell, the harmonic oscillator admits three polarization vectors $\{\epsilon_{\mathbf{k},1}, \epsilon_{\mathbf{k},2}, \epsilon_{\mathbf{k},3}\}$ that form an orthonormal basis. Typical examples of these polarizations are transverse, longitudinal, and general. The atomic displacement can then be written as

$$\mathbf{u}_{\mathbf{k}\lambda} \equiv f_{\mathbf{k}\lambda} \frac{1}{\sqrt{2}} \left(b^{\dagger}_{-\mathbf{k}\lambda} + b_{\mathbf{k}\lambda} \right) \boldsymbol{\epsilon}_{\mathbf{k}\lambda} \tag{1.28}$$

with

$$f_{\mathbf{k}\lambda} = \sqrt{\frac{\hbar}{M\omega_{\mathbf{k}\lambda}}}, \qquad \left[b_{\mathbf{k}\lambda}, b^{\dagger}_{\mathbf{k}'\lambda'} \right] = \delta_{\mathbf{k},\mathbf{k}'}\, \delta_{\lambda,\lambda'}.$$

The phonon Hamiltonian is

$$H_{ph} = \sum_{\mathbf{k}\lambda} \hbar\omega_{\mathbf{k}\lambda} \left(b^{\dagger}_{\mathbf{k}\lambda} b_{\mathbf{k}\lambda} + \frac{1}{2} \right).$$

If the number of atoms in the unit cell is increased from 1 to s, then it is possible to show that there are 3 acoustic modes and $3(s-1)$ optical modes. The λ index is used to distinguish index both the polarisation and the mode.

1.4.1 Electron-Phonon Interaction

Having established a model for the phonons, we proceed to examine the coupling between electrons and lattice ions. As previously discussed, the electron-ion interaction in a crystalline solid can be decomposed into two distinct contributions [5], the interaction with the static lattice potential and the phonons:

$$V_{\text{el-ion}} = V_{\text{el-latt}} + V_{\text{el-ph}}.$$

Let us denote the electron density at position $\mathbf{r}$ by $\rho_{\text{el}}(\mathbf{r})$. Each ion is displaced by a quantity $\mathbf{u}_j$ from its lattice site $\mathbf{R}^0_j$, so its position is $\mathbf{R}_j = \mathbf{R}^0_j + \mathbf{u}_j$. The Coulomb potential between an electron in $\mathbf{r}$ and an ion located at $\mathbf{R}_j$ is given by $V_{\text{ion}}(\mathbf{r} - \mathbf{R}_j)$. To account for all N ions, sum over the index j:

$$V_{el-ion} = \int d^3\mathbf{r} \left\{ (-e)\, \rho_{el}\left(\mathbf{r}\right) \sum_{j=1}^{N} V_{ion}\left(\mathbf{r} - \mathbf{R}_j\right) \right\}, \tag{1.29}$$

and consider the Taylor expansion around the equilibrium position $\mathbf{R}^0_j$:

$$V_{ion}(\mathbf{r} - \mathbf{R}_j) \approx V_{ion}\left(\mathbf{r} - \mathbf{R}^0_j\right) - \nabla_{\mathbf{r}} V_{ion}\left(\mathbf{r} - \mathbf{R}^0_j\right) \cdot \mathbf{u}_j.$$

Eq. (1.29) is then evaluated as

$$V_{\text{el}-\text{ion}} = \int d\mathbf{r}(-e)\rho_{\text{el}}(\mathbf{r}) \sum_{j=1}^{N} V_{\text{ion}}\left(\mathbf{r}-\mathbf{R}_j^0\right) - \int d\mathbf{r}(-e)\rho_{\text{el}}(\mathbf{r}) \times$$

$$\times \sum_{j=1}^{N} \nabla_{\mathbf{r}} V_{\text{ion}}\left(\mathbf{r}-\mathbf{R}_j^0\right)\cdot \mathbf{u}_j. \quad (1.30)$$

The first term $V_{el-latt}$ is the static interaction with the lattice. This term was already studied Sect. 1.3.1, in the crystal Hamiltonian H_{Bloch}: it is already taken into account in the Bloch bands. The dynamic part of the interaction is the electron-phonon interaction, which is the second term in Eq. (1.30):

$$V_{\text{el}-\text{ph}} = \int d\mathbf{r}\rho_{\text{el}}(\mathbf{r}) \left\{ \sum_j e\mathbf{u}_j \cdot \nabla_{\mathbf{r}} V_{\text{ion}}\left(\mathbf{r}-\mathbf{R}_j^0\right) \right\}. \quad (1.31)$$

First, consider the Fourier transform of $V_{ion}(\mathbf{r}-\mathbf{R}_j^0)$:

$$V_{ion}(\mathbf{r}-\mathbf{R}_j^0) = \frac{1}{\mathcal{V}}\sum_{\mathbf{p}} V_{\mathbf{p}} e^{i\mathbf{p}\cdot\left(\mathbf{r}-\mathbf{R}_j^0\right)} = \frac{1}{\mathcal{V}} \sum_{\substack{\mathbf{k}\in\text{FBZ}\\ \mathbf{G}\in\text{RL}}} V_{\mathbf{k}+\mathbf{G}} e^{i(\mathbf{k}+\mathbf{G})\cdot\left(\mathbf{r}-\mathbf{R}_j^0\right)},$$

where

$$V_{\mathbf{p}} = \int_{\mathcal{V}} d^3\mathbf{r} \left\{ e^{-i\mathbf{p}\cdot\mathbf{r}} V_{ion}(\mathbf{r}) \right\}.$$

The derivative in Eq. (1.30) is computed as

$$\nabla_{\mathbf{r}} V_{ion}(\mathbf{r}-\mathbf{R}_j^0) = \frac{1}{\mathcal{V}} \sum_{\substack{\mathbf{k}\in\text{FBZ}\\ \mathbf{G}\in\text{RL}}} V_{\mathbf{k}+\mathbf{G}}\, i\left(\mathbf{k}+\mathbf{G}\right) e^{i(\mathbf{k}+\mathbf{G})\cdot(\mathbf{r}-\mathbf{R}_j^0)}.$$

Then use the relation in Eq. (1.28):

$$\mathbf{u}_{\mathbf{k}\lambda} \equiv \sqrt{\frac{\hbar}{2M\omega_{\mathbf{k}\lambda}}} \left(b^\dagger_{-\mathbf{k}\lambda} + b_{\mathbf{k}\lambda}\right) \epsilon_{\mathbf{k}\lambda},$$

and compute the sum:

$$\sum_j e \frac{1}{\sqrt{N}} \sum_{\mathbf{k}\in\text{FBZ}} u_{\mathbf{k}} e^{i\mathbf{k}\cdot\mathbf{R}_j^0} = \sum_j e \frac{1}{\sqrt{N}} \sum_{\mathbf{k}\in\text{FBZ}} \sqrt{\frac{\hbar}{2M\omega_{\mathbf{k}\lambda}}} \left(b^\dagger_{-\mathbf{k}\lambda} + b_{\mathbf{k}\lambda}\right) \boldsymbol{\epsilon}_{\mathbf{k}\lambda} e^{i\mathbf{k}\cdot\mathbf{R}_j^0}.$$

We obtain:

$$\frac{1}{\mathcal{V}}\sum_j e\mathbf{u}_j\cdot\nabla_{\mathbf{r}}V_{\text{ion}}\left(\mathbf{r}-\mathbf{R}_j^0\right)=\frac{1}{\mathcal{V}}\sum_j e\frac{1}{\sqrt{N}}\sum_{\mathbf{k}\in\text{FBZ}}\sum_{\substack{\mathbf{q}\in\text{FBZ}\\ \mathbf{G}\in\text{RL}}}\sqrt{\frac{\hbar}{2M\omega_{\mathbf{k}\lambda}}}\times$$

$$\times\left(b^{\dagger}_{-\mathbf{k}\lambda}+b_{\mathbf{k}\lambda}\right)e^{i\mathbf{k}\cdot\mathbf{R}_j^0}\boldsymbol{\epsilon}_{\mathbf{k}\lambda}\cdot V_{\mathbf{k}+\mathbf{G}}\,i\left(\mathbf{q}+\mathbf{G}\right)e^{i(\mathbf{q}+\mathbf{G})\cdot\left(\mathbf{r}-\mathbf{R}_j^0\right)}\qquad(1.32)$$

The exponential term with the sum over j yields

$$\sum_{j=1}^{N}e^{i\mathbf{R}_j^0\cdot(\mathbf{k}-\mathbf{q}-\mathbf{G})}=\sqrt{N}\delta_{\mathbf{k},\mathbf{q}+\mathbf{G}},$$

and summing over $\mathbf{k}$, Eq. (1.32) is rewritten as

$$\sum_j e\mathbf{u}_j\cdot\nabla_{\mathbf{r}}V_{\text{el}}\left(\mathbf{r}-\mathbf{R}_j^0\right)=\frac{1}{V}\sum_{\substack{\mathbf{q}\in\text{FBZ}\\ \mathbf{G}\in\text{RL}\\ \lambda}}M_{\mathbf{q},\mathbf{G},\lambda}\left(b_{\mathbf{q}\lambda}+b^{\dagger}_{-\mathbf{q}\lambda}\right)e^{i(\mathbf{q}+\mathbf{G})\cdot\mathbf{r}},$$

with the *electron-phonon coupling strength* defined as

$$M_{\mathbf{q},\mathbf{G},\lambda}=ie\sqrt{\frac{N\hbar}{2M\omega_{\mathbf{q}\lambda}}}(\mathbf{q}+\mathbf{G})\cdot\boldsymbol{\epsilon}_{\mathbf{q}\lambda}V_{\mathbf{q}+\mathbf{G}}.$$

Finally, we consider in Eq. (1.31) the electron density term. This is written using the number operator as[6]

$$\rho_{el}(\mathbf{r})=\frac{1}{\mathcal{V}}\sum_{\mathbf{k},\mathbf{p},\sigma}e^{-i\mathbf{p}\cdot\mathbf{r}}c^{\dagger}_{\mathbf{k}+\mathbf{p},\sigma}c_{\mathbf{k}\sigma}$$

This term in inserted in Eq. (1.29) and yields

$$\begin{aligned}V_{el-ph}&=\int d^3\mathbf{r}\left\{\frac{1}{\mathcal{V}}\sum_{k,p,\sigma}e^{-i\mathbf{p}\cdot\mathbf{r}}c^{\dagger}_{\mathbf{k}+\mathbf{p},\sigma}c_{\mathbf{k},\sigma}\frac{1}{\mathcal{V}}\sum_{\mathbf{q},\mathbf{G}}M_{\mathbf{q},\mathbf{G},\lambda}\left(b_{\mathbf{q},\lambda}+b^{\dagger}_{-\mathbf{q},\lambda}\right)e^{i(\mathbf{q}+\mathbf{G})\cdot\mathbf{r}}\right\}\\&=\frac{1}{\mathcal{V}}\sum_{\mathbf{k},\mathbf{q},\mathbf{G}}M_{\mathbf{q},\mathbf{G},\lambda}c^{\dagger}_{\mathbf{k}+\mathbf{q}+\mathbf{G},\sigma}c_{\mathbf{k},\sigma}\left(b_{\mathbf{q}\lambda}+b^{\dagger}_{-\mathbf{q}\lambda}\right)\end{aligned}$$

In conclusion, the electron-phonon interaction is written in second quantisation as

$$V_{el-ph}=\frac{1}{\mathcal{V}}\sum_{\mathbf{k}\sigma}\sum_{\mathbf{q}\lambda}\sum_{\mathbf{G}}M_{\mathbf{q},\mathbf{G},\lambda}c^{\dagger}_{\mathbf{k}+\mathbf{q}+\mathbf{G},\sigma}c_{\mathbf{k},\sigma}\left(b_{\mathbf{q}\lambda}+b^{\dagger}_{-\mathbf{q}\lambda}\right).\qquad(1.33)$$

---

[6] To obtain this expression, simply take the Fourier transform of the electron density operator.

The processes where $\mathbf{G} \neq 0$ are called *umklapp* processes and they are often negligible when compared to normal processes ($\mathbf{G} = 0$); this is because the term $V_{\mathbf{q}+\mathbf{G}}$ depends on $\frac{1}{(\mathbf{q}+\mathbf{G})^2}$. For this reason, in this thesis we will consider $\mathbf{G} = 0$. Furthermore, we consider only one phonon mode λ, so the sum over λ is removed as well:

$$V_{el-ph} = \frac{1}{\mathcal{V}} \sum_{\mathbf{k}\sigma} \sum_{\mathbf{q}} M_{\mathbf{q}} c^{\dagger}_{\mathbf{k}+\mathbf{q},\sigma} c_{\mathbf{k}\sigma} \left(b_{\mathbf{q}} + b^{\dagger}_{-\mathbf{q}} \right). \tag{1.34}$$

Green's Functions

2

In this chapter, we introduce the Green's functions, which are the quantity we ultimately aim to calculate through the Diagrammatic Monte Carlo for the Holstein polaron. We start by introducing the interaction representation in Sect. 2.1 and the Dyson series in Sect. 2.2. Sects. 2.3 – 2.5 will give a brief overview of the Green's functions formalism. Finally, Sect. 2.6 will address how to extract observables relevant to the polaron problem from the imaginary-time Green's function. In this chapter, we follow Mahan's notation once again and set $\hbar = 1$ [7].

2.1 Interaction Representation

Before introducing the Green's functions formalism, we turn our attention to three different representations in Quantum Mechanics [7]: *Schrödinger*, *Heisenberg*, and *interaction representation*.

Schrödinger representation. The most common representation when working with a time-independent Hamiltonian is the *Schrödinger representation*:

$$i\hbar \frac{\partial}{\partial t} |\psi(t)\rangle = H |\psi(t)\rangle \implies |\psi(t)\rangle = e^{-\frac{i}{\hbar}Ht} |\psi_0\rangle .$$

Thus, the wave functions $|\psi(t)\rangle$ are time dependent, whereas operators are independent of time[1].

Heisenberg representation. In contrast, the *Heisenberg representation* treats the wave functions as time independent, and the operators as dependent on time. The time evolution of an operator $O(t)$ is given by

$$i\hbar \frac{\partial O(t)}{\partial t} = [O(t), H] \implies O(t) = e^{iHt} O(0) e^{-iHt}.$$

---

[1] Unless the operator explicitly depends on time t. However, in this thesis we will not consider such cases.

Notice how the time dependence of these operators appear to be contrary. However, they actually yield the same physical results. To see this, simply evaluate the matrix element of an operator $O(t)$ between two wave functions $|\psi_1\rangle$ and $|\psi_2\rangle$:

$$\langle\psi_1|O(t)|\psi_2\rangle = \langle\psi_1|e^{\frac{i}{\hbar}Ht}O(0)e^{-\frac{i}{\hbar}Ht}|\psi_2\rangle = \langle\psi_1(t)|O(0)|\psi_2(t)\rangle\,.$$

Because of this, the Heisenberg representation is equivalent to the Schrödinger representation.

Interaction representation. Finally, consider a Hamiltonian of the form:

$$H = H_0 + V,$$

where H_0 is the unperturbed part, which is taken to be exactly solvable, and V contains the interactions. In the *interaction representation*, both the operators and the wave functions are time dependent and are defined as:

$$\hat{O}(t) \equiv e^{iH_0t}Oe^{-iH_0t}, \qquad |\hat{\psi}(t)\rangle \equiv e^{iH_0}e^{-iHt}\,|\psi(t)\rangle\,. \tag{2.1}$$

Note that, in general, $e^{iH_0t}e^{-iHt} \neq e^{iH_0t-iHt}$, as the equality only holds if the operators commute: $[H_0, H] = [H_0, V] = 0$. However, if that is not usually the case. If the operators were to commute, then the problem would be trivial and it would not require the use of many-body theory.

Notation. Let us repeat again a few important remarks about the notation that was used up to to this point and will be used in further chapters. We shall use a common notation in many-body physics that was adopted by Mahan [7]:

- In the Schrödinger representation, the wave function and the operator are denoted by $|\psi(t)\rangle$ and O, respectively.
- In the Heisenberg representation, the wave function and the operator are denoted by $|\psi\rangle$ and $O(t)$, respectively.
- In the interaction picture, the wave function and the operator are denoted by $|\hat{\psi}(t)\rangle$ and $\hat{O}(t)$, respectively.

Lastly, we show that the matrix elements in the interaction representation are equivalent to those of the other representations:

$$\begin{aligned}\left\langle\hat{\psi}_1(t)\middle|\hat{O}(t)\middle|\hat{\psi}_2(t)\right\rangle &= \left\langle\psi_1(0)\middle|e^{iHt}e^{-iH_0t}\left(e^{iH_0t}Oe^{-iH_0t}\right)e^{iH_0t}e^{-iHt}\middle|\psi_2(0)\right\rangle \\ &= \left\langle\psi_1(0)\middle|e^{iHt}O(0)e^{-iHt}\middle|\psi_2(0)\right\rangle \\ &= \langle\psi_1(t)|O(0)|\psi_2(t)\rangle\,.\end{aligned}$$

2.2 Dyson Series

By Eq. (2.1), in the interaction representation the time evolution of an operator is governed by the unperturbed Hamiltonian H_0. We show that the time dependence of the wave functions is given by the interactions [7]:

$$\begin{aligned}\frac{\partial}{\partial t}|\hat{\psi}(t)\rangle &= ie^{iH_0t}\left(H_0 - H\right)e^{-iHt}|\psi(0)\rangle \\ &= -ie^{iH_0t}Ve^{-iHt}|\psi(0)\rangle \\ &= -ie^{iH_0t}Ve^{-iH_0t}\left[e^{iH_0t}e^{-iHt}|\psi(0)\rangle\right] \\ &= -i\hat{V}(t)|\psi\hat{\rangle}(t), \end{aligned} \tag{2.2}$$

This is referred to as *equation of motion*. Next, we define the time-evolution operator.

Definition 2.1 (Time-evolution operator). *The* ***time-evolution operator*** $\hat{U}(t)$ *is defined in the interaction picture as*

$$\hat{U}(t) \equiv e^{iH_0t}e^{-iHt} \implies |\hat{\psi}(t)\rangle = \hat{U}(t)\,|\psi(0)\rangle\,, \tag{2.3}$$

By Eq. (2.2), the equation of motion for the operator $\hat{U}(t)$ is

$$\frac{\partial}{\partial t}\hat{U}(t) = -i\hat{V}(t)\hat{U}(t) \implies \hat{U}(t) = 1 - i\int_0^t dt_1\hat{V}(t_1)\hat{U}(t_1). \tag{2.4}$$

This is a recursive relation, i.e. we write $\hat{U}(t_1)$ as

$$\hat{U}(t_1) = 1 - i\int_0^{t_1} dt_2\hat{V}(t_2)\hat{U}(t_2),$$

and replace into Eq. (2.4):

$$\hat{U}(t) = 1 - i\int_0^t dt_1\hat{V}(t_1) + (-i)^2\int_0^t dt_1\int_0^{t_1} dt_2\hat{V}(t_2)\hat{U}(t_2).$$

By iterating this process repeatedly, we find

$$\begin{aligned}\hat{U}(t) &= 1 - i\int_0^t dt_1\,\hat{V}(t_1) + (-i)^2\int_0^t dt_1\int_0^{t_1} dt_2\,\hat{V}(t_1)\hat{V}(t_2) + \cdots \\ &= \sum_{n=0}^{\infty}(-i)^n\int_0^t dt_1\int_0^{t_1} dt_2\cdots\int_0^{t_{n-1}} dt_n\,\hat{V}(t_1)\hat{V}(t_2)\ldots\hat{V}(t_n)\end{aligned} \tag{2.5}$$

Time-ordering operator. Next, we introduce the *time-ordering operator* $\mathcal{T}$, whose action on a group of time-dependent operator is to arrange them by placing the earliest times to the right. For example, suppose that $t_1 > t_2 > t_3$, we have

$$\mathcal{T}V(t_2)V(t_3)V(t_1) = V(t_1)V(t_2)V(t_3).$$

If the operators upon which $\mathcal{T}$ acts are fermionic, then by the anticommutation rule in Eq. (1.8) the expression must be multiplied by -1.

Notation. When considering a group of operators upon which $\mathcal{T}$ acts, we omit the parenthesis. For example, by notation

$$\mathcal{T}ABC$$

we are referring to

$$\mathcal{T}\left(ABC\right).$$

Eq. (2.5) can be rewritten using $\mathcal{T}$ as follows. Consider the integral

$$\frac{1}{2!}\int_0^t dt_1\int_0^t dt_2\mathcal{T}\hat{V}(t_1)\hat{V}(t_2) =$$
$$= \frac{1}{2!}\int_0^t dt_1\int_0^{t_1} dt_2\hat{V}(t_1)\hat{V}(t_2) + \frac{1}{2!}\int_0^t dt_2\int_0^{t_2} dt_2\hat{V}(t_2)\hat{V}(t_1),$$

the second term in the RHS is the same as the first (simply swap integration variables t_1 and t_2). Thus, the $n = 2$ term in Eq. (2.5) is rewritten as

$$\int_0^t dt_1\int_0^{t_1} dt_2\hat{V}(t_1)\hat{V}(t_2) = \frac{1}{2!}\int_0^t dt_1\int_0^t dt_2\mathcal{T}\hat{V}(t_1)\hat{V}(t_2).$$

It can be shown similarly that this is true for any number n of operators. Therefore, Eq. (2.5) is rewritten as

$$\hat{U}(t) = 1 + \sum_{n=1}^{\infty}\frac{(-i)^n}{n!}\int_0^t dt_1\int_0^t dt_2\cdots\int_0^t dt_n\mathcal{T}\left[\hat{V}\left(t_1\right)\hat{V}\left(t_2\right)\cdots\hat{V}\left(t_n\right)\right], \qquad (2.6)$$

which is known as *Dyson series*. It is often abbreviated as

$$\hat{U}(t) = \mathcal{T}\exp\left[-i\int_0^t dt_1\hat{V}(t_1)\right],$$

which is just an alternative notation to represent the series in Eq. (2.6).

S-matrix operator. Similarly to how we defined $\hat{U}(t)$, we now define the *S-matrix* operator.

Definition 2.2 (S-matrix)**.** *The* ***S-matrix*** *is defined as the operator that evolves* $|\hat{\psi}(t')\rangle$ *from* t' *to* t

$$\hat{\psi}(t) = S(t,t')\hat{\psi}(t').$$

We can find an expression for $S(t,t')$ in terms of the operator $\hat{U}(t)$:

$$\hat{\psi}(t) = \hat{U}(t)\hat{\psi}(0) = S(t,t')\hat{U}(t')\hat{\psi}(0),$$

which implies

$$S(t,t') = \hat{U}(t)\hat{U}^{\dagger}(t').$$

2.3 Real-Time Green's Functions

2.3.1 Electron Green's Function

Let us now state the definition of the electron real-time Green's function at zero temperature [7].

Definition 2.3 (Electron Green's function at zero temperature)**.** *The* ***electron Green's function at zero temperature*** *is defined in the Heisenberg representation as*

$$G(\lambda, t-t') = -i\,\langle|\, \mathcal{T} c_{\lambda}(t) c_{\lambda}^{\dagger}(t')\,|\rangle\,, \tag{2.7}$$

In particular, the operator $c_{\lambda}^{\dagger}(t)$ is the electron's creation operator in the Heisenberg representation for some quantum numbers λ (e.g. $\lambda = (\mathbf{p},\sigma)$). $|\rangle$ is the ground state of the Hamiltonian $H = H_0 + V$. Since we are using the Heisenberg representation, $|\rangle$ is independent of time, whereas the operator $c_{\lambda}(t)$ is given by

$$c_{\lambda}(t) = e^{iHt} c_{\lambda} e^{-iHt}.$$

We now use the notation $\langle| \ldots |\rangle$ to differentiate from $\langle \ldots \rangle$: the latter will be employed later as the thermodynamic average.

Now consider $t > t'$: Eq. (2.7) becomes

$$G(\lambda, t-t') = -i\,\langle|\, c_{\lambda}(t) c_{\lambda}^{\dagger}(t')\,|\rangle\,,$$

which can be seen as taking the ground state $|\rangle$, creating an excitation λ at time t', and later destroying such excitation at time t. Suppose now that $t' > t$ instead; in this case, the Green's function is

$$G(\lambda, t' > t) = i \langle | \, c^\dagger_\lambda(t') c_\lambda(t) \, | \rangle \,,$$

which is interpreted as the destruction of an electron in the state λ at time t and the creation of that same state at a later time t'. Note that this is only possible if $|\rangle$ contains an electron in the state λ at the initial time t.

2.3.2 Phonon Green's Function

Consider now the electron-phonon interaction as defined in Eq. (1.33). The operators $A_{\mathbf{q}\lambda}$ and $A^\dagger_{\mathbf{q}\lambda}$ are defined as [7]:

$$A_{\mathbf{q}\lambda} \equiv \left(b_{\mathbf{q}\lambda} + b^\dagger_{-\mathbf{q}\lambda} \right), \qquad A^\dagger_{\mathbf{q}\lambda} \equiv \left(b^\dagger_{\mathbf{q}\lambda} + b_{-\mathbf{q}\lambda} \right).$$

$A_{\mathbf{q}\lambda}$ can be thought of as the operator removing $\mathbf{q}$; this can be done either by annihilating a phonon of momentum $\mathbf{q}$ through $b_{\mathbf{q}}$ or by creating a phonon of opposite momentum $-\mathbf{q}$ through $b^\dagger_{-\mathbf{q}}$. Similarly, $A^\dagger_{\mathbf{q}\lambda}$ is seen as the operator that adds $\mathbf{q}$, and that is done by creating a phonon of momentum $-\mathbf{q}$ or destroying one of momentum $\mathbf{q}$.

Definition 2.4 (Phonon Green's Function). *The* ***phonon Green's function at zero temperature*** *is defined in the Heisenberg representation as*[2]

$$D(\mathbf{q}, t - t') \equiv -i \langle | \, \mathcal{T} A_{\mathbf{q}}(t) A_{-\mathbf{q}}(t') \, | \rangle \,,$$

2.4 Matsubara Green's Function

2.4.1 Definition

In this section, we aim to introduce the effects of temperature in the Green's functions formalism. We will work in the grand-canonical ensemble and use the Hamiltonian [14]:

$$\bar{H} \equiv H - \mu N = \bar{H}_0 + V$$

and

$$\bar{H}_0 = H_0 - \mu N,$$

---

[2] From now on we ignore the polarization λ of the phonons.

where μ is the chemical potential and N the number of particles. The Hamiltonians under consideration usually have the property that they commute with the number operator, that is

$$[H_0, N] = 0,$$
$$[H, N] = 0.$$

It is therefore possible to define simultaneous eigenstates of H_0 and N, as well of H and N. We now call $\bar{H}_0$, defined as above, the non-interacting problem, which is then affected by the perturbation V. Once again, we suppose that the non-interacting problem H_0 is fully solvable, so that by extent $\bar{H}_0$ is as well.

We may now introduce the effects of temperature in real time by redefining Eq. (2.7) as an average over the grand-canonical ensemble. That is indeed what we will do in Sect. 4.3. However, the thermal average requires the introduction of the factor $e^{-\beta \bar{H}}$ in the numerator of Eq. (2.7), whereas the operators $c^\dagger(t)$ evolves according to $e^{\pm i\bar{H}t}$. This mismatch in the exponents, one real and one imaginary, renders the perturbation theory that we will soon see a difficult task. It is easier to work in imaginary time, by substituting $it \to \tau$. As for the real time, we define an imaginary-time Heisenberg picture as

$$O(\tau) = e^{\tau \bar{H}} O e^{-\tau \bar{H}},$$

and the interaction representation as

$$\hat{O}(\tau) = e^{\tau \bar{H}_0} O e^{-\tau \bar{H}_0}. \tag{2.8}$$

$\hat{U}(t)$ can easily be generalised to the imaginary-time version:

$$\hat{U}(\tau) = e^{\tau \bar{H}_0} e^{-\tau \bar{H}}. \tag{2.9}$$

After introducing the imaginary time τ and the grand-canonical Hamiltonian $\bar{H}$, we may now define the *Matsubara Green's function*.

Definition 2.5 (Matsubara Green's function for the electron). *The* ***Matsubara*** *or* ***imaginary-time Green's function*** *for the electron is defined in the Heisenberg representation as*

$$\mathcal{G}(\lambda, \tau, \tau') \equiv -\left\langle \mathcal{T}_\tau c_\lambda(t) c_\lambda^\dagger(t') \right\rangle. \tag{2.10}$$

The notation[3] $\langle A \rangle$ is now used to refer to the thermodynamic average of an operator A. $\mathcal{T}_\tau$ is the imaginary time-ordering operator, and acts identically to the real time-ordering operator $\mathcal{T}$. Eq. (2.10) is then written as the trace

$$\mathcal{G}(\lambda,\tau,\tau') = -\frac{1}{Z}\mathrm{Tr}\left(e^{-\beta\bar{H}}\mathcal{T}_\tau e^{\tau\bar{H}}\hat{c}_\lambda e^{-(\tau-\tau')\bar{H}}\hat{c}_\lambda^\dagger e^{-\tau'\bar{H}}\right), \tag{2.11}$$

where Z is the grand-canonical partition function:

$$Z = \mathrm{Tr}\left[e^{-\beta\bar{H}}\right].$$

2.4.2 Properties

It is easy to show[4] that the Matsubara Green's function only depends on the time difference $\tau-\tau'$ and that $\beta \leq \tau \leq \beta$. As a consequence, we can set $\tau'=0$ and study

$$\mathcal{G}(\lambda,\tau) = -\left\langle \mathcal{T}_\tau c_\lambda(\tau)c_\lambda^\dagger\right\rangle \qquad \text{with} \qquad \beta \leq \tau \leq \beta \tag{2.12}$$

By using the cyclic property of the trace, we can show that the Matsubara Green's function is periodic (aperiodic) for bosons (fermions) in the imaginary time:

$$\mathcal{G}(\lambda,\tau) = \pm\mathcal{G}(\lambda,\tau-\beta). \tag{2.13}$$

We make use of this property and use the formalism of discrete Fourier transform to expand the Matsubara Green's function in terms of discrete frequencies:

$$\mathcal{G}(\lambda,\tau) = \frac{1}{\beta}\sum_{n=-\infty}^{+\infty} e^{-i\omega_n\tau}\mathcal{G}(\lambda,i\omega_n).$$

We then impose the constraint in Eq. (2.13) to find that

$$e^{-i\omega_n\tau} = \pm e^{-i\omega_n(\tau-\beta)} \implies e^{i\omega_n\beta} = \pm 1,$$

which implies

$$\omega_n = \begin{cases} 2n\pi/\beta & n\in\mathbb{Z} \quad \text{for bosons,} \\ (2n+1)\pi/\beta & n\in\mathbb{Z} \quad \text{for fermions.}\end{cases}$$

ω_n are know known as *Matsubara frequencies*. The inverse transformation is

$$\mathcal{G}(\lambda,i\omega_n) = \frac{1}{2}\int_{-\beta\hbar}^{\beta\hbar} e^{i\omega_n\tau}\mathcal{G}(\lambda,\tau)\,d\tau.$$

---

[3] This is different from the notation $\langle| A |\rangle$ used before, which simply denoted the term $\langle\psi| A |\psi\rangle$.

[4] See [14] for a detailed proof.

2.4.3 Green's Functions and the U-operator

We now take the wave vector $\mathbf{k}$ and the spin index σ as the quantum numbers, i.e. $\lambda = (\mathbf{k}, \sigma)$. Consider the Matsubara Green's function for the electron:

$$\mathcal{G}(\mathbf{k}\sigma, \tau) = -\frac{1}{Z}\mathrm{Tr}\left[e^{-\beta\bar{H}}\mathcal{T}_\tau e^{\tau\bar{H}} c_{\mathbf{k}\sigma} e^{-\tau\bar{H}} c^\dagger_{\mathbf{k}\sigma}\right], \tag{2.14}$$

with

$$\bar{H} = \bar{H}_0 + V = H_0 - \mu N + V,$$

and the partition function

$$Z = \mathrm{Tr}\left[e^{-\beta\bar{H}}\right].$$

Then we consider the $\hat{U}$ operators in the interaction representation:

$$\hat{U}(\tau) = e^{\tau\bar{H}_0}e^{-\tau\bar{H}}, \qquad \hat{U}^{-1}(\tau) = e^{\tau\bar{H}}e^{-\tau\bar{H}_0}.$$

The creation and annihilation operators are written in the interaction representation as in Eq. (2.8):

$$\hat{c}_{\mathbf{k}\sigma}(\tau) = e^{\tau\bar{H}_0}c_{\mathbf{k}\sigma}e^{-\tau\bar{H}_0}.$$

Eq. (2.14) is then written for $\tau > 0$ as

$$\begin{aligned}\mathcal{G}(\mathbf{k}\sigma, \tau) &= -\frac{\mathrm{Tr}\left[e^{-\beta\bar{H}_0}e^{\beta\bar{H}_0}e^{-\beta\bar{H}}e^{\tau\bar{H}}e^{-\tau\bar{H}_0}e^{\tau\bar{H}_0}c_{\mathbf{k}\sigma}e^{-\tau\bar{H}_0}e^{\tau\bar{H}_0}e^{-\tau\bar{H}}c^\dagger_{\mathbf{k}\sigma}\right]}{\mathrm{Tr}\left[e^{-\beta\bar{H}_0}e^{\beta\bar{H}_0}e^{-\beta\bar{H}}\right]} \\ &= -\frac{\mathrm{Tr}\left[e^{-\beta\bar{H}_0}\hat{U}(\beta)\hat{U}^{-1}(\tau)\hat{c}_{\mathbf{k}\sigma}(\tau)\hat{U}(\tau)\hat{c}^\dagger_{\mathbf{k}\sigma}\right]}{\mathrm{Tr}\left[e^{-\beta\bar{H}_0}\hat{U}(\beta)\right]},\end{aligned} \tag{2.15}$$

where we used the cyclical property of the trace and the identity $1 = e^{\alpha}e^{-\alpha}$. The operator $\hat{U}(\beta)$ is then solved in terms of the τ-ordered products. The *equation of motion* is

$$\begin{aligned}&\frac{\partial}{\partial\tau}\hat{U}(\tau) = e^{\tau\bar{H}_0}\left(\bar{H}_0 - \bar{H}\right)e^{-\tau\bar{H}} = -e^{\tau\bar{H}_0}Ve^{-\tau\bar{H}} = -e^{-\tau\bar{H}_0}Ve^{-\tau\bar{H}_0}e^{\tau\bar{H}_0}e^{-\tau\bar{H}} \\ &\frac{\partial}{\partial\tau}\hat{U}(\tau) = -\hat{V}(\tau)\hat{U}(\tau),\end{aligned}$$

which is then formally solved as was done in Sect. 2.2, with minor changes:

$$\begin{aligned}\hat{U}(\tau) &= \sum_{n=0}^{\infty}\frac{(-1)^n}{n!}\int_0^\tau d\tau_1\int_0^\tau d\tau_2\cdots\int_0^\tau d\tau_n\mathcal{T}_\tau\hat{V}(\tau_1)\hat{V}(\tau_2)\ldots\hat{V}(\tau_n) = \\ &= \mathcal{T}_\tau\exp\left[-\int_0^\tau d\tau_1\hat{V}(\tau_1)\right].\end{aligned}$$

Next, the S-matrix in imaginary time is

$$S(\tau_1, \tau_2) = \mathcal{T}_\tau \exp\left[-\int_{\tau_1}^{\tau_2} d\tau \hat{V}(\tau)\right],$$

which implies the usual relations:

$$S(\tau_2, \tau_1) = \hat{U}(\tau_2)\hat{U}^{-1}(\tau_1), \quad S(\tau_3, \tau_2)S(\tau_2, \tau_1) = S(\tau_3, \tau_1).$$

Also, we denote $S(\tau) \equiv S(\tau, 0) = U(\tau)$. Finally, these equations are inserted into (2.15) to produce the result

$$\mathcal{G}(\mathbf{k}\sigma, \tau) = -\frac{\mathrm{Tr}\left[e^{-\beta\bar{H}_0}\mathcal{T}_\tau S(\beta, \tau)\hat{c}_{\mathbf{k}\sigma}(\tau)S(\tau)\hat{c}^\dagger_{\mathbf{k}\sigma}(0)\right]}{\mathrm{Tr}\left[e^{-\beta\bar{H}_0}S(\beta)\right]} \tag{2.16}$$

Then, we define the average over the non-interacting state energies as

$$\langle A\rangle_0 \equiv \mathrm{Tr}\left[Ae^{-\beta\bar{H}_0}\right],$$

and Eq. (2.16) is written more compactly as

$$\mathcal{G}(\mathbf{k}\sigma, \tau) = -\frac{\left\langle \mathcal{T}_\tau S(\beta)\hat{c}_{\mathbf{k}\sigma}(\tau)\hat{c}^\dagger_{\mathbf{k}\sigma}(0)\right\rangle_0}{\langle S(\beta)\rangle_0} \tag{2.17}$$

Finally, let us mention that a similar expression can be derived for the real-time Green's function at zero temperature. The procedure is similar, but particular care is required to bridge the non-interacting and the interacting states. The necessary result is from the Gell-Mann and Low theorem [15]. The Green's function is found to be:

$$G(\lambda, t - t') = -i\frac{\langle |_0\, \mathcal{T}\hat{c}_\lambda(t)\hat{c}^\dagger_\lambda(t')S(\infty, -\infty)\, |\rangle_0}{\langle |_0\, \mathcal{T}S(\infty, -\infty)\, |\rangle_0}.$$

2.4.4 Free Propagators

An important result that we will use in the diagrammatic expansion is the Green's function for the free electron $\mathcal{G}(\mathbf{k}, \theta)$. In this case, the interaction term V is zero, hence the S-matrix operator is the identity. Eq. (2.17) becomes [14]:

$$\begin{aligned}
\mathcal{G}^0(\mathbf{k}\sigma, \tau) &= -\langle \mathcal{T}c_{\mathbf{k}\sigma}(\tau)c^\dagger_{\mathbf{k}\sigma}(0)\rangle_0 \\
&= -\theta(\tau)\langle c_{\mathbf{k}\sigma}(\tau)c^\dagger_{\mathbf{k}\sigma}(0)\rangle_0 + \theta(-\tau)\langle c^\dagger_{\mathbf{k}\sigma}(0)c_{\mathbf{k}\sigma}(\tau)\rangle_0 \\
&= \left[-\theta(\tau)\langle c_{\mathbf{k}\sigma}(0)c^\dagger_{\mathbf{k}\sigma}(0)\rangle_0 + \theta(-\tau)\langle c^\dagger_{\mathbf{k}\sigma}(0)c_{\mathbf{k}\sigma}(0)\rangle_0\right] e^{-\bar{\varepsilon}_{\mathbf{k}\sigma}\tau/\hbar} \\
&= \left[-\theta(\tau)(1 - n_f(\bar{\varepsilon}_{\mathbf{k}\sigma}) + \theta(-\tau)n_f(\bar{\varepsilon}_{\mathbf{k}\sigma})\right] e^{-\bar{\varepsilon}_{\mathbf{k}\sigma}\tau},
\end{aligned}$$

where $\theta(\tau)$ is the step function, and $n_f(\bar{\varepsilon}_{\mathbf{k}\sigma})$ is the Fermi-Dirac distribution. In this thesis, we are interested in the zero-temperature limit $T \to 0$. With similar calculations for the bosonic case we find the *electron* and *boson* free propagators at zero temperature[5]:

$$\mathcal{G}_0(\mathbf{k},\tau) = -e^{-\varepsilon_{\mathbf{k}}\tau} \qquad \text{if } \tau > 0, \tag{2.18}$$

$$\mathcal{D}_0(\mathbf{q},\tau) = -e^{-\omega_{\mathbf{q}}\tau} \qquad \text{if } \tau > 0. \tag{2.19}$$

2.5 Retarded Green's Function

The retarded Green's functions are particularly important in the nonzero-temperature theory [14]: all measurable quantities, such as conductivities, are retarded correlation functions. For the scope of this thesis, here we just give some brief results that will be used later.

Definition 2.6 (Unperturbed Green's function)**.** *The* ***retarded Green's function*** *is defined in the Heisenberg representation as*

$$G^R(\mathbf{k}\sigma,t) = -i\theta(t)\left\langle\left[c_{\mathbf{k}\sigma}(t), c^\dagger_{\mathbf{k}\sigma}(0)\right]\right\rangle \tag{2.20}$$

where $[A,B]$ is the commutator (anti-commutator) for bosons (fermions), $\langle\dots\rangle$ is the thermodynamic average, and $\theta(t)$ is the step function.

An important observable is the *spectral density function* $A(\mathbf{k}\sigma,\omega)$, which gives information about the distribution of the energies of the system. It can be shown that:

$$G^R(\mathbf{k}\sigma,\omega) = \lim_{\eta\to 0^+}\int_{-\infty}^{\infty}\frac{A(\mathbf{k}\sigma,\epsilon)}{\omega-\epsilon+i\eta}\frac{d\epsilon}{2\pi},$$

which implies:

$$A(\mathbf{k}\sigma,\omega) = -2\,\mathrm{Im}\,G^R(\mathbf{k}\sigma,\omega). \tag{2.21}$$

2.6 Ground-State Energy and Quasiparticle Weight

We now introduce a new observable that we may infer from the Green's function [16]. Let us consider a set of orthonormal eigenstates $\psi_{\mathbf{k}}$ such that $H\left|\psi_{\mathbf{k}}\right\rangle = \varepsilon_{\mathbf{k}}\left|\psi_{\mathbf{k}}\right\rangle$.

---

[5] Setting $\mu = 0$ and suppressing the spin indexes.

Then the Matsubara Green's function in Eq. (2.11) is taken in the zero temperature limit and rewritten using the completeness relation [16]:

$$\begin{aligned}
\mathcal{G}(\mathbf{k},\tau) &= -\left\langle \psi_0 \mid c_{\mathbf{k}}(\tau) c_{\mathbf{k}}^{\dagger}(0) \mid \psi_0 \right\rangle \\
&= -\sum_{\mathbf{p}} \left\langle \psi_0 \mid e^{H\tau} c_{\mathbf{k}}(0) e^{-H\tau} \mid \psi_{\mathbf{p}} \right\rangle \left\langle \psi_{\mathbf{p}} \mid c_{\mathbf{k}}^{\dagger}(0) \mid \psi_0 \right\rangle \\
&= -\sum_{\mathbf{p}} e^{-\varepsilon_{\mathbf{p}}\tau} \left| \left\langle \psi_{\mathbf{p}} \mid c_{\mathbf{k}}^{\dagger}(0) \mid \psi_0 \right\rangle \right|^2
\end{aligned}$$

For each excited state we may define the *quasiparticle weight* as

$$Z_0(\mathbf{k}) \equiv \left| \left\langle \psi_0 \mid c_{\mathbf{k}} \mid \psi_{\mathbf{p}} \right\rangle \right|^2 = \left| \left\langle \psi_{\mathbf{p}} \mid c_{\mathbf{k}}^{\dagger} \mid \psi_0 \right\rangle \right|^2$$

We take the limit $\tau \to \infty$ and the dominant term is the first excited state with nonzero matrix element, say $|\psi_{\mathbf{q}}\rangle$. Thus:

$$\mathcal{G}(\mathbf{k},\tau) \xrightarrow{\tau\to\infty} \left| \left\langle \psi_0 \mid c_{\mathbf{k}} \mid \psi_{\mathbf{q}} \right\rangle \right|^2 e^{-\varepsilon_{\mathbf{k}}^0 \tau} = Z_{0,\mathrm{GS}}(\mathbf{k})\, e^{-\varepsilon_{\mathbf{k}}^0 \tau}$$

By taking the limit, we have selected the lowest excited energy $\varepsilon_{\mathbf{k}}^0$. The quasiparticle weight $Z_{0,\mathrm{GS}}(\mathbf{k})$ quantifies how much the first excited state resembles a free particle, measuring the overlap between the interacting state and the bare-electron state.

Let us make a few clarifications in the case of our interest: an interaction between the electron and the phonons. By knowing the Green's function limit for $\tau \to \infty$ we can therefore determine the quasiparticle weight $Z_{0,GS}(\mathbf{k})$ as well as the ground-state energy of the polaron E_{GS}. When $Z_{0,GS} = 1$, the overlap between the state with one free electron and the particle state is maximum: hence, the particle behaves like a free electron. Conversely, when $Z_{0,GS} = 0$, the particle loses its bare-electron behaviour and is in fact a polaron, which is a bound state of the electron and the phonon cloud.

Feynman Diagrams

3

Feynman introduced in 1949 the idea of representing Green's functions (GF) through series of diagrams [17]. Since then, this approach have become a standard tool in quantum field theory and many body physics for studying perturbative expansions. Essentially, Feynman diagrams allow to visualise each term of the perturbative expansion of the GF through a graphical representation, where each line represents a specific free propagator and each vertex represents an interaction. The theoretical justification of this approach is based on *Wick's theorem*, whose main result is that the GF of a many-body system can be written as a sum of products of free GFs. Each of these product is translated into a diagram.

We begin this chapter with a summary of the Wick's theorem in Sect. 3.1, then we show how to use it to expand the electron-phonon interaction in Sect. 3.2. In Sect. 3.3 we prove an important theorem, called *cancellation theorem*, which greatly simplifies the evaluation of diagrams. Finally, in Sect. 3.4 we collect all the results previously obtained in a series of ready-to-use rules for drawing Feynman diagrams.

3.1 Wick's Theorem

In Sect. 2.4, we wrote the expression for the imaginary-time Green's function $\mathcal{G}(\mathbf{k}\sigma,\tau)$ using the non-interacting states. Using the Dyson series of the S-matrix operator (Eq. (2.6)), we rewrite the numerator of the GF as

$$\begin{aligned}&\left\langle \mathcal{T}_\tau S(\beta)\hat{c}_{\mathbf{k}\sigma}(\tau)\hat{c}^\dagger_{\mathbf{k}\sigma}(0)\right\rangle_0 \\ &\quad = -\sum_{n=0}^{\infty}\frac{(-1)^n}{n!}\int_0^\beta d\tau_1\dots\int_0^\beta d\tau_n \left\langle \mathcal{T}_\tau \hat{c}_{\mathbf{k}\sigma}(\tau)\hat{V}(\tau_1)\cdots\hat{V}(\tau_n)\,\hat{c}^\dagger_{\mathbf{k}\sigma}(0)\right\rangle_0 . \qquad (3.1)\end{aligned}$$

However, Eq. (3.1) does not really tell us how to calculate the GF: we still do not know how to evaluate $\langle\dots\rangle_0$, which is a thermal average over the non-interacting states. Using Wick's theorem, it is possible to expand it in terms of the free GFs in Eqs. (2.18) and (2.19). Let us first define the *contraction* of two operators [14].

Definition 3.1 (Contraction). *Let $\hat{A}$ and $\hat{B}$ be two operators in the interaction picture. Their **contraction** is defined as*

$$\wick{\c{\hat{A}}\c{\hat{B}}} = \langle \mathcal{T}\hat{A}\hat{B}\rangle_0 ,$$

If $\hat{A}, \hat{B}, \hat{C}, \hat{D}$ are fermionic operators, a term such as $\wick{\c1{\hat{A}}\c2{\hat{B}}\c1{\hat{C}}\c2{\hat{D}}}$ is to be interpreted as $-\wick{\c{\hat{A}}\c{\hat{C}}\c{\hat{B}}\c{\hat{D}}}$, because $\hat{B}$ and $\hat{C}$ need to be interchanged. From the definition, we see that (suppose $\tau > \tau'$)

$$\wick{\c{\hat{c}_{\mathbf{k}}(\tau)}\c{\hat{c}^{\dagger}_{\mathbf{k}}}}(\tau') = \langle \mathcal{T}_\tau \hat{c}_{\mathbf{k}}(\tau)\hat{c}^{\dagger}_{\mathbf{k}}(\tau')\rangle_0 = -\mathcal{G}_0(\mathbf{k}, \tau - \tau') \tag{3.2}$$

Let us now state Wick's theorem [18].

Theorem 3.1 (Wick's theorem). *The ensemble average over a noninteracting system of the time-ordered product of interaction picture operators is equal to the sum over all possible contracted pairs:*

$$\langle \mathcal{T}\hat{A}\hat{B}\hat{C}\hat{D}\rangle_0 = \wick{\c{\hat{A}}\c{\hat{B}}\c{\hat{C}}\c{\hat{D}}}\cdots + \wick{\c1{\hat{A}}\c2{\hat{B}}\c1{\hat{C}}\c2{\hat{D}}}\cdots + \wick{\c1{\hat{A}}\c2{\hat{B}}\c2{\hat{C}}\c1{\hat{D}}}\cdots + \ldots$$

A alternative statement of Wick's theorem is as follows. Let $\hat{a}_1, \hat{a}_2, \ldots, \hat{a}_{2n}$ be operators in the interaction picture. Then,

$$\left\langle \mathcal{T}\prod_{i=1}^{2n}\hat{a}_i \right\rangle_0 = \sum_{\pi\in\mathcal{P}_{2n}} \operatorname{sgn}(\pi) \prod_{k=1}^{n} \left\langle \mathcal{T}\hat{a}_{\pi(2k-1)}\hat{a}_{\pi(2k)} \right\rangle_0 \tag{3.3}$$

where the sum is over all pairwise partitions π of the set $\{1, 2, \ldots, 2n\}$, and $\operatorname{sgn}(\pi)$ is the sign of the permutation required to bring the operators into the order specified by the pairing. For bosons, $\operatorname{sign}(\pi)$ is always $+1$; for fermions, $\operatorname{sign}(\pi)$ is $+1$ if π is an even permutation, -1 if it is odd.

Basically, Wick's theorem states that we need to sum over all possible ways of pairing the operators in the time-ordered product, and for each possible way of pairing we calculate the product of the expectation values of each pair. For each partition, if we are working with fermionic operators, we need to account for the sign of the permutation required to bring the operators into the order specified by the pairing. For instance, suppose we need to evaluate the ensemble average of 4 *fermionic* operators:

$$\langle \mathcal{T}\hat{A}\hat{B}\hat{C}\hat{D}\rangle_0 = \langle \mathcal{T}\hat{A}\hat{B}\rangle_0 \langle \mathcal{T}\hat{C}\hat{D}\rangle_0 - \langle \mathcal{T}\hat{A}\hat{C}\rangle_0 \langle \mathcal{T}\hat{B}\hat{D}\rangle_0 + \langle \mathcal{T}\hat{A}\hat{D}\rangle_0 \langle \mathcal{T}\hat{B}\hat{C}\rangle_0 . \tag{3.4}$$

Because of Eq. (3.2), if the operators are $\hat{c}^\dagger_{\mathbf{q}}$ and $\hat{c}^\dagger_{\mathbf{q}}$, then Eq. (3.4) is actually a sum of products of free propagators, which we can easily calculate.

3.2 Diagrammatic Expansion of the Electron-Phonon Interaction

Let us recall the GF that was previously evaluate in Eq. (2.17):

$$\mathcal{G}(\mathbf{k}\sigma,\tau) = -\frac{\left\langle \mathcal{T}_\tau S(\beta)\hat{c}_{\mathbf{k}\sigma}(\tau)\hat{c}^\dagger_{\mathbf{k}\sigma}(0)\right\rangle_0}{\langle S(\beta)\rangle_0}. \tag{3.5}$$

We take the interaction $\hat{V}(\tau)$ to be the electron-phonon interaction, which was evaluated in Eq. (1.34):

$$\hat{V}(\tau) = \sum_{\mathbf{q}\mathbf{k}s} M_{\mathbf{q}}\hat{A}_{\mathbf{q}}(\tau)\hat{c}^\dagger_{\mathbf{k}+\mathbf{q},s'}(\tau)\hat{c}_{\mathbf{k}s}(\tau).$$

We take the first two orders of the Dyson series in Eq. (3.1) and write the GF as[1]:

$$\begin{aligned}
&\mathcal{G}\left(\mathbf{p}\sigma,\tau-\tau'\right) \\
&\quad= \mathcal{G}^{(0)}\left(\mathbf{p},\tau-\tau'\right) + (-1)^2\int_0^\beta d\tau_1 \left\langle \mathcal{T}_\tau \hat{c}_{\mathbf{p}\sigma}(\tau)\hat{V}\left(\tau_1\right)\hat{c}^\dagger_{\mathbf{p}\sigma}\left(\tau'\right)\right\rangle_0 + \\
&\qquad + \frac{(-1)^3}{2!}\int_0^\beta d\tau_1 \int_0^\beta d\tau_2 \left\langle \mathcal{T}_\tau \hat{c}_{\mathbf{p}\sigma}(\tau)\hat{V}\left(\tau_1\right)\hat{V}\left(\tau_2\right)\hat{c}^\dagger_{\mathbf{p}\sigma}\left(\tau'\right)\right\rangle_0
\end{aligned} \tag{3.6}$$

The first term, at the 0-th order, is the free electron GF. The term at the first order is cancelled out because it contains an odd number of phonon operators $\hat{A}_{\mathbf{q}}$, so we only need to evaluate the second integral:

$$\begin{aligned}
&\left\langle \mathcal{T}_\tau \hat{c}_{\mathbf{p}\sigma}(\tau)\hat{V}\left(\tau_1\right)\hat{V}\left(\tau_2\right)\hat{c}^\dagger_{\mathbf{p}\sigma}\left(0\right)\right\rangle_0 = \sum_{\substack{\mathbf{q}_1,\mathbf{q}_2\\ \mathbf{k}_1,\mathbf{k}_2\\ s,s'}} M_{\mathbf{q}_1}M_{\mathbf{q}_2}\times \\
&\quad\times \left\langle \mathcal{T}_\tau \hat{c}_{\mathbf{p}\sigma}(\tau)\hat{A}_{\mathbf{q}_1}(\tau_1)\hat{c}^\dagger_{\mathbf{k}_1+\mathbf{q}_1,s}(\tau_1)\hat{c}_{\mathbf{k}_1 s}(\tau_1)\hat{A}_{\mathbf{q}_2}(\tau_2)\hat{c}^\dagger_{\mathbf{k}_2+\mathbf{q}_2,s'}(\tau_2)\hat{c}_{\mathbf{k}_2 s'}(\tau_2)\hat{c}^\dagger_{\mathbf{p}\sigma}(0)\right\rangle_0
\end{aligned}$$

---

[1] Let us ignore the denominator for now: it will be evaluated later.

$$
\begin{aligned}
\sum_{\substack{\mathbf{q}_1,\mathbf{q}_2\\ \mathbf{k}_1,\mathbf{k}_2}} M_{\mathbf{q}_1} M_{\mathbf{q}_2} \left\langle \mathcal{T}_\tau \hat{A}_{\mathbf{q}_1}\left(\tau_1\right) \hat{A}_{\mathbf{q}_2}\left(\tau_2\right) \right\rangle_0 &= \sum_{\substack{\mathbf{q}_1,\mathbf{q}_2\\ \mathbf{k}_1,\mathbf{k}_2}} M_{\mathbf{q}_1} M_{\mathbf{q}_2}\, \delta_{\mathbf{q}_1,-\mathbf{q}_2}\, \mathcal{D}_0\left(\mathbf{q}_1, \tau_1 - \tau_2\right) \\
&= \sum_{\substack{\mathbf{k}_1,\mathbf{k}_2\\ \mathbf{q}_1}} M_{\mathbf{q}_1} M_{-\mathbf{q}_1}\, \mathcal{D}_0\left(\mathbf{q}_1, \tau_1 - \tau_2\right) \qquad (3.7)
\end{aligned}
$$

where we denoted with $\mathcal{D}_0$ the free phonon imaginary-time Green's function. The sum over $\mathbf{q}_2$ has yielded $\mathbf{q}_1 = -\mathbf{q}_2$, which we now use to calculate the electron term. We now apply the Wick's theorem (Th. 3.1) and consider all the possible pairings between the operators in the average. There are 6 possible pairings:

$$
\begin{aligned}
&\left\langle \mathcal{T}_\tau\, \hat{c}_{\mathbf{p}\sigma}(\tau)\, \hat{c}^\dagger_{\mathbf{k}_1+\mathbf{q}_1,s}(\tau_1)\, \hat{c}_{\mathbf{k}_1 s}(\tau_1)\, \hat{c}^\dagger_{\mathbf{k}_2-\mathbf{q}_1,s'}(\tau_2)\, \hat{c}_{\mathbf{k}_2 s'}(\tau_2)\, \hat{c}^\dagger_{\mathbf{p}\sigma}(\tau') \right\rangle_0 = \\
&\underbrace{\left\langle \mathcal{T}_\tau\, \hat{c}_{\mathbf{p}\sigma}(\tau)\, \hat{c}^\dagger_{\mathbf{k}_1+\mathbf{q}_1,s}(\tau_1) \right\rangle_0 \left\langle \mathcal{T}_\tau\, \hat{c}_{\mathbf{k}_1 s}(\tau_1)\, \hat{c}^\dagger_{\mathbf{k}_2-\mathbf{q}_1,s'}(\tau_2) \right\rangle_0 \left\langle \mathcal{T}_\tau\, \hat{c}_{\mathbf{k}_2 s'}(\tau_2)\, \hat{c}^\dagger_{\mathbf{p}\sigma}(\tau') \right\rangle_0}_{\text{(a)}} \\
&+ \underbrace{\left\langle \mathcal{T}_\tau\, \hat{c}_{\mathbf{p}\sigma}(\tau)\, \hat{c}^\dagger_{\mathbf{k}_2-\mathbf{q}_1,s'}(\tau_2) \right\rangle_0 \left\langle \mathcal{T}_\tau\, \hat{c}_{\mathbf{k}_1 s}(\tau_1)\, \hat{c}^\dagger_{\mathbf{p}\sigma}(\tau') \right\rangle_0 \left\langle \mathcal{T}_\tau\, \hat{c}_{\mathbf{k}_2 s'}(\tau_2)\, \hat{c}^\dagger_{\mathbf{k}_1+\mathbf{q}_1,s}(\tau_1) \right\rangle_0}_{\text{(b)}} \\
&+ \underbrace{\left\langle \mathcal{T}_\tau\, \hat{c}_{\mathbf{p}\sigma}(\tau)\, \hat{c}^\dagger_{\mathbf{k}_1+\mathbf{q},s}(\tau_1) \right\rangle_0 \left\langle \mathcal{T}_\tau\, \hat{c}_{\mathbf{k}_1,s}(\tau_1)\, \hat{c}^\dagger_{\mathbf{p}\sigma}(\tau') \right\rangle_0 \left\langle \mathcal{T}_\tau\, \hat{c}^\dagger_{\mathbf{k}_2-\mathbf{q}_1,s'}(\tau_2)\, \hat{c}_{\mathbf{k}_2 s'}(\tau_2) \right\rangle_0}_{\text{(c)}} \\
&+ \underbrace{\left\langle \mathcal{T}_\tau\, \hat{c}_{\mathbf{p}\sigma}(\tau)\, \hat{c}^\dagger_{\mathbf{k}_2-\mathbf{q}_1,s'}(\tau_2) \right\rangle \left\langle \mathcal{T}_\tau\, \hat{c}_{\mathbf{k}_2,s'}(\tau_2)\, \hat{c}^\dagger_{\mathbf{p}\sigma}(\tau') \right\rangle_0 \left\langle \mathcal{T}_\tau\, \hat{c}^\dagger_{\mathbf{k}_1+\mathbf{q}_1,s}(\tau_1)\, \hat{c}_{\mathbf{k}_1 s}(\tau_1) \right\rangle_0}_{\text{(d)}} \\
&+ \underbrace{\left\langle \mathcal{T}_\tau\, \hat{c}_{\mathbf{p}\sigma}(\tau)\, \hat{c}^\dagger_{\mathbf{p}\sigma}(\tau') \right\rangle_0 \left\langle \mathcal{T}_\tau\, \hat{c}^\dagger_{\mathbf{k}_1+\mathbf{q}_1,s}(\tau_1)\, \hat{c}_{\mathbf{k}_1 s}(\tau_1) \right\rangle_0 \left\langle \mathcal{T}_\tau\, \hat{c}^\dagger_{\mathbf{k}_2-\mathbf{q}_1,s'}(\tau_2)\, \hat{c}_{\mathbf{k}_2 s'}(\tau_2) \right\rangle_0}_{\text{(e)}} \\
&- \underbrace{\left\langle \mathcal{T}_\tau\, \hat{c}_{\mathbf{p}\sigma}(\tau)\, \hat{c}^\dagger_{\mathbf{p}\sigma}(\tau') \right\rangle_0 \left\langle \mathcal{T}_\tau\, \hat{c}_{\mathbf{k}_1 s}(\tau_1)\, \hat{c}^\dagger_{\mathbf{k}_2-\mathbf{q}_1,s'}(\tau_2) \right\rangle_0 \left\langle \mathcal{T}_\tau\, \hat{c}_{\mathbf{k}'}(\tau_2)\, \hat{c}^\dagger_{\mathbf{k}_1+\mathbf{q}_1,s}(\tau_1) \right\rangle_0}_{\text{(f)}} .
\end{aligned}
\qquad (3.8)
$$

Notice that

$$
\left\langle \mathcal{T}_\tau \hat{c}_{\mathbf{p}s}(\tau_2) \hat{c}^\dagger_{\mathbf{q}s'}(\tau_1) \right\rangle_0 = -\delta_{\mathbf{p}=\mathbf{q}} \delta_{s=s'} \mathcal{G}_0\left(\mathbf{p}, \tau_2 - \tau_1\right),
$$

which is the free electron GF, and was already evaluated in Eq. (2.18). Also, remember that $\mathbf{q}_1$ is the wave vector of the phonon in Eq. (3.7). The expressions

(c), (d), and (e) imply $\mathbf{q}_1 = 0$, which means that the phonon has a null wave vector. Such phonons do not exist, so these terms simply vanish. We thus have

$$\begin{aligned}
&\left\langle \mathcal{T}_\tau \, \hat{c}_{\mathbf{p}\sigma}(\tau) \, \hat{c}^\dagger_{\mathbf{k}_1+\mathbf{q}_1,s}(\tau_1) \, \hat{c}_{\mathbf{k}_1,s}(\tau_1) \, \hat{c}^\dagger_{\mathbf{k}_2-\mathbf{q}_1,s'}(\tau_2) \, \hat{c}_{\mathbf{k}_2 s'}(\tau_2) \, \hat{c}^\dagger_{\mathbf{p}\sigma}(\tau') \right\rangle_0 = \\
&\qquad \delta_{\mathbf{p}=\mathbf{k}_2=\mathbf{k}_1+\mathbf{q}_1} \, \delta_{s=s'=\sigma} \, \mathcal{G}_0\left(\mathbf{p}, \tau-\tau_1\right) \, \mathcal{G}_0\left(\mathbf{p}-\mathbf{q}_1, \tau_1-\tau_2\right) \, \mathcal{G}_0\left(\mathbf{p}, \tau_2-\tau'\right) \\
&\qquad + \delta_{\mathbf{p}=\mathbf{k}_1=\mathbf{k}_2-\mathbf{q}_1} \, \delta_{s=s'=\sigma} \, \mathcal{G}_0\left(\mathbf{p}, \tau-\tau_2\right) \, \mathcal{G}_0\left(\mathbf{p}+\mathbf{q}_1, \tau_2-\tau_1\right) \, \mathcal{G}_0\left(\mathbf{p}, \tau_1-\tau'\right) \\
&\qquad - \delta_{\mathbf{k}_1=\mathbf{k}_2-\mathbf{q}_1} \, \delta_{s'=s} \, \mathcal{G}_0\left(\mathbf{p}, \tau-\tau'\right) \, \mathcal{G}_0\left(\mathbf{k}_1, \tau_1-\tau_2\right) \, \mathcal{G}_0\left(\mathbf{k}_1+\mathbf{q}_1, \tau_2-\tau_1\right). \qquad (3.9)
\end{aligned}$$

In summary, the expectation value in the second-order term of Eq. (3.6) for the electron-phonon Green's function can be explicitly written as:

$$\begin{aligned}
&\left\langle \mathcal{T}_\tau \hat{c}_{\mathbf{p}\sigma}(\tau) \hat{V}\left(\tau_1\right) \hat{V}\left(t_2\right) \hat{c}^\dagger_{\mathbf{p}\sigma}\left(0\right) \right\rangle_0 = \sum_{\mathbf{k}_1\mathbf{k}_2\mathbf{q}_1} |M_{\mathbf{q}_1}|^2 \mathcal{D}_0\left(\mathbf{q}_1, \tau_1-\tau_2\right) \times \{ \\
&\qquad \delta_{\mathbf{p}=\mathbf{k}_2=\mathbf{k}_1+\mathbf{q}_1} \, \delta_{s=s'=\sigma} \, \mathcal{G}_0\left(\mathbf{p}, \tau-\tau_1\right) \, \mathcal{G}_0\left(\mathbf{p}-\mathbf{q}_1, \tau_1-\tau_2\right) \, \mathcal{G}_0\left(\mathbf{p}, \tau_2-\tau'\right) + \\
&\qquad + \delta_{\mathbf{p}=\mathbf{k}_1=\mathbf{k}_2-\mathbf{q}_1} \, \delta_{s=s'=\sigma} \, \mathcal{G}_0\left(\mathbf{p}, \tau-\tau_2\right) \, \mathcal{G}_0\left(\mathbf{p}+\mathbf{q}_1, \tau_2-\tau_1\right) \, \mathcal{G}_0\left(\mathbf{p}, \tau_1-\tau'\right) + \\
&\qquad - \delta_{\mathbf{k}_1=\mathbf{k}_2-\mathbf{q}_1} \, \delta_{s'=s} \, \mathcal{G}_0\left(\mathbf{p}, \tau-\tau'\right) \, \mathcal{G}_0\left(\mathbf{k}_1, \tau_1-\tau_2\right) \, \mathcal{G}_0\left(\mathbf{k}_1+\mathbf{q}_1, \tau_2-\tau_1\right)\} \qquad (3.10)
\end{aligned}$$

Drawing Feynman diagrams. Let us now now explain how to construct *Feynman diagrams*. The central idea is that a Green's function $\mathcal{G}(\mathbf{p}, \tau-\tau')$ can be represented as a series of diagrams. Each diagram corresponds to a term in the perturbative expansion and consists of a set of lines, where each line represents a free Green's function $\mathcal{G}_0$ or $\mathcal{D}_0$, as seen in the expressions above. In particular, we represent the electron's Green's function $\mathcal{G}_0$ with a solid line and the phonon's Green's function $\mathcal{D}_0$ with a dashed line. The electron's GF has an orientation in time, which is depicted with an arrow, but the phonon's GF does not. As a matter of fact, the following rules apply:

$$\mathcal{D}_0\left(\mathbf{q}, \tau-\tau'\right) = \mathcal{D}_0\left(-\mathbf{q}, \tau'-\tau\right).$$

By using these rules, the three diagrams resulting from Eq. (3.10) are depicted in Fig. 3.1.

Topologically distinct diagrams Notice however that the first two diagrams (a) and (b) are equivalent. This can be shown by considering the integral

$$\begin{aligned}
&\int_0^\beta d\tau_1 \int_0^\beta d\tau_2 \sum_{\mathbf{q}} \left|M_{\mathbf{q}}\right|^2 \mathcal{D}_0\left(\mathbf{q}, \tau_2\right) \\
&\times \Big[\mathcal{G}_0\left(\mathbf{p}, \tau-\tau_1\right) \mathcal{G}_0\left(\mathbf{p}-\mathbf{q}, \tau_1-\tau_2\right) \mathcal{G}_0\left(\mathbf{p}, \tau_2-\tau'\right) \\
&\qquad + \mathcal{G}_0\left(\mathbf{p}, \tau-\tau_2\right) \mathcal{G}_0\left(\mathbf{p}+\mathbf{q}, \tau_2-\tau_1\right) \mathcal{G}_0\left(\mathbf{p}, \tau_1-\tau'\right)\Big].
\end{aligned}$$

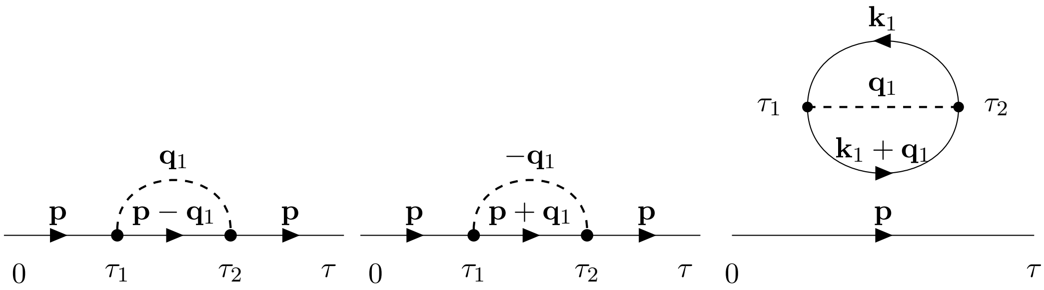

(a) (b) (f)

Fig. 3.1: Second-order Feynman diagrams for the electron-phonon Green's function.

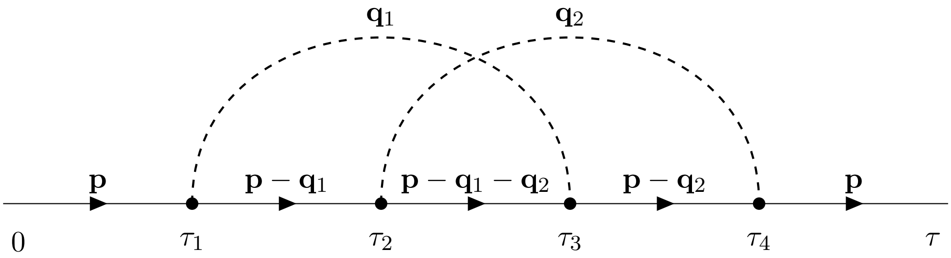

(e)

Fig. 3.2: Fourth-order Feynman diagrams for the electron-phonon Green's function.

It is evident that the two terms in the square brackets are equivalent, as they differ only by the exchange of the integration variables τ_1 and τ_2. Relabelling $\tau_1 \leftrightarrow \tau_2$ in the second term yields the first, so both integrals contribute equally[2]. Therefore, diagrams (a) and (b) represent the same physical process and contribute identically to the expansion. Such diagrams are said to be *topologically equivalent*. Now see that in the perturbative expansion in Eq. (3.8) has a prefactor of $\frac{1}{2!}$ in front of the integral. With prefactor cancels out exactly the factor of 2 that arises from the two equivalent diagrams (a) and (b). The same reasoning applies at higher orders: for example, at fourth order ($n = 4$), a diagram such as that shown in Fig. 3.2 would appear. There are $4!$ equivalent diagrams corresponding to all permutations of the vertices, but the $1/4!$ prefactor in the expansion cancels this multiplicity. In general, we conclude that *only topologically distinct diagrams need to be drawn, with each diagram counted once in the perturbative expansion*.

Finally, the diagram (f) in Fig. 3.1 is not equivalent to the other two, as it is a topologically distinct diagram. It is in fact a *disconnected* diagram. It is shown in the next section that disconnected diagrams do not contribute to the Green's function.

---

[2] This equivalence is also apparent from diagrams (a) and (b) in Fig. 3.1: swapping the two vertices (corresponding to τ_1 and τ_2) transforms diagram (a) into (b).

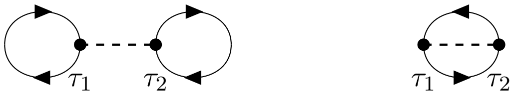

(g) (h)

Fig. 3.3: Second-order vacuum polarisation diagrams.

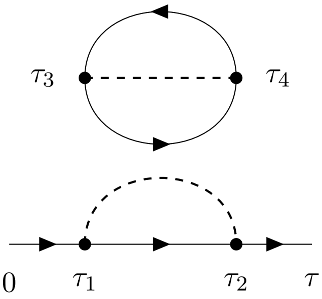

(i)

Fig. 3.4: Example of a disconnected diagram originating from diagram (a) in Fig. 3.1.

3.3 Disconnected Diagrams

The diagrammatic expansion of the GF for the electron-phonon interaction has given rise to a *disconnected diagram*, depicted in Fig. 3.1 (f). First, let us clearly define what a disconnected diagram is.

Definition 3.2 (Disconnected diagram)**.** *A Feynman diagram is said to be* ***disconnected*** *if at least one of its internal points* $\tau_1, \tau_2, .., \tau_n$ *is not connected to the external points* 0 *and* τ*.*

If we now were to expand the S-matrix operator $S(\beta)$ in the denominator of Eq. (3.5), a series of diagrams like those in Fig. 3.3 would appear:

$$\langle S(\beta)\rangle_0 = -\sum_{j=1}^{\infty} \frac{(-1)^j}{j!} \int_0^{\beta\hbar} d\tau_1 \cdots \int_0^{\beta\hbar} d\tau_j \left\langle \mathcal{T}_\tau \hat{V}(\tau_1) \cdots \hat{V}(\tau_j) \right\rangle_0 \equiv 1 + S^{(1)} + S^{(2)} + \ldots$$

These are called *vacuum polarisation diagrams*. It is then possible to show that those diagrams exactly cancel out the disconnected diagrams appearing in the numerator of Eq. (2.17), so that only connected diagrams contribute to the GF. The claim is that the numerator of Eq. (2.17) can always written as

$$\langle \mathcal{T}_\tau \, \hat{c}_\lambda(\tau) \hat{c}_\lambda^\dagger(0) S(\beta) \rangle_0 = \mathcal{G}_c(\lambda, \tau) \left(1 + S^{(1)} + S^{(2)} + \ldots \right),$$

where $\mathcal{G}_c\,(\lambda,\tau)$ is the sum of only the connected diagrams' GFs. For example, the disconnected diagram in Fig. 3.4 is just the product of the connected part of diagram (a) in Fig. 3.1 and the second-order disconnected part in Fig. 3.3 (h). Then the same factor appearing in both numerator and denominator cancels out, leaving only the connected diagrams' GF $\mathcal{G}_c$. This is called the *cancellation theorem* [14].

Theorem 3.2 (Cancellation theorem). *The numerator of any disconnected diagram may be written as:*

$$\langle \mathcal{T}_\tau\, \hat{c}_\lambda(\tau)\hat{c}^\dagger_\lambda(0)S(\beta)\rangle_0 = \mathcal{G}_c(\lambda,\tau)\,\langle S(\beta)\rangle_0$$

where $\mathcal{G}_c$ is the Green's function for the connected part.

Proof. From Eq. (3.1), for a disconnected diagram the n-th order term can be written as the product of a connected part c and a disconnected part:

$$\begin{aligned}
&\delta\mathcal{G}^{(n)} \\
&= -\sum_{m=0}^{n}\frac{(-1)^n}{m!(n-m)!}\left(\int_0^\beta d\tau_1\cdots\int_0^\beta d\tau_m\right)\left\langle \mathcal{T}_\tau\,\hat{c}_{\mathbf{k}\sigma}(\tau)\hat{c}^\dagger_{\mathbf{k}\sigma}(0)\hat{V}(\tau_1)\cdots\hat{V}(\tau_m)\right\rangle_{0,c} \\
&\qquad\qquad\times\left(\int_0^\beta d\tau_{m+1}\cdots\int_0^\beta d\tau_n\right)\left\langle \mathcal{T}_\tau\,\hat{V}(\tau_{m+1})\cdots\hat{V}(\tau_n)\right\rangle_0,
\end{aligned}$$

where m is the number of disconnected points. The binomial coefficient term is the number of ways to choose m disconnected points from n total points. Then the summation over m is rewritten as

$$\sum_{m=0}^{n}\frac{1}{m!(n-m)!}\cdots = \sum_{m=0}^{\infty}\sum_{j=0}^{\infty}\delta_{n,m+j}\frac{1}{m!j!}\cdots,$$

and the numerator is rewritten as the sum of all order terms from $n=0$ to ∞:

$$\begin{aligned}
&\langle \mathcal{T}_\tau\, \hat{c}_\lambda(\tau)\hat{c}^\dagger_\lambda(0)S(\beta)\rangle_0 \\
&\qquad= -\sum_{n=0}^{\infty}\sum_{m=0}^{\infty}\sum_{j=0}^{\infty}\delta_{n,m+j}\frac{1}{m!j!}\left(-\frac{1}{\hbar}\right)^n\int_0^{\beta\hbar}d\tau_1\cdots\int_0^{\beta\hbar}d\tau_m \\
&\qquad\qquad\times\left\langle \mathcal{T}\hat{c}_{\mathbf{k}\sigma}(0)\hat{c}^\dagger_{\mathbf{k}\sigma}(0)\hat{V}(\tau_1)\cdots\hat{V}(\tau_m)\right\rangle_{0,c} \\
&\qquad\qquad\qquad\times\int_0^\beta d\tau_1\cdots\int_0^\beta d\tau_j\left\langle \mathcal{T}\hat{V}(\tau_1)\cdots\hat{V}(\tau_j)\right\rangle_0,
\end{aligned}$$

where we relabelled the time variables $\tau_{m+1}, \ldots, \tau_n \to \tau_1, \ldots, \tau_j$, which was possible because of the delta (only terms with $j = n - m$ are nonzero). Summing over n then yields:

$$
\begin{aligned}
&\langle \mathcal{T}_\tau\, \hat{c}_\lambda(\tau)\hat{c}^\dagger_\lambda(0)S(\beta)\rangle_0 \\
&\quad = -\sum_{m=0}^{\infty} \frac{1}{m!}\left(-\frac{1}{\hbar}\right)^m \int_0^\beta d\tau_1 \cdots \int_0^\beta d\tau_m \left\langle \mathcal{T}\hat{c}_{\mathbf{k}\sigma}(\tau)\hat{c}^\dagger_{\mathbf{k}\sigma}(0)\hat{V}(\tau_1)\cdots\hat{V}(\tau_m)\right\rangle_{0,c} \\
&\qquad\qquad \times \sum_{j=0}^{\infty} \frac{1}{j!}\left(-\frac{1}{\hbar}\right)^j \int_0^\beta d\tau_1 \cdots \int_0^\beta d\tau_j \left\langle \mathcal{T}\hat{V}(\tau_1)\cdots\hat{V}(\tau_j)\right\rangle_0 .
\end{aligned}
$$

The last factor is exactly the Dyson series expansion of the denominator $\langle S(\beta)\rangle_0$. Thus, the theorem is proved. ☐

3.4 Feynman Rules

Having established the rules for constructing Feynman diagrams, we hereby summarise the rules [14] relevant to the electron-phonon interaction to calculate the Matsubara Green's function in the momentum space $\mathcal{G}(\mathbf{p}\sigma, \tau)$.

Rules for the electron-phonon interaction.

1. Only even orders $2n$ are nonzero.
2. For each order $2n$, draw all **topologically distinct** and **connected** diagrams with: n phonon lines, 2 external electron lines, and $2n - 1$ internal electron lines.
3. Momentum and spin must be conserved at each vertex.
4. Each electron line of momentum $\mathbf{p}$ with vertices τ_1 to τ_2 is assigned the factor $\mathcal{G}_0(\mathbf{k}\sigma, \tau_2 - \tau_1)$.
5. Each phonon line of momentum $\mathbf{q}$ with vertices τ_1 to τ_2 is assigned the factor $|M_\mathbf{q}|^2 D(\mathbf{q}, \tau_2 - \tau_1)$.
6. Multiply each electron loop by a factor of -1.
7. Sum or integrate over all internal coordinates.

Let us briefly justify the rules above based on what we have learned in the previous sections. Rule 2 is derived: i) from the discussion in Sect. 3.2, where it was established that only topologically distinct diagrams contribute to the perturbative expansion; and ii) from Th. 3.2, which states that only connected diagrams contribute to the GF. Rules 1–7 are a direct consequence of the expansion that was established in in Sect. 3.2.

4

Holstein Hamiltonian in the Atomic Limit

In his original paper [4], Holstein introduced a model to describe the polaron problem in a one-dimensional molecular crystal. The polaron problem involves an electron interacting with the lattice vibrations, which are described as phonons. The Hamiltonian is regarded as the sum of three terms that we have already derived and discussed in the previous chapter: the electronic term H_{el}, the phononic term H_{ph}, and the electron-phonon interaction term H_{el-ph}. It is often the case that the electron-phonon interaction may not treated as a perturbation, and gives in fact rise to the self-trapping of the electron in the lattice. One can imagine that an electron is initially fixed at some site in the lattice: the surrounding lattice particles, due to the electron-lattice interactions, are displaced in new equilibrium positions. These displacements will provide a potential well for the electron; if such a well is sufficiently deep, then the electron will be trapped in a bound state and unable to move unless accompanied by the well. The unit formed by the electron and the lattice is called a *polaron*.

In this chapter, the Holstein Hamiltonian in its first-quantised form will be introduced in Sect. 4.1. In Sect. 4.2, we elaborate its second-quantised form in the atomic limit, which is the one that will be used in the rest of the thesis. The Holstein Hamiltonian in the atomic limit will be solved exactly in Sect. 4.3, where we find an exact form for the ground-state polaron energy and the ground-state quasiparticle weight. Such values are used as a benchmark in Ch. 5.

4.1 The Holstein Hamiltonian

The molecular-crystal model in the original Holstein's formulation [4] is assumed to be a linear chain on N identical diatomic molecules. Only the internuclear separation of the molecules may vary, giving rise to the lattice vibrations. The Hamiltonian of the lattice reads

$$H_{ph} = \frac{1}{2M} \sum_{n=1}^{N} p_n^2 + \frac{1}{2} \sum_{n=1}^{N} M\omega_0^2 x_n^2,$$

where x_n is the deviation of the internuclear separation from its equilibrium position, p_n is the associated canonical momentum of the n-th molecule, M is the relative

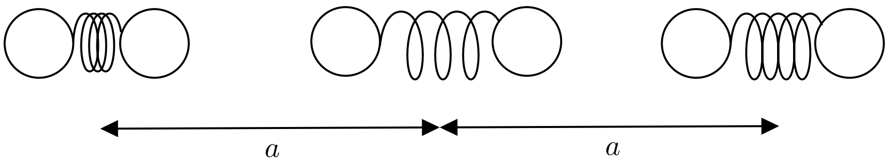

Fig. 4.1: Schematic representation of the one-dimensional Holstein Model. There exist N identical diatomic molecules that are separated by a distance a. Each diatomic molecule is represented by a pair of atoms, which are connected by a spring.

mass, and ω_0 is the harmonic vibrational frequency. The phonons are thus assumed to be optical and dispersionless. This model is illustrated in Fig. 4.1. Adding the electron kinetic energy we get the full Hamiltonian:

$$H = \sum_n \left(-\frac{\hbar^2}{2M} \frac{\partial^2}{\partial x_n^2} + \frac{1}{2} M \omega_0^2 x_n^2 \right) - \frac{\hbar^2}{2m} \frac{\partial^2}{\partial r^2} + \sum_n U\left(r - R_n, x_n\right) \tag{4.1}$$

A single electron is studied in the tight-binding approximation, which was discussed in Sect. 1.3.2. It will be briefly presented here for the Holstein model. The state of the system is taken to be the linear superposition of the molecular electron wave functions $\phi(r - na, x_n)$:

$$\psi(r, x_n) = \sum_{n=1}^{N} a_n(x_1, \ldots, x_N) \phi(r - na, x_n).$$

Each wave function $\phi(r - na, x_n)$ is a solution of the Schrödinger equation for a single electron in the potential of the n-th molecule:

$$\left[-\frac{\hbar^2}{2m} \nabla^2 + U\left(r - na, x_n\right) \right] \phi\left(r - na, x_n\right) = E\left(x_n\right) \phi\left(r - na, x_n\right).$$

A complete calculation leads to a differential equation for the coefficients a_n:

$$\begin{aligned} &\left[i\hbar \frac{\partial}{\partial t} - \sum_p \left(-\frac{\hbar^2}{2M} \frac{\partial^2}{\partial x_p^2} + \frac{1}{2} M \omega_0^2 x_p^2 \right) - E\left(x_n\right) - W_n\left(x_1 \ldots x_N\right) \right] \alpha_n\left(x_1 \ldots x_N\right) \\ &= \sum_{(\pm)} J\left(x_n, x_{n\pm1}\right) \alpha_{n\pm1}\left(x_1 \ldots x_N\right) \end{aligned} \tag{4.2}$$

with

$$\begin{aligned} W_n\left(x_1 \ldots x_N\right) &= \int \left|\phi_n\left(r - na, x_n\right)\right|^2 \sum_{p \neq n} U\left(r - pa, x_p\right) dr, \\ J\left(x_r, x_m\right) &= \int \phi_n^*\left(r - na, x_n\right) U\left(r - na, x_n\right) \phi\left(r - ma, x_m\right) dr. \end{aligned}$$

The sum $\sum_{(\pm)}$ is taken to be over the nearest neighbours of the n-th molecule, i.e. $n-1$ and $n+1$. The term $W_n(x_1, \dots, x_N)$ is the potential energy of the n-th molecule due to all the other molecules in the lattice, and $J(x_n, x_{n\pm 1})$ is the hopping term between the n-th molecule and its nearest neighbours.

The Holstein Hamiltonian in its first-quantised form in Eq. (4.1) is outside the scope of this thesis, so the solution written above will not be discussed further. Rather, it is interesting to explain the approximations that were introduced by Holstein, understand their physical meaning, and how they can be reformulated in the second quantisation formalism.

Holstein approximations. The first approximation to do in Eq. (4.2) is to neglect the term $W_n(x_1, \dots, x_N)$: the rationale behind this is that the electron is assumed to be localised in a single molecule by a short-range potential, and therefore the interaction with the other molecules is negligible. The second approximation is to assume that the hopping term $J(x_n, x_{n\pm 1})$ is constant, i.e. it does not depend on the position of the molecules in the lattice. Such approximation was already justified in the tight-binding model, and $-J$ corresponds in fact to the hopping parameter $-t$ in Eq. (1.20). Lastly, the energy $E_n(x_n)$ is assumed to depend linearly from the displacement x_n of the n-th molecule from its equilibrium position: $E_n(x_n) = -Ax_n$.

It is found in the original Holstein's formulation that the Schrödinger's equation under these approximations reads:

$$i\hbar \frac{\partial}{\partial t} \alpha_n = \sum_p \left(-\frac{\hbar^2}{2M} \frac{\partial^2}{\partial x_p^2} + \frac{1}{2} M \omega_0^2 x_p^2 \right) \alpha_n - t \left(\alpha_{n+1} + \alpha_{n-1} \right) \alpha_n - A x_n \alpha_n. \quad (4.3)$$

4.2 Holstein Hamiltonian in Second Quantisation

We have already encountered the first term of Eq. (4.3) when discussing phonons. The assumption made by Holstein is that the phonons are dispersionless, with a constant frequency ω_0. The phonon Hamiltonian is written in second quantisation as[1]

$$H_{ph} = \omega_0 \sum_{\mathbf{q}} \left(b^\dagger_{\mathbf{q}} b_{\mathbf{q}} + \frac{1}{2} \right).$$

The second term in Eq. (4.3) includes the energy of the electron and the hopping term. In the wave-vector notation and in the tight-binding approximation, this is written as

$$H_{el} = \sum_{\mathbf{k}} \varepsilon_{\mathbf{k}} c^\dagger_{\mathbf{k}} c_{\mathbf{k}}.$$

---

[1] This is the three-dimensional formulation.

The energy $\varepsilon_{\mathbf{k}}$ has a dispersion relation that is found in the tight-binding approximation, e.g. in Eq. (1.21) for the nearest-neighbour approximation. Finally, the electron-phonon interaction was already encountered in Sect. 1.4.1. Such assumption derives from the fact that the potential in the Holstein model grows linearly with the distance, and the matrix elements of the interaction are derivative of the potential. The electron-phonon interaction term in the Holstein model was derived in Eq. (1.33). Umklapp processes are assumed to be negligible, hence $\mathbf{G} = 0$. Furthermore, the interaction term in Eq. (4.3) does not depend on the momentum. We then consider the interaction matrix as constant, and equal to $\frac{g}{\sqrt{N}}$. The electron-phonon interaction reads[2]:

$$H_{el-ph} = \frac{g}{\sqrt{N}} \sum_{\mathbf{k},\mathbf{q}} c^\dagger_{\mathbf{k}+\mathbf{q}} c_{\mathbf{k}} \left(b^\dagger_{-\mathbf{q}} + b_{\mathbf{q}} \right).$$

In its second-quantised formulation, the Holstein Hamiltonian reads

$$H_{\text{Holstein}} = \sum_{\mathbf{k}} \varepsilon_{\mathbf{k}} c^\dagger_{\mathbf{k}} c_{\mathbf{k}} + \omega_0 \sum_{\mathbf{q}} \left(b^\dagger_{\mathbf{q}} b_{\mathbf{q}} + \frac{1}{2} \right) + \frac{g}{\sqrt{N}} \sum_{\mathbf{k},\mathbf{q}} c^\dagger_{\mathbf{k}+\mathbf{q}} c_{\mathbf{k}} \left(b^\dagger_{-\mathbf{q}} + b_{\mathbf{q}} \right). \tag{4.4}$$

Atomic limit. However, this Hamiltonian cannot be solved exactly. Rather, here we are interested in the *atomic limit*. In the atomic limit, the electrons are considered tightly bound to the atoms, so much that they cannot hop between the sites: the hopping term t is set to 0. More formally, the hopping matrix in Eq. (1.18) must be $t_{ij} \propto \delta_{ij}$, so that it is nonzero only when $i = j$. From Eq. (1.18) one can also see that, for this to be satisfied, the site energy ε_i is constant: $\varepsilon_i = \varepsilon$. By using the relations in Eq. (1.16) for the electron operators, the Hamiltonian is written as

$$H_{\text{atom}} = \varepsilon c^\dagger c + \omega_0 \sum_{\mathbf{q}} \left(b^\dagger_{\mathbf{q}} b_{\mathbf{q}} + \frac{1}{2} \right) + c^\dagger c \sum_{\mathbf{q}} M_{\mathbf{q}} \left(b^\dagger_{-\mathbf{q}} + b_{\mathbf{q}} \right), \tag{4.5}$$

where $M_{\mathbf{q}} = \frac{g}{\sqrt{N}} e^{i\mathbf{q}\cdot\mathbf{R}_i}$. Since the sites are now decoupled, we study the single-site Hamiltonian, where $c \equiv c_i$. Further application of Eq. (1.16) for the boson operators leads to:

$$H_{\text{atom}} = \varepsilon c^\dagger c + \omega_0 b^\dagger b + g c^\dagger c \left(b^\dagger + b \right). \tag{4.6}$$

4.3 Exact Solution in the Atomic Limit

The Holstein Hamiltonian in the atomic limit in Eq. (4.5) has an exact solution. Here, we consider a more general model where the phonon frequency is not assumed to

---

[2] We omit the indexes for the spin.

be constant. This is called the *independent boson model*. Later on, we will specialise to the case of constant phonon frequency and coupling. The Hamiltonian we wish to solve is [7]

$$H = c^{\dagger}c\left[\varepsilon + \sum_{\mathbf{q}} M_{\mathbf{q}}\left(b_{\mathbf{q}} + b^{\dagger}_{-\mathbf{q}}\right)\right] + \sum_{\mathbf{q}} \omega_{\mathbf{q}} b^{\dagger}_{\mathbf{q}} b_{\mathbf{q}}. \tag{4.7}$$

This Hamiltonian describes a single electron coupled to phonons, where ε is the energy of the electron, $M_{\mathbf{q}}$ is the coupling strength between the electron and the phonon with wave vector $\mathbf{q}$, and $\omega_{\mathbf{q}}$ is the frequency of the phonon with wave vector $\mathbf{q}$. Before tackling this Hamiltonian, we need to perform the so-called *Lang-Firsov transformation*, which is a unitary transformation.

4.3.1 Lang-Firsov Transformation

The Hamiltonian is rewritten by a transformation of the type

$$\bar{H} = e^{S} H e^{-S} = c^{\dagger}c\left(\varepsilon - \Delta\right) + \sum_{\mathbf{q}} \omega_{\mathbf{q}} b^{\dagger}_{\mathbf{q}} b_{\mathbf{q}}, \tag{4.8}$$

where

$$\Delta = \sum_{\mathbf{q}} \frac{M^2_{\mathbf{q}}}{\omega_{\mathbf{q}}}.$$

We now show that applying the transformation in Eq. (4.8) to any product of operators is simply the product of the transformed operators. This is easily shown by considering

$$e^{S} A_1 A_2 \cdots A_{\nu} e^{-S} = \left(e^{S} A_1 e^{-S}\right)\left(e^{S} A_2 e^{-S}\right)\cdots\left(e^{S} A_{\nu} e^{-S}\right) = \bar{A}_1 \bar{A}_2 \cdots \bar{A}_{\nu},$$

where we have used the identity $e^{S}e^{-S} = \mathbf{1}$, and we denoted with $\bar{A}_j$ the transformed operator A_j. Furthermore, the transformation of a function of operators is the function of the transformed operators:

$$e^{S} f(A) e^{-S} = e^{S} \sum_{n=0}^{\infty} a_n A^n e^{-S} = \sum_{n=0}^{\infty} a_n (\bar{A})^n = f(\bar{A}). \tag{4.9}$$

Using these properties, we can compute the transformed Hamiltonian $\bar{H}$ by applying the transformation to each operator individually. This is done by evaluating

$$e^{S} = \sum_{n} \frac{S^n}{n!} \implies \bar{A} = e^{S} A e^{S} = A + [S, A] + \frac{1}{2!}\left[S, [S, A]\right] + \ldots,$$

with the operator

$$S = c^\dagger c \sum_{\mathbf{q}} \frac{M_{\mathbf{q}}}{\omega_{\mathbf{q}}} \left(b^\dagger_{\mathbf{q}} - b_{\mathbf{q}} \right).$$

The transformation is applied to each operator in Eq. (4.8),

$$\begin{aligned} \bar{c} &= cX, \\ \bar{c}^\dagger &= c^\dagger X^\dagger, \\ \bar{b}_{\mathbf{q}} &= b_{\mathbf{q}} - \frac{M_{\mathbf{q}}}{\omega_{\mathbf{q}}} c^\dagger c, \\ \bar{b}^\dagger_{\mathbf{q}} &= b^\dagger_{\mathbf{q}} - \frac{M_{\mathbf{q}}}{\omega_{\mathbf{q}}} c^\dagger c, \end{aligned}$$

where we introduced the operator

$$X \equiv e^{-\sum_{\mathbf{q}} \frac{M_{\mathbf{q}}}{\omega_{\mathbf{q}}} \left(b^\dagger_{\mathbf{q}} - b_{\mathbf{q}} \right)}. \tag{4.10}$$

This operator commutes with c, hence the number operator is the same in the new representation:

$$\bar{c}^\dagger \bar{c} = c^\dagger c X^\dagger X = c^\dagger c.$$

The Hamiltonian in Eq. (4.7) is then rewritten as

$$\begin{aligned} \bar{H} = \varepsilon_c \bar{c}^\dagger \bar{c} + \sum_{\mathbf{q}} \omega_{\mathbf{q}} \left(b^\dagger_{\mathbf{q}} - \frac{M_{\mathbf{q}}}{\omega_{\mathbf{q}}} c^\dagger c \right) \left(b_{\mathbf{q}} - \frac{M_{\mathbf{q}}}{\omega_{\mathbf{q}}} c^\dagger c \right) + \\ + \sum_{\mathbf{q}} M_{\mathbf{q}} \left(b^\dagger_{\mathbf{q}} + b_{\mathbf{q}} - 2 \frac{M_{\mathbf{q}}}{\omega_{\mathbf{q}}} c^\dagger c \right) c^\dagger c, \end{aligned}$$

which simplifies into

$$\bar{H} = c^\dagger c \left(\varepsilon_c - \Delta \right) + \sum_{\mathbf{q}} \omega_{\mathbf{q}} b^\dagger_{\mathbf{q}} b_{\mathbf{q}} = H_e + H_p.$$

In the last equality, $\overline{H}$ was separated into an electronic part H_e and a phonon part H_p:

$$H_e \equiv c^\dagger c \left(\varepsilon_c - \Delta \right), \qquad H_p \equiv \sum_{\mathbf{q}} \omega_{\mathbf{q}} b^\dagger_{\mathbf{q}} b_{\mathbf{q}}. \tag{4.11}$$

4.3.2 Green's Function

The aim is to compute the Green's function (GF) of the Holstein Hamiltonian. To account for the temperature, we will use the grand canonical ensemble by averaging over the trace:

$$G(t) = -\frac{i}{Z}\mathrm{Tr}\left(e^{-\beta H}e^{iHt}ce^{-iHt}c^{\dagger}\right), \quad \text{for } t > 0.$$

Notice that it is not necessary here to use the Matsubara formalism. We introduce the identity $1 = e^{-S}e^{S}$:

$$G(t) = -\frac{i}{Z}\mathrm{Tr}\left(e^{-\beta H}e^{iHt}ce^{-iHt}c^{\dagger}e^{-S}e^{S}\right),$$

and make use of the cyclic properties of the trace to rewrite the GF as

$$G(t) = -\frac{i}{Z}\mathrm{Tr}\left(e^{S}e^{-\beta H}e^{iHt}ce^{-iHt}c^{\dagger}e^{-S}\right) = -\frac{i}{Z}\mathrm{Tr}\left(e^{-\beta \bar{H}}e^{i\bar{H}t}\bar{c}e^{-i\bar{H}t}\bar{c}^{\dagger}\right).$$

This evaluation is non-trivial: the operators $\bar{c}$ and $\bar{c}^{\dagger}$ do not commute with $b^{\dagger}$ and b because they depend on X, which was defined in Eq. (4.10). We write the X dependence explicitly:

$$G(t) = -\frac{i}{Z}\mathrm{Tr}\left(e^{-\beta \bar{H}}e^{i\bar{H}t}cXe^{-i\bar{H}t}c^{\dagger}X^{\dagger}\right).$$

The part in the middle can be computed as follows:

$$e^{i\bar{H}t}cXe^{-i\bar{H}t} = e^{-i(\varepsilon_c-\Delta)t}ce^{i\bar{H}t}Xe^{-i\bar{H}t} = e^{-i(\varepsilon_c-\Delta)t}cX(t), \tag{4.12}$$

where

$$X(t) \equiv \exp\left[-\sum_{\mathbf{q}}\frac{M_{\mathbf{q}}}{\omega_{\mathbf{q}}}\left(b^{\dagger}_{\mathbf{q}}e^{i\omega_{\mathbf{q}}t} - b_{\mathbf{q}}e^{-i\omega_{\mathbf{q}}t}\right)\right].$$

Now call

$$\bar{\varepsilon}_c \equiv \varepsilon - \Delta.$$

By making use of Eq. (4.12), the Green's function is written as

$$G(t) = -i\frac{1}{Z}\,\mathrm{Tr}\left(e^{-\beta\bar{\varepsilon}_c n}cc^{\dagger}\right)\mathrm{Tr}\left[e^{-\beta H_p}X(t)X^{\dagger}(0)\right], \tag{4.13}$$

where we separated the expression into an electronic and a phonon part. This is possible because the Hamiltonian was itself separated into the electronic and the phonon part, defined in Eq. (4.11). The partition functions are Z_{el} and Z_{ph} respectively, such that $Z = Z_{el}Z_{ph}$.

The electronic part is easily calculated as

$$\begin{aligned}
\frac{1}{Z_{el}}\,\mathrm{Tr}\left(e^{-\beta\bar{\varepsilon}n}cc^{\dagger}\right) &= \frac{1}{Z_{el}}\,\mathrm{Tr}\left(e^{-\beta\bar{\varepsilon}n}(1-n)\right) \\
&= \frac{1}{Z_{el}}\left[\mathrm{Tr}\left(e^{-\beta\bar{\varepsilon}n}\right) - \mathrm{Tr}\left(e^{-\beta\bar{\varepsilon}n}n\right)\right] \\
&= \frac{1}{Z_{el}}\left(1 + e^{-\beta\bar{\varepsilon}} - e^{-\beta\bar{\varepsilon}}\right) \\
&= \frac{1}{Z_{el}}\cdot 1 \\
&= 1 - n_f(\bar{\varepsilon})
\end{aligned}$$

where $n_f(\bar{\varepsilon})$ is the Fermi-Dirac distribution.

Phonon part

Evaluating the phonon part

$$F(t) \equiv \frac{1}{Z_{ph}}\mathrm{Tr}\left[e^{-\beta H_P}X(t)X^{\dagger}(0)\right]$$

is more difficult, but it can be done exactly. First, $F(t)$ is arranged as

$$F(t) = \frac{1}{Z_{ph}}\,\mathrm{Tr}\left[e^{-\beta\sum_q \omega_q n_q}X(t)X^{\dagger}(0)\right] = \prod_{\mathbf{q}}\mathscr{F}_{\mathbf{q}}(t), \tag{4.14}$$

where we introduced

$$\begin{aligned}
\mathscr{F}_{\mathbf{q}} &\equiv \frac{1}{Z_{\mathbf{q}}}\sum_{n=0}^{\infty} e^{-\beta n\omega}\,\langle n|X(t)X^{\dagger}(0)|n\rangle = \\
&= \frac{1}{Z_{\mathbf{q}}}\sum_{n_{\mathbf{q}}=0}^{\infty} e^{-\beta n_{\mathbf{q}}\omega_{\mathbf{q}}}\,\langle n_{\mathbf{q}}|\,e^{-\lambda_{\mathbf{q}}B_{\mathbf{q}}(t)}e^{\lambda_{\mathbf{q}}B_{\mathbf{q}}(0)}\,|n_{\mathbf{q}}\rangle\,, \\
B_{\mathbf{q}}(t) &\equiv b_{\mathbf{q}}^{\dagger}\,e^{i\omega_{\mathbf{q}}t} - b_{\mathbf{q}}\,e^{-i\omega_{\mathbf{q}}t}, \\
\lambda_{\mathbf{q}} &\equiv \frac{M_{\mathbf{q}}}{\omega_{\mathbf{q}}}
\end{aligned}$$

The partition function Z is given by

$$Z = \prod_{\mathbf{q}} Z_{\mathbf{q}}, \quad Z_{\mathbf{q}} = \sum_{n_q=0}^{\infty} e^{-\beta n_q\omega_q} \implies \quad \frac{1}{Z_{\mathbf{q}}} = 1 - e^{-\beta\omega_{\mathbf{q}}}.$$

Now let us drop all $\mathbf{q}$ subscripts in the expression for a more concise notation. We have

$$\mathscr{F}_{\mathbf{q}}(t) = \left(1 - e^{-\beta\omega}\right) \sum_{n=0}^{\infty} e^{-\beta n\omega} \langle n| e^{-\lambda\left(b^{\dagger}e^{i\omega t} - be^{-i\omega t}\right)} e^{\lambda\left(b^{\dagger} - b\right)} |n\rangle,$$

where the state $|n\rangle$ is

$$|n\rangle = \frac{\left(b^{\dagger}\right)^{n}}{\sqrt{n!}} |0\rangle.$$

In order to separate the operators into the exponentials, we make use of Feynman's theorem on the disentangling of operators [19].

Theorem 4.1 (Feynman's theorem on disentangling of operators)**.** *Let A and B be two operators. If their commutator $C = [A, B]$ commutes with both of them, that is*

$$[C, A] = [C, B] = 0,$$

then

$$e^{A+B} = e^{A} e^{B} e^{-1/2[A,B]}.$$

This theorem will not be proved. Now recall that

$$\mathscr{F}_{\mathbf{q}}(t) = \left(1 - e^{-\beta\omega}\right) \sum_{n=0}^{\infty} e^{-\beta n\omega} \left\langle n| X(t) X^{\dagger}(0) |n\right\rangle, \tag{4.15}$$

with

$$X(t) = e^{-\lambda\left(b^{\dagger}e^{i\omega t} - be^{-i\omega t}\right)},$$
$$X(0) = e^{\lambda\left(b^{\dagger} - b\right)}.$$

We set

$$A \equiv -\lambda b^{\dagger} e^{i\omega t}$$
$$B \equiv \lambda b e^{-i\omega t}$$

which yields

$$[A, B] = -\lambda^{2} \left[b^{\dagger}, b\right] = \lambda^{2},$$

and the operators $X(t)$ and $X^{\dagger}(0)$ may be rewritten as

$$X(t) = e^{A+B} = e^{-\lambda^{2}/2} e^{-\lambda b^{\dagger} e^{i\omega t}} e^{\lambda b e^{-i\omega t}},$$
$$X^{\dagger}(0) = e^{-\lambda^{2}/2} e^{\lambda b^{\dagger}} e^{-\lambda b}.$$

Eq. (4.15) becomes

$$\mathscr{F}_{\mathbf{q}}(t) = \left(1 - e^{-\beta\omega}\right) \sum_{n=0}^{\infty} e^{-\beta n\omega} \left\langle n| e^{-\lambda^{2}} e^{-\lambda b^{\dagger} e^{i\omega t}} e^{\lambda b e^{-i\omega t}} e^{\lambda b^{\dagger}} e^{-\lambda b} |n\right\rangle. \tag{4.16}$$

We now need to get all the annihilation operators on the right and the creation operators on the left. To do so, we exchange the operators in the middle. They are written as

$$e^{\lambda b(t)} e^{\lambda b^\dagger} = e^{\lambda b^\dagger} \left(e^{-\lambda b^\dagger} e^{\lambda b(t)} e^{\lambda b^\dagger} \right) \tag{4.17}$$

The term in the parenthesis is exactly the same as Eq. (4.9) by setting

$$S \equiv -\lambda b^\dagger.$$

With the same reasoning, we notice that the boson annihilation operator is rewritten as

$$\begin{aligned} e^{-\lambda a^\dagger} a e^{\lambda a^\dagger} &= a - \lambda \left[a^\dagger, a \right] + \frac{\lambda^2}{2!} \left[a^\dagger, \left[a^\dagger, a \right] \right] \ldots \\ &= a + \lambda, \end{aligned}$$

so the term in Eq. (4.17) is rewritten as

$$e^{-\lambda a^\dagger} e^{\lambda a(t)} e^{\lambda a^\dagger} = \exp \left[\lambda e^{-i\omega t} (a + \lambda) \right] = e^{\lambda^2 e^{-i\omega t}} e^{\lambda a(t)}.$$

Finally, inserting this back into Eq. (4.16) we get

$$\mathscr{F}_{\mathbf{q}}(t) = \left(1 - e^{-\beta\omega} \right) e^{-\lambda^2 \left(1 - e^{-i\omega t} \right)} \sum_{n=0}^{\infty} e^{-\beta\omega n} \langle n | e^{\lambda b^\dagger \left(1 - e^{i\omega t} \right)} e^{-\lambda b \left(1 - e^{-i\omega t} \right)} | n \rangle$$

Now, rename $u \equiv \lambda \left(1 - e^{-i\omega t} \right)$, such that

$$\mathscr{F}_{\mathbf{q}}(t) = \left(1 - e^{-\beta\omega} \right) \sum_{n=0}^{\infty} e^{-\beta n\omega} \langle n | e^{u^* b^\dagger} e^{-ub} | n \rangle \tag{4.18}$$

which we want to rewrite using $N = \frac{1}{e^{\beta\omega} - 1}$. First of all the exponential is expanded in a power series

$$e^{-ub} | n \rangle = \sum_{l=0}^{\infty} \frac{(-u)^l}{l!} b^l | n \rangle. \tag{4.19}$$

The result is computed by using the properties of the boson annihilation operators that were outlined in Sect. 1.2.1. The result of $b^l \, |n\rangle$ is calculated iteratively. First see that if $l > n$ then $b^l \, |n\rangle = 0$; that is because by applying the operator n times we arrive at $b^{l-n} \, |0\rangle$, which is 0 if $l - n > 0$.

If $l \leq n$, the following applies:

$$\begin{aligned} b|n\rangle &= n^{1/2}|n-1\rangle \\ b^2|n\rangle &= [n(n-1)]^{1/2}|n-2\rangle \\ &\vdots \\ b^l|n\rangle &= \left[\frac{n!}{(n-l)!}\right]^{1/2}|n-l\rangle \end{aligned}$$

The expansion in Eq. (4.19) is therefore written as follows, where we make use of the fact that the sum is truncated when $l > n$:

$$e^{-ua}|n\rangle = \sum_{l=0}^{n} \frac{(-u)^l}{l!} \left[\frac{n!}{(n-l)!}\right]^{1/2} |n-l\rangle. \tag{4.20}$$

The next term to be calculated in Eq. (4.18) is of course the other exponential acting on on the left. However, the term $\langle n|\, e^{u^* b^\dagger}$ is simply the Hermitian conjugate of Eq. (4.20), so that the left term is written as

$$\langle n|e^{u^* a^\dagger} = \sum_{m=0}^{n} \frac{(u^*)^m}{m!} \left[\frac{n!}{(n-m)!}\right]^{1/2} \langle n-m|.$$

Inserting this into Eq. (4.18), the bra and the ket are multiplied and by their property of orthonormality they yield a delta $\langle n-m|n-l\rangle = \delta_{n-m,n-l} = \delta_{m,l}$. Their product is then

$$\langle n|e^{u^* a^\dagger} e^{-ua}|n\rangle = \sum_{l=0}^{n} \frac{\left(-|u|^2\right)^l}{(l!)^2} \frac{n!}{(n-l)!} = L_n\left(|u|^2\right),$$

where we found that this power series is just the Laguerre polynomial of order n. Next, consider the generating function of Laguerre polynomials:

$$(1-y)\sum_{n=0}^{\infty} L_n\left(|u|^2\right) y^n = e^{|u|^2 y/(y-1)}$$

If we rename $y \equiv e^{-\beta\omega}$, then $\frac{y}{y-1} = -N = -\frac{1}{e^{\beta\omega}-1}$. We finally find a simpler expression for $\mathscr{F}(t)$:

$$\begin{aligned} \mathscr{F}_{\mathbf{q}}(t) &= \left(1-e^{-\beta\omega}\right) e^{-\lambda^2\left(1-e^{-i\omega t}\right)} \langle n|e^{u^* b^\dagger} e^{-ub}|n\rangle \\ &= e^{-\lambda^2\left(1-e^{-i\omega t}\right)} e^{-|u|^2 N} \\ &\equiv e^{-\eta_{\mathbf{q}}(t)} \end{aligned}$$

with

$$N = \frac{1}{e^{\beta\omega} - 1}, \quad u = \lambda\left(1 - e^{-i\omega t}\right).$$

The phase $\eta_{\mathbf{q}}(t)$ in the exponential is then computed as

$$\begin{aligned}
\eta_{\mathbf{q}}(t) &= \lambda^2\left(1 - e^{-i\omega t}\right) + |u|^2 N \\
&= \lambda^2\left[\left(1 - e^{-i\omega t}\right) + \left(1 - e^{-i\omega t}\right)\left(1 - e^{i\omega t}\right) N\right] \\
&= \lambda^2\left[(N+1)\left(1 - e^{-i\omega t}\right) + N\left(1 - e^{i\omega t}\right)\right].
\end{aligned}$$

Recall from Eq. (4.14) that the phonon contribution to the Green's function is given by

$$F(t) = \prod_{\mathbf{q}} \mathscr{F}_{\mathbf{q}}(t) = e^{-\sum_{\mathbf{q}} \eta_{\mathbf{q}}(t)} \equiv e^{-\eta(t)},$$

where (restoring the subscripts):

$$\begin{aligned}
\eta(t) &= \sum_{\mathbf{q}} \eta_{\mathbf{q}}(t) = \sum_{\mathbf{q}} \left(\frac{M_{\mathbf{q}}}{\omega_{\mathbf{q}}}\right)^2 \left[N_{\mathbf{q}}\left(1 - e^{i\omega_{\mathbf{q}} t}\right) + (N_{\mathbf{q}} + 1)\left(1 - e^{-i\omega_{\mathbf{q}} t}\right)\right] \\
N_{\mathbf{q}} &= \frac{1}{e^{\beta\omega_{\mathbf{q}}} - 1}
\end{aligned} \tag{4.21}$$

Finally, we combine the phonon and the electronic part in Eq. (4.13), and obtain the Green's function:

$$G(t) = -i\, e^{-it(\varepsilon - \Delta)}\, e^{-\eta(t)}\left[1 - n_F(\bar{\varepsilon})\right], \tag{4.22}$$

4.3.3 Observables in the Atomic Limit

Building on the derivation of the Green's function in Eq. (4.22), we now focus on the Holstein Hamiltonian in the atomic limit, where all phonons share the same frequency, $\omega_{\mathbf{q}} = \omega_0$. For simplicity, we assume a constant coupling $M_{\mathbf{q}} = \frac{g}{\sqrt{N}}$. At zero temperature, all phonon modes are in their ground state, i.e., $N_{\mathbf{q}} = 0$. Under these conditions, the energy shift in Eq. (4.8) simplifies to

$$\Delta = \sum_{\mathbf{q}} \frac{M_{\mathbf{q}}^2}{\omega_0} = \frac{g^2}{\omega_0}$$

Then the phase is greatly simplified:

$$\eta(t) = \sum_{\mathbf{q}} \left(\frac{g^2/N}{\omega_0}\right)\left(1 - e^{-i\omega_0 t}\right) = \frac{g^2}{\omega_0^2}\left(1 - e^{-i\omega_0 t}\right),$$

and the Green's function in Eq. (4.22) becomes:

$$G(t) = -i\theta(t) \exp\left[-it\varepsilon - \frac{g^2}{\omega_0^2}\left(1 - i\omega_0 t - e^{-i\omega_0 t}\right)\right].$$

Frequency Distribution

We now wish to evaluate the distribution of the energies. Recall from Eq. (2.21) that the spectral density function is given by

$$\begin{aligned} A(\omega) &= -2\mathrm{Im}G^R(\mathbf{k}\sigma, \omega) = \\ &= -2\,\mathrm{Im}\left\{-i\int_0^\infty dt\, e^{i\omega t} e^{-it\varepsilon - \frac{g^2}{\omega_0^2}\left(1 - i\omega_0 t - e^{-i\omega_{n'}}\right)}\right\} \\ &= 2\,\mathrm{Re}\left\{\int_0^\infty dt\, e^{i\omega t} e^{-it\varepsilon - \frac{\Delta}{\omega_0}\left(1 - i\omega_0 t - e^{-i\omega_{n'} t}\right)}\right\} \end{aligned}$$

The exponential is expanded in a power series:

$$e^{\Delta e^{-i\omega_0 t}} = \sum_r \frac{(\Delta/\omega_0)^r}{r!} e^{-i\omega_0 t r}$$

By a proper evaluation of the oscillating integral, we find

$$A(\omega) = 2\pi e^{-\Delta/\omega_0} \sum_{r=0}^{\infty} \frac{(\Delta/\omega_0)^r}{r!} \delta(\omega - \varepsilon + \Delta - r\omega_0). \tag{4.23}$$

The spectral function is given by a sum of delta functions. The peak heights are distributed according to a Poisson distribution. In case of weak coupling $g \to 0$ ($\Delta \to 0$), a single peak is found at $\omega = \varepsilon$. For strong coupling $g \to \infty$ ($\Delta \to \infty$), the peaks are distributed over a wider range and states with energies $\omega_r = \varepsilon + r\omega_0 - \Delta$ are found. These states do indeed occur when the electron is coupled to some phonons. The number n of excitations ω_0 is distributed according to a Poisson distribution:

$$N_{p0} = \frac{\Delta}{\omega_0} = \frac{g^2}{\omega_0^2}, \quad n \sim \text{Poisson}(N_{p0}) \implies P(n) = \frac{N_{p0}^n}{n!} e^{-N_{p0}}.$$

The average binding energy however is still ε:

$$\langle\omega\rangle = \frac{1}{2\pi}\int_{-\infty}^{\infty} A(\omega)\omega\,\mathrm{d}\omega = e^{-N_{p0}} \sum_r \frac{N_{p0}^r}{r!}(\varepsilon - \Delta + \omega_0 r) = \varepsilon - \Delta + N_{p0}\omega_0 = \varepsilon$$

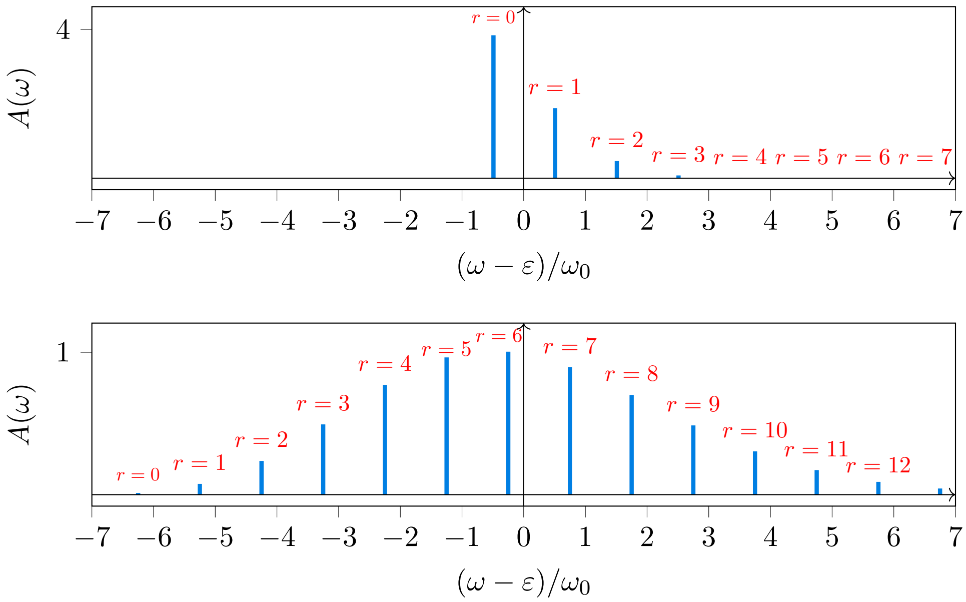

Fig. 4.2: Spectral function $A(\omega)$ in the atomic limit of the Holstein model.

Quasiparticle Weight and Binding Energy

Finally, recall that in Sect. 2.6 an expression for the quasiparticle weight and the binding energy of the polaron was found by taking the limit of the Matsubara Green's function for $\tau \to \infty$:

$$\mathcal{G}(\mathbf{k},\tau) \xrightarrow{\tau\to\infty} Z_0\left(\mathbf{k}\right) e^{-\varepsilon^0_{\mathbf{k}}\tau}$$

Then we take Eq. (4.22) and find the Matsubara Green's function by replacing t with $-i\tau$. By taking the limit $\tau \to \infty$, we find:

$$\mathcal{G}(\tau) \xrightarrow{\tau\to\infty} -e^{-\varepsilon\tau-\frac{g^2}{\omega_0^2}(1-\omega_0\tau)} = e^{-g^2/\omega_0^2} e^{-\left(\varepsilon-\frac{g^2}{\omega_0}\right)\tau} \tag{4.24}$$

We have found $E_{GS} = -\frac{g^2}{\omega_0}$ to be the ground-state energy of the polaron. In conclusion, the observables of interest are

$$E_{GS} = -\frac{g^2}{\omega_0}, \tag{4.25}$$

$$Z_{0,\mathrm{GS}} = e^{-g^2/\omega_0^2}, \tag{4.26}$$

and they can be computed through a linear fit of Eq. (4.24).

5

Diagrammatic Monte Carlo

Diagrammatic Monte Carlo (DiagMC) was first introduced in the 1998 by Prokof'ev and Svistunov [2] who applied it to the polaron problem. In its most general form, DiagMC is a numeric method based on the Markov chain Monte Carlo that enables the calculation of quantities that are described in terms of diagrammatic expansions [1]. In Sects. 5.1–5.2, we will introduce the theoretical framework of DiagMC. In Sect. 5.3, we will apply the Feynman rules of the electron-phonon interaction to formulate the DiagMC method for the Holstein Hamiltonian in the atomic limit. Finally, in Sects. 5.4–5.5 we will discuss our own application of the DiagMC and the results obtained.

5.1 Markov Chain Monte Carlo

The term *Markov chain Monte Carlo* (MCMC) refers to a class of algorithms based on the *Markov chains* used to draw samples from a probability distribution [20].

Definition 5.1 (Markov chain). *Let S be a countable set called the* ***state space****. A sequence of random variables $X = \{X_1, X_2, \ldots, X_n, \ldots\}$ taking values in S is called a* ***Markov chain*** *if, for all n, the conditional probability satisfies*

$$P(X_n = x \mid X_{n-1}, \ldots, X_1) = P(X_n = x \mid X_{n-1}),$$

That is to say that the probability density function of X_n only depends on the random variable immediately before X_{n-1} and not on the others. Let us now define the probability to be in the state $x_i \in S$ at step n. Such probability is denoted by

$$p_i^{(n)} \equiv P(X_n = x_i).$$

Let us now define a *transition matrix*

$$P_{ij} \equiv P(X_{n+1} = x_i | X_n = x_j),$$

and suppose that the above definition does not depend on the step n.

Definition 5.2 (Stochastic matrix). *P_{ij} is a* ***stochastic matrix*** *if:*

$$\sum_i P_{ij} = 1 \quad \forall\, j, \qquad P_{ij} > 0 \quad \forall\, i,\, j,$$

By definition of conditional probability we can thus evaluate the probability that $X_{n+1} = x_i$ as:

$$p_i^{(n+1)} = \sum_j P_{ij} p_j^{(n)}.$$

When working with a MCMC it is often the case that the transition matrix P_{ij} is known, as well as the initial probabilities $p_i^{(0)}$, where of course $\sum_i p_i^{(0)} = 1$. It is easy to show that $\sum_i p_i^{(n+1)} = 1$ as well.

What we are mostly interested in is that, under very general conditions and independent of the starting distribution $p_i^{(0)}$, with enough steps the probability distribution converges to a certain distribution p:

$$P(X_n = x) \to p(x),$$

which is called *stationary distribution*. We now introduce some definitions that will be useful to understand the conditions under which the Markov chain converges to a unique stationary distribution.

Definition 5.3 (Period of a State). *Consider a state $x_i \in \mathcal{S}$ of a Markov chain $\{X_1, X_2, \dots\}$. The state x_i has period d if d is the greatest common divisor of all possible number of steps n such that the chain can return to x_i in n steps: $P(X_n = x_i \mid X_0 = x_i) > 0$.*

In other words, if the state x_i has a period of d, then the Markov chain can only return to x_i in $d, 2d, 3d, \dots$ steps. For example, if the period is $d = 3$, then starting from x_i, the chain can return to x_i only after $3, 6, 9, \dots$ steps, but never after $1, 2, 4, 5, \dots$ steps.

Definition 5.4 (Aperiodic Markov Chain). *A Markov chain $\{X_1, X_2, \dots\}$ is* ***aperiodic*** *if all its possible states $x_i \in S$ are* ***aperiodic****; that is, if their period is $d = 1$.*

Definition 5.5 (Irreducible Markov Chain). *A Markov chain is* ***irreducible*** *if for any two states $x_i, x_j \in S$, there exists some integer n such that*

$$P(X_n = x_j \mid X_0 = x_i) > 0.$$

The intuitive meaning of this condition is that the state space is "connected": it is always possible to go from any state to any other state with enough steps. We now state a very important theorem that is the basis of the MCMC methods.

Theorem 5.1 (Existence and uniqueness of the stationary distribution)**.** *Let P_{ij} be a stochastic matrix, and consider a Markov chain that is irreducible, aperiodic, and has a finite state space. Then there exists a unique stationary distribution p_i such that*

$$\lim_{n\to\infty} p_i^{(n)} = p_i, \qquad p_i = \sum_j P_{ij} p_j, \tag{5.1}$$

where $p_i^{(n)}$ is the probability of being in state x_i at step n. In other words, regardless of the initial distribution, the Markov chain converges to a unique stationary distribution p_i as $n \to \infty$.

The latter of (5.1) is called *stationarity condition*. A Markovian process that satisfies the above conditions and therefore has a unique stationary distribution is said to be *ergodic*. We now define another condition for the distribution p_i.

Definition 5.6 (Detailed Balance Condition)**.** *A probability distribution p_i and a transition matrix P_{ij} satisfy the* ***detailed balance condition*** *if, for all states $x_i, x_j \in \mathcal{S}$:*

$$p_i P_{ij} = p_j P_{ji}, \tag{5.2}$$

The intuitive meaning is that at equilibrium the probability of a transition from i to j is exactly the same as the probability of transitioning from j to i. It is immediate to see that the detailed balance condition in Eq. (5.2) does in fact imply the stationarity condition in Eq. (5.1).

Let us take a moment to appreciate the implications of Th. 5.1. Under the conditions of ergodicity, after a certain time (called *thermalisation time*), the Markov chain will converge to a unique stationary distribution p_i. The first surprising aspect is that p_i *does not* depend on the initial distribution $p_i^{(0)}$. The second important aspect is that the stationary distribution p_i is *unique*. This enables us with a powerful tool for sampling: we can devise an algorithm whose transition matrix P_{ij} satisfies the detailed balance condition with respect to a desired probability distribution p_i, which is the target distribution we want to sample from. The transition matrix P_{ij} is already designed with p_i in mind. Then we know that p_i is a stationary distribution for the Markov chain and, because of its *uniqueness*, the theorem guarantees that the sampled distribution will converge to the desired p_i in a sufficient number of steps.

Finally, a quick note on the detailed balance condition. It is not necessary to satisfy the detailed balance condition for a probability density function p_i to be stationary. In fact, the condition Eq. (5.1) does not imply detailed balance, which is a stronger condition. However, here we are interested in the Metropolis-Hastings algorithm, which is a detailed-balance method.

5.1.1 Metropolis-Hastings Algorithm

Extension to continuous state spaces. So far, we have considered the Markov chain with a discrete state space $S = \{x_1, x_2, \dots\}$ and transition probabilities denoted by the matrix elements $P_{ij} = P(X_{n+1} = x_i \mid X_n = x_j)$. However, for the DiagMC, the state space is continuous, and the states are represented by continuous variables $x \in \mathbb{R}^d$ (or some continuous domain).

The transition probabilities are described by a *transition kernel* or *density*, which we denote as $\pi(x \leftarrow y)$. This represents the probability density of transitioning from state y to state x in one step of the Markov chain. Formally,

$$\pi(x \leftarrow y)\, dx = P(X_{n+1} \in [x, x + dx) \mid X_n = y).$$

The transition kernel $\pi(x \leftarrow y)$ generalizes the discrete transition matrix P_{ij} to continuous state spaces, and it satisfies the normalisation condition

$$\int \pi(x \leftarrow y)\, dx = 1 \quad \forall y.$$

Correspondingly, the probability distribution at step n is described by a density function $p^{(n)}(x)$, and the evolution of the distribution is given by the integral equation

$$p^{(n+1)}(x) = \int \pi(x \leftarrow y)\, p^{(n)}(y)\, dy.$$

Metropolis-Hastings Algorithm The idea behind the *Metropolis-Hastings algorithm* is as follows [21]. Suppose the system is in some state $y \in S$. A new state $x \in S$ is then proposed according to a certain *proposal distribution* $q(x \mid y)$. The proposed variable x is then either accepted or rejected according to the *acceptance ratio* A:

$$\mathcal{A}(x \leftarrow y) = \min\left\{1, \frac{q(y \mid x) f(x)}{q(x \mid y) f(y)}\right\}. \tag{5.3}$$

If the proposed variable is accepted, then the state is set to x; otherwise, it remains at y. This algorithm has the transition kernel:

$$\pi(x \leftarrow y) = q(x \mid y) A(x \leftarrow y) \quad \text{if } x \neq y.$$

It is easy to see that the Metropolis-Hastings transition kernels satisfy the detailed balance condition for the desired target distribution $f(x)$:

$$\pi(x \leftarrow y) \frac{f(y)}{\int f(z)\, dz} = \pi(y \leftarrow x) \frac{f(x)}{\int f(z)\, dz}.$$

Algorithm 1 Metropolis-Hastings Algorithm

```
Input: Target density $f(x)$, proposal distribution $q(x \mid y)$, initial state $x_0$, number of samples $N$
Set $x \leftarrow x_0$
for $i = 1$ to $N$ do
    Sample $x'$ from $q(x' \mid x)$
    Compute acceptance ratio: $\mathcal{A} = \min\left\{1, \frac{q(x|x')f(x')}{q(x'|x)f(x)}\right\}$
    Draw $u \sim \mathrm{Uniform}(0,1)$
    if $u < \mathcal{A}$ then
        $x \leftarrow x'$
    end if
    Record $x$ as the $i$-th sample
end for
```

It was stated before that the detailed balance condition implies the stationarity condition, so $f(x)$ is a stationary distribution for the Markov chain under consideration. Under the assumption that $\pi(x \leftarrow y)$ is ergodic, by Th. 5.1 the Markov chain must be unique. This means that after a certain number of steps, called *thermalisation time*, the samples x_i obtained from the algorithm will be distributed according to the desired probability density function

$$x_i \sim \frac{f(x)}{\int f(z)\,dz}.$$

In Alg. 1, we write the Metropolis-Hastings algorithm in pseudocode.

5.2 Diagrammatic Monte Carlo

In Ch. 3, we discussed how the Green's function can be expanded as a series, with each term represented by a Feynman diagram. More generally, a diagrammatic expansion of a physical quantity Q takes the form of a series of integrals, each with an increasing number of integration variables:

$$Q(y) = \sum_{m=0}^{\infty} \sum_{\xi_m} \int dx_1 \cdots dx_m \, \mathcal{F}(\xi_m, y, x_1, x_2, \ldots, x_m) \tag{5.4}$$

Here, y denotes a set of parameters on which $Q(y)$ depends. The index m indicates the order of the diagrams, and ξ_m labels different diagrams of the same order. The variables x_i are the integration variables associated with each diagram.

Diagrammatic Monte Carlo (DiagMC) is a computational technique that enables the simulation of quantities defined by such diagrammatic series [1]. In this approach, $Q(y)$ is interpreted as a distribution function over the variables y. The value of $Q(y)$ is then estimated using a Markov chain Monte Carlo process, which samples diagrams stochastically. In the context of the polaron problem, $Q(y)$ is naturally associated with the Matsubara Green's function in the momentum-time representation, $\mathcal{G}(\mathbf{k}, \tau)$. Thus, Q corresponds to the Matsubara Green's function G, and y represents the variables $(\mathbf{k}, t)$. The integration variables x_i correspond to the internal times and momenta of each diagram ξ_m.

The terms $\mathcal{F}(\xi_m, y, x_1, \ldots, x_m)$ represent the weights of the diagrams ξ_m. The $m = 0$ term corresponds to the free-particle Green's function (GF) $\mathcal{G}_0(\tau)$. According to Wick's expansion, higher-order terms ($m > 0$) are products of non-interacting GFs and interaction vertices $M_{\mathbf{q}}(\mathbf{k})$. As established earlier,

$$\mathcal{G}^{(0)}(\mathbf{k}, \tau_2 - \tau_1) = e^{-\varepsilon_{\mathbf{k}}(\tau_2 - \tau_1)} \quad \text{if } \tau_2 > \tau_1,$$

for the electron, and

$$\mathcal{D}_0(\mathbf{q}, \tau_2 - \tau_1) = e^{-\omega_{\mathbf{q}}(\tau_2 - \tau_1)} \quad \text{if } \tau_2 > \tau_1,$$

for the phonon.

To simulate the distribution $Q(y)$, diagrams relevant to the physical problem are generated stochastically. This is achieved using a Metropolis-Hastings algorithm, where each step involves proposing an update to the current diagram. The algorithm was introduced in the previous section; here, we reiterate its application to DiagMC. At each step, a modification to the current diagram is proposed, the acceptance ratio (Eq. (5.3)) is evaluated, and the update is accepted or rejected accordingly. If accepted, the diagram is updated.

In their original formulation [2], Prokof'ev *et al.* classified the possible updates into two categories:

Type I updates These updates modify a variable of the current diagram without altering its structure. Such updates are analogous to simulating a continuous distribution for a fixed function $\mathcal{F}$. An example of a type I update, which will be used later, is changing the electron's time of flight τ.

For a type I update, suppose we propose a change in the variables from $\vec{x} = (x_1, \ldots, x_m)$ to $\vec{x}' = (x'_1, \ldots, x'_m)$. The acceptance ratio is then:

$$A(x \to x') = \min\left\{1, \frac{\mathcal{F}(\xi_m, y', \vec{x}')}{\mathcal{F}(\xi_m, y, \vec{x})} \cdot \frac{q\,(\vec{x} \mid \vec{x}')}{q\,(\vec{x}' \mid \vec{x})}\right\},$$

where $q(\vec{x}' \mid \vec{x})$ is the probability of proposing $\vec{x}'$ given the current state $\vec{x}$.

Type II updates. These updates alter the structure of the diagram, i.e., they change the form of the function $\mathcal{F}$. An example is the addition of a phonon line, which modifies the diagram's structure. Suppose that a process $\mathcal{A}$ transforms the diagram as follows:

$$\mathcal{F}(\xi_m, y, x_1, \ldots, x_m) \xrightarrow{\mathcal{A}} \mathcal{F}(\xi_{m+n}, y, x_1, \ldots, x_m, x_{m+1}, \ldots, x_{m+n})$$

The update $\mathcal{A}$ introduces n new variables $\vec{x} = (x_{m+1}, \ldots, x_{m+n})$. The new variables $\vec{x}$ are chosen according to a distribution function $W(\vec{x})$, and the update is proposed with probability[1] $p_{\mathcal{A}}$. The function $W(\vec{x})$ does not require a specific form, but it must ensure (a) that physical constraints are respected and (b) that the updates are ergodic, so the resulting transition kernel is ergodic.

To ensure ergodicity, it is natural to define the complementary process $\mathcal{B}$, which is the reverse of $\mathcal{A}$ and removes the variables $\vec{x}$:

$$\mathcal{F}(\xi_m, y, x_1, \ldots, x_m) \xleftarrow{\mathcal{B}} \mathcal{F}(\xi_{m+n}, y, x_1, \ldots, x_m, x_{m+1}, \ldots, x_{m+n}).$$

This update is proposed with probability $p_{\mathcal{B}}$.

Given the forward and reverse processes, the acceptance ratio for the Metropolis-Hastings algorithm can be computed. For the process $\mathcal{A}$, which modifies the diagram by adding variables $\vec{x} = (x_1, \ldots, x_n)$, the acceptance ratio is given by Eq. (5.3):

$$A_{\mathcal{A}} = \min\left\{1, \frac{p_{\mathcal{B}}}{p_{\mathcal{A}}} \cdot \frac{\mathcal{F}(\xi_{m+n}, y, x_1, \ldots, x_m, \vec{x})}{\mathcal{F}(\xi_m, y, x_1, \ldots, x_m)} \cdot \frac{1}{W(\vec{x})}\right\}.$$

Here, $q(\text{new state with added variables } \vec{x} \mid \text{old state}) = p_{\mathcal{A}} \cdot W(\vec{x})$ is the product of the probabilities of two independent events: (a) proposing the update $\mathcal{A}$ with probability $p_{\mathcal{A}}$, and (b) choosing the new variables $\vec{x}$ according to $W(\vec{x})$. The acceptance ratio for the reverse process $\mathcal{B}$ is analogous:

$$A_{\mathcal{B}} = \min\left\{1, \frac{p_{\mathcal{A}}}{p_{\mathcal{B}}} \cdot \frac{\mathcal{F}(\xi_m, y, x_1, \ldots, x_m)}{\mathcal{F}(\xi_{m+n}, y, x_1, \ldots, x_m, \vec{x})} \cdot W(\vec{x})\right\},$$

Before proceeding to the implementation for the Holstein Hamiltonian, let us consider the acceptance ratio A and the distribution function $W(\vec{x})$. As previously stated, $W(\vec{x})$ can be chosen arbitrarily, provided that the resulting diagram is physically valid and all possible diagrams are accessible (ergodicity condition). However, $W(\vec{x})$ should ideally be chosen to closely match the actual distribution given of $\mathcal{F}(\xi_m, x_1, \ldots, x_m, \vec{x})$. If these distributions coincide, the acceptance ratio

---

[1] $p_{\mathcal{A}}$ generally depends on $W(\vec{x})$.

becomes $A_{\mathcal{A}} = 1$, resulting in an optimal algorithm. Conversely, if $W(\vec{x})$ is poorly chosen, the acceptance ratio decreases, leading to longer thermalisation times.

Finally, recall that $p_{\mathcal{A}}$ is the proposal probability for process $\mathcal{A}$, and $p_{\mathcal{B}}$ for process $\mathcal{B}$. For example, consider the processes [21]

$$A = \text{add a phonon line}, \quad \mathcal{B} = \text{remove a phonon line},$$

It may seem reasonable to assume that creation and annihilation are proposed with equal probability, implying $p_{\mathcal{A}}/p_{\mathcal{B}} = 1$. However, this is not generally the case. Even if the update types ($\mathcal{A}$ or $\mathcal{B}$) are proposed with the same frequencies, their overall probability depends on how the variables are chosen. For example, $\mathcal{A}$ requires choosing two points τ_i and τ_{i+1} to insert the new phonon line, whereas $\mathcal{B}$ involves choosing one of the N_{ph} phonon lines to remove. Such choices generally lead to different proposal probabilities for the two processes $p_{\mathcal{A}} \neq p_{\mathcal{B}}$.

5.3 DiagMC for the Holstein Hamiltonian in the Atomic Limit

5.3.1 Diagram Weights

Let us now consider the Holstein Hamiltonian in the atomic limit that was previously stated in Eq. (4.6) in the form[2]

$$H = \varepsilon c^\dagger c + \omega_0 \sum_{\mathbf{q}} b^\dagger_{\mathbf{q}} b_{\mathbf{q}} + \frac{g}{\sqrt{N}} c^\dagger c \sum_{\mathbf{q}} \left(b_{\mathbf{q}} + b^\dagger_{\mathbf{q}} \right),$$

which is equivalent to

$$H = \varepsilon c^\dagger c + \omega_0 b^\dagger b + g c^\dagger c \left(b + b^\dagger \right).$$

We shall now consider the zero-temperature case in the Matsubara formalism. For a correct implementation of the DiagMC for Holstein Hamiltonian, we need to establish the possible diagrams that can be generated by the electron-phonon interaction. To do that, we make use of the Rules 1–7 of Sect. 3.4 to generate each diagram and later to calculate its weight. Some of the resulting diagrams are shown in Fig. 5.1. In order to respect the rules, one electron line of momentum $\mathbf{p}$ is always present and connected to the external vertices at times 0 and τ. Several phonon lines are

---

[2] In this form, the electron-coupling constant is actually g with a certain phase, as denoted in Eq. (4.5). However, we see that later the squared module of the coupling constant appears, so we can safely drop the phase factor.

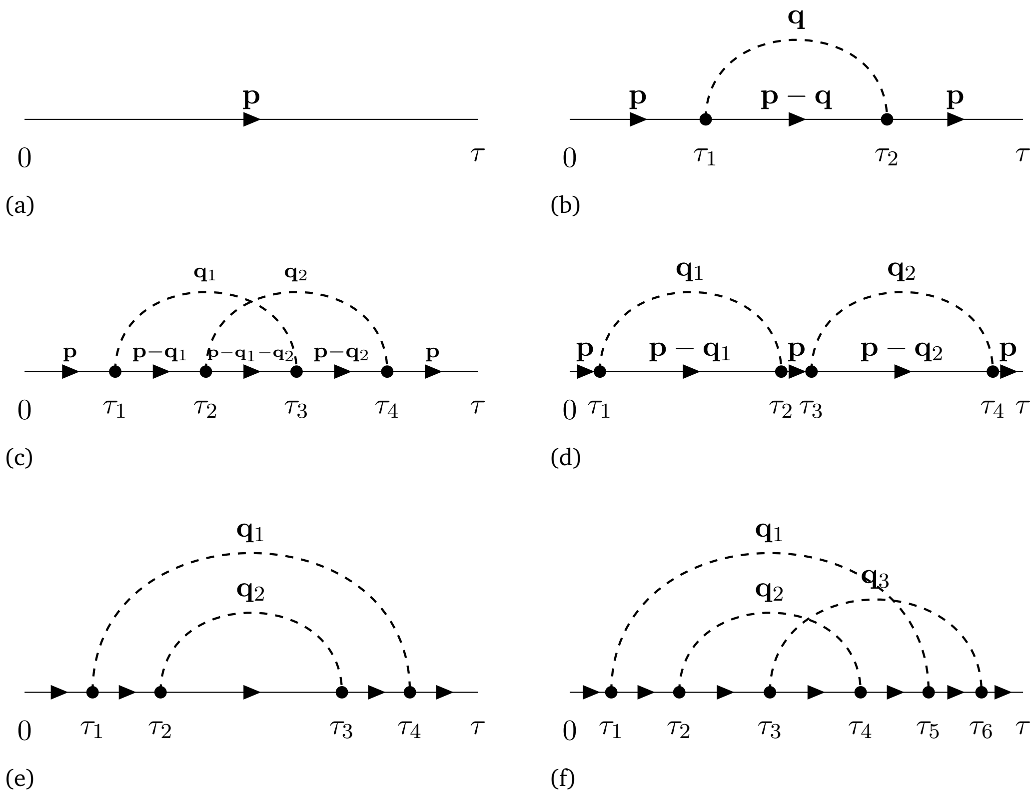

Fig. 5.1: Several Feynman diagrams for the atomic limit Holstein Hamiltonian.

connected to the electron line at different times. Each vertex must conserve the momentum and spin.

Later, we need to evaluate the weight of each diagram. Each electron line contributes as $\mathcal{G}_0(\mathbf{p}, \tau_2 - \tau_1)$; each phonon lines contributes as $\mathcal{D}_0(\mathbf{k}, \tau_2 - \tau_1)$. Each electron-phonon vertex contribute with the interaction $\frac{g}{\sqrt{N}}$. For example, the diagram in Fig. 5.1 (b) has the diagram weight as follows, where we sum over the possible momentum $\mathbf{q}$ of the phonons:

$$\begin{aligned}\mathcal{F}(\mathbf{p}, \{\tau_i\}) &= \frac{g^2}{N}\mathcal{G}_0(\mathbf{p}, \tau_1)\mathcal{G}_0(\mathbf{p}, \tau - \tau_2)\sum_{\mathbf{q}}\mathcal{G}_0(\mathbf{p} - \mathbf{q}, \tau_2 - \tau_1)\mathcal{D}_0(\mathbf{q}, \tau_2 - \tau_1) = \\ &= \frac{g^2}{N}e^{-\varepsilon\tau_1}e^{-\varepsilon(\tau_2-\tau_1)}e^{-\varepsilon(\tau-\tau_2)}\sum_{\mathbf{q}}e^{-\omega_0(\tau_2-\tau_1)}.\end{aligned}$$

Over a 1-dimensional lattice of N sites, there are exactly N distinct momenta derived from the conditions in Eq. (1.24). Under the assumption of working with dispersionless phonons with the same energy, we see that the phonon Green's function is in fact identical for all momenta. The sum over $\mathbf{q}$ thus yields exactly N identical terms, so a prefactor of N appears and cancels out with the denominator. The electron part does not depend on the momentum either, since we have assumed that electrons can only have a single energy ε. The diagram weight for Fig. 5.1 (b) therefore is

$$\mathcal{F}(\mathbf{p}, \{\tau_i\}) = g^2 e^{-\varepsilon\tau} e^{-\omega_0(\tau_2-\tau_1)}. \tag{5.5}$$

Let us now generalise this result by supposing there are m phonon lines. The term in Eq. (5.5) that is related to the electron is always the ending time τ, as all times τ_i cancels out in the sum. However, by Feynman rules the phonon part is the product of all different phonon's GFs:

$$\prod_i^m e^{-\omega_0(\tau_{2i-1}-\tau_{2i})} = e^{-\omega_0 \sum_i (\tau_{2i-1}-\tau_{2i})} \equiv e^{-\omega_0 \sum_i L_i},$$

where $L_i \equiv \tau_{2i} - \tau_{2i-1}$ is the length of the i-th phonon. Furthermore, we know that for m phonons there must be $2m$ coupling vertices. The diagram weight therefore is

$$\mathcal{F}(\mathbf{p}, \{\tau_i\}) = g^{2m} e^{-\varepsilon\tau} e^{-\omega_0 \sum_i^m L_i}.$$

5.3.2 Updates

Now that we have established the weight of all possible connected diagrams, it is necessary to implement the updates that will allow us to sample the diagrams stochastically [21]. The updates need to be ergodic, meaning that they must allow the Markov chain to explore the entire configuration space of diagrams. This is a necessary condition for the Markov chain to converge to the correct distribution.

Change τ

The first update to be performed is of type 1 and consists in changing the length τ of the electron line by choosing a new value τ'. The only constraint is that $\tau' > \tau_{2m} \equiv \tau_p$, where τ_p is the time of the latest electron-phonon vertex. This update and its complementary are represented in Fig. 5.2.

As stated in the previous section, for code efficiency it is important to choose τ' with a proper distribution. Let us consider the acceptance ratio for this update:

$$A\left(\tau \to \tau'\right) = \frac{\mathcal{F}(\xi_m, x_1, \ldots, \tau', \ldots, x_m)}{\mathcal{F}(\xi_m, x_1, .., \tau, \ldots, x_m)} \cdot \frac{q(\tau \mid \tau')}{q(\tau' \mid \tau)} = e^{-\varepsilon(\tau'-\tau)} \cdot \frac{q(\tau \mid \tau')}{q(\tau' \mid \tau)}.$$

Then, for an acceptance ratio of $A = 1$, it we should choose

$$\frac{q(\tau' \mid \tau)}{q(\tau \mid \tau')} = e^{-\varepsilon(\tau'-\tau)}, \tag{5.6}$$

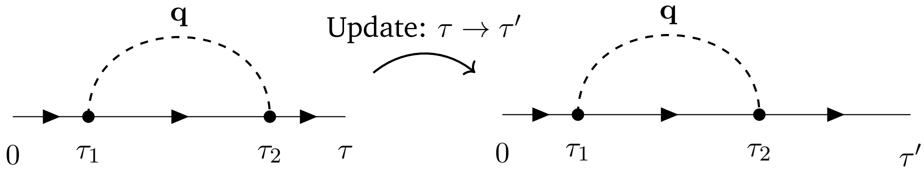

Fig. 5.2: Diagrammatic representation of the change τ update.

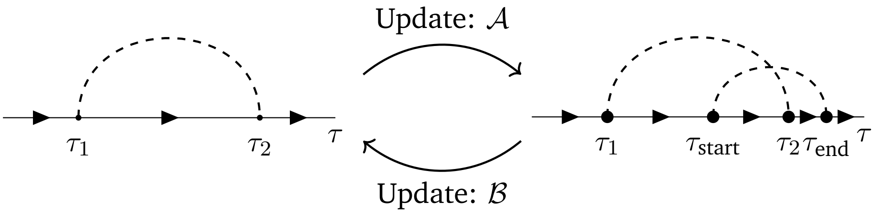

Fig. 5.3: Diagrammatic representation of the add/remove phonons updates.

then our variable τ' should be chosen as en exponential distribution from τ_p to ∞:

$$\tau' - \tau_p \sim \text{Exp}\left(\lambda\left(\tau_p\right)\right),$$

Thus, τ also has the same distribution and the condition in Eq. (5.6) is satisfied. By using this proposal distribution we achieve a perfect acceptance ratio of 1.

A common way of sampling τ' in this way is through the *inverse transform sampling* method. The idea is that the cumulative density function of the variable τ is uniformly distributed. This can easily be seen by considering $r \sim$ Uniform(τ_{min}, τ_{max}) (say $q(\tau \mid \tau') \equiv F(\tau)$):

$$P(F(\tau) \leq r) = P(\tau \leq F^{-1}(r)) = F\left(F^{-1}(r)\right) = r.$$

To sample our variable τ then we can simply generate r uniformly between 0 and 1 and then calculate

$$\tau = F^{-1}(r) = \tau_p - \frac{\ln(r)}{\varepsilon}.$$

Add/Remove phonon lines

The next updates to be implemented are of type II and consist in adding or removing phonon lines. Let us call them

$$\mathcal{A} \equiv \text{add a phonon line}, \quad \mathcal{B} \equiv \text{remove a phonon line}.$$

They are depicted in Fig. 5.3. In order to calculate $p_{\mathcal{A}}/p_{\mathcal{B}}$ it is necessary to state the procedure for choosing each update clearly. Let us call $\mathcal{S}_{N_{ph}}$ the initial state and $\mathcal{S}_{N_{ph}+1}$ the final state. The first step of the implementation is that, in the most general case, we choose to either add ($\mathcal{A}$) or remove ($\mathcal{B}$) phonon lines with some probabilities: $w_{\mathcal{A}}$ and $w_{\mathcal{B}}$, respectively. For the add phonon lines update $\mathcal{A}$ we need to choose the starting and the ending position of the phonon lines. The starting position is chosen uniformly from 0 to τ, whereas the ending position is chosen exponentially distributed from τ_{start} to τ:

$$q_s(\tau_{\text{start}}) = \frac{1}{\tau}, \quad q_e(\tau_{\text{end}}) = \frac{\omega_0\, e^{-\omega_0(\tau_{\text{end}}-\tau_{\text{start}})}}{1 - e^{-\omega_0(\tau-\tau_{\text{start}})}}$$

The total proposal probability for $\mathcal{A}$ therefore is

$$p_{\mathcal{A}} \cdot W(\{\tau_{\text{start}}, \tau_{\text{end}}\}) = w_{\mathcal{A}} \cdot q_s(\tau_{\text{start}}) \cdot q_e(\tau_{\text{end}}) = w_{\mathcal{A}} \cdot \frac{1}{\tau} \cdot \frac{\omega_0\, e^{-\omega_0(\tau_{\text{end}}-\tau_{\text{start}})}}{1 - e^{-\omega_0(\tau-\tau_{\text{start}})}}.$$

For updates of type $\mathcal{B}$ we need to choose the phonon line to be removed. The phonon line is chosen uniformly among all. For the reverse update ($N_{ph}+1 \to N_{ph}$), the proposal probability of $\mathcal{B}$ is:

$$p_{\mathcal{B}} = w_{\mathcal{B}} \cdot \frac{1}{N_{\text{ph}}}.$$

Finally, the diagram weight ratio is evaluated:

$$\frac{\mathcal{F}\left(S_{N_{ph}+1}, \vec{x}, \{\tau_{\text{start}}, \tau_{\text{end}}\}\right)}{\mathcal{F}\left(S_{N_{ph}}, \vec{x}\right)} = g^2 e^{-\omega_0(\tau_{\text{end}}-\tau_{\text{start}})}.$$

The acceptance ratio for the update $\mathcal{A}(N_{ph} \to N_{ph}+1)$ is (from Eq. (5.3)):

$$A_{\mathcal{A}}\left(N_{ph} \to N_{ph}+1\right) = g^2 e^{-\omega_0(\tau_{\text{end}}-\tau_{\text{start}})} \tau \frac{1 - e^{-\omega_0(\tau-\tau_{\text{start}})}}{\omega_0\, e^{-\omega_0(\tau_{\text{end}}-\tau_{\text{start}})}} \cdot \frac{1}{N_{ph}+1} \cdot \frac{w_{\mathcal{A}}}{w_{\mathcal{B}}}.$$

5.4 Implementation

The DiagMC method for this thesis was implemented in `C++`. The work was largely based on a DiagMC package developed by Thomas Hahn [22]. For reference, we rewrite the atomic limit Holstein Hamiltonian here:

$$H = \varepsilon c^\dagger c + \omega_0 b^\dagger b + g c^\dagger c \left(b + b^\dagger\right). \tag{5.7}$$

The following parameters are initially chosen for the simulations:

- The site energy ε of the electron.
- The phonon frequency ω_0.
- The electron-phonon coupling strength g.
- The maximum imaginary time τ_{max} and the number of bins N_{bins} for the histogram.
- The weight or probability w_i for each update type to be chosen.
- The time length t of the simulation.

The code is structured in two parts: the thermalisation phase and the sampling phase. The thermalisation phase is almost identical to the sampling phase, except that the diagram state is not measured. For this reason in Alg. 2 the thermalisation phase is not explicitly shown. The sampling phase is performed according to the Metropolis-Hastings algorithm that was largely discussed in the previous sections. The time length of the sampling phase is decided by the time length t of the simulation; for the sake of simplicity, in Alg. 2 the loop is shown for a number of fixed steps N_{sample}. We now briefly describe the procedure of each sampling step.

Update proposal. In this step, an update type is chosen according to the weights w_i. The update types were already discussed in Sect. 5.3.2 and they are:

- Change τ: the length of the electron line is changed to a new value τ' that is drawn from the proposal distribution $q(\tau' \mid \tau')$, which is exponential.
- Add phonon line: a new phonon line is added to the diagram. The start time τ_{start} is drawn uniformly from the interval $[0, \tau]$ and the end time τ_{end} is drawn from an exponential distribution $q_e(\tau_{\text{end}})$ between τ_{start} and τ.
- Remove phonon line: a phonon line is removed from the diagram. The phonon line to be removed is chosen uniformly from the list of all phonon lines in the current diagram.

After the update type is chosen and the parameters are drawn, the acceptance ratio A is computed according to the diagram weights $\mathcal{F}$ and the proposal probabilities. The acceptance ratio was already determined in Sect. 5.3.2.

Acceptance step. In this step, a random number u is drawn from a uniform distribution in the interval $[0, 1]$. If $u < A$, the update is accepted and the diagram state is updated accordingly. Otherwise, the diagram state remains unchanged.

Measurement. The bin corresponding to the current time τ is updated in the histogram.

At the end of the sampling phase, we estimate the probability density function $p(\tau)$ by dividing the number of samples in each bin $n(\tau)$ by the total number of samples N:

$$p(\tau) = \frac{n(\tau)}{N\delta_\tau},$$

where δ_τ is the size of the bin. $p(\tau)$ differs from the GF by a unknown normalisation constant K:

$$p(\tau) = \frac{\mathcal{G}(\tau)}{K}. \tag{5.8}$$

However, it is possible to calculate the normalisation constant K_0 of the free GF by integrating it over the time interval $[0, \tau_{\text{max}}]$. Then, let N_0 be the number of 0-th order diagrams, the ratio between the normalisation constants is the same as the ratio between the number of 0-th order diagrams and the total number of diagrams:

$$\frac{N_0}{N} = \frac{K_0}{K}.$$

The GF is extracted from Eq. (5.8):

$$\mathcal{G}(\tau) = \frac{K_0}{N_0\delta_\tau} n(\tau).$$

5.5 Results

The results of the simulations are presented in this section. The main observables of interest are the ground-state quasiparticle weight $Z_{0,GS} \equiv Z_0$ and the ground-state energy E_{GS} of the polaron. These can be extracted from the measured Green's function $\mathcal{G}(\tau)$ such that (from Eq. (4.24))

$$|\mathcal{G}(\tau)| \sim Z_0 e^{-(E_{GS}+\varepsilon)\tau}. \tag{5.9}$$

Then a linear fit of the logarithm is performed:

$$\ln|\mathcal{G}(\tau)| = a + b\tau,$$

and thus the quasiparticle weight and energy are extracted as

$$Z_0 = e^a, \quad E_{GS} = -b - \varepsilon.$$

Such values are then compared to the exact results in Eqs. (4.26) and (4.25) to verify the correctness of the implementation.

Algorithm 2 DiagMC of the atomic Holstein Hamiltonian

```
Input: $\varepsilon$, $\omega_0$, $g$, $\tau_{\text{max}}$, number of samples $N$, number of thermalisation steps $N_{\text{therm}}$, update type weights $w_i$ (i=1, 2, 3)
Initialise diagram state as free electron line (e.g., $m = 0$ phonon lines, $\tau$ initialised)
Set $x \leftarrow x_0$                                    ▷ Thermalisation phase
for $i = 1$ to $N_{\text{therm}}$ do
    Thermalisation step
end for                                                   ▷ Sampling phase
for $i = 1$ to $N_{\text{sample}}$ do
    Draw $up$ according to weights $w_i$ from the list [change $\tau$, add phonon line, remove phonon line]
    Propose an update to the diagram (change $\tau$, add/remove phonon line, etc.)
    if $up$ is "change $\tau$" then
        Draw $\tau$ from $q(\tau \mid \tau')$
    else if $up$ is "add phonon line" then
        Draw $\tau_{\text{start}} \sim \mathrm{Uniform}(0, \tau)$
        Draw $\tau_{\text{end}} \sim q_e(\tau_{end})$
    else if $up$ is "remove phonon line" then
        Draw phonon line $n \in [1, 2, \dots, N_{ph}]$
    end if
    Compute $A$ with diagram weights $\mathcal{F}$ and proposal probabilities
    Draw $b \sim \mathrm{Uniform}(0, 1)$
    if $b < A$ then
        Update the diagram state
    end if
    Measure $\mathcal{G}(\tau)$
end for
```

The update weights w_i were all set to 1, so all update types were equiprobable. The parameters chosen for the simulations are reported in Table 5.1. The execution time of each simulation was set to $t = 20$ seconds.

Careful consideration must be given to the choice of the parameter ε. If ε is chosen to be too small in absolute value ($\varepsilon \ll |E_{GS}|$), then the the Green's function in Eq. (5.9) will be an increasing exponential, leading to poor statistics at small τ. Conversely, if ε is too large ($\varepsilon \gg |E_{GS}|$), then the Green's function will decay too quickly, leading to a small number of diagrams at large τ. For this reason, the value of ε must be chosen such that it is close to that of the energy $|E_{GS}|$. This is not an issue, since we already have an exact solution for the energy in Eq. (4.25), which can be used to set ε accordingly.

The results of the simulations are presented in Table 5.2. For each value of g, several values of ε were tested to find the optimal parameters. Figs. 5.4 and 5.5 display the logarithm of the GF $\mathcal{G}(\tau)$ and its linear fit for values of $g = 1$ and $g = 2$, respectively. The results show that the fitted values for the energy and quasiparticle

Parameter	τ_{init}	τ_{max}	ω_0
Value	5.0	10.0	1.0

Tab. 5.1: Simulation parameters. ε and g are not listed here since they are changed at every simulation.

#	g	ε	E_{exact}	Z_{exact}	E_{fit}	std(E_{fit})	Z_{fit}	std(Z_{fit})
1	0	0.1	0.00	1.00	0.0005	0.0007	1.002	0.006
2	0.25	0.25	-0.0625	0.939	-0.0619	0.0005	0.943	0.004
3	0.50	0.375	-0.25	0.779	-0.248	0.001	0.790	0.005
4	1.0	1.1	-1.00	0.368	-1.001	0.001	0.365	0.003
5	1.5	2.3	-2.25	0.1054	-2.249	0.001	0.106	0.001
6	2.0	4.04	-4.00	0.0183	-4.012	0.004	0.0183	0.0006

Tab. 5.2: Comparison of the exact and fitted values for the polaron energy and quasiparticle weight for different coupling strengths g and site energies ε.

weight are in good agreement with the analytical results, confirming the correctness of the implementation.

Finally, 200 simulations were performed with g sweeping from 0 to 4. The value of ε was chosen to be $\varepsilon = \frac{g^2}{\omega_0} + 0.2$. Notice that this choice is suboptimal, because in Tab. 5.2 we observed that the optimal value of ε is not a linear function of the polaron energy. Nevertheless, the results in Figs. 5.6 and 5.7 show a good agreement with their analytical counterparts.

Next follows an interpretation of the results. In Fig. 5.6 we see that the ground-state energy E_{GS} is zero when the coupling constant is null. This is of course expected: if $g = 0$, then Eq. (5.7) is that of a free electron with constant energy ε decoupled from the phonons. As g increases, the energy becomes more negative, indicating that the polaron is becoming more bound. The quasiparticle weight Z_0 in Fig. 5.7 is 1 when $g = 0$, which is also expected. Recall that the quasiparticle weight is the weight of the bare-electron state. For the zero-interaction case, this is of course 1 as the electron is free. As g increases, Z_0 decreases because the electron gets dressed by the phonons.

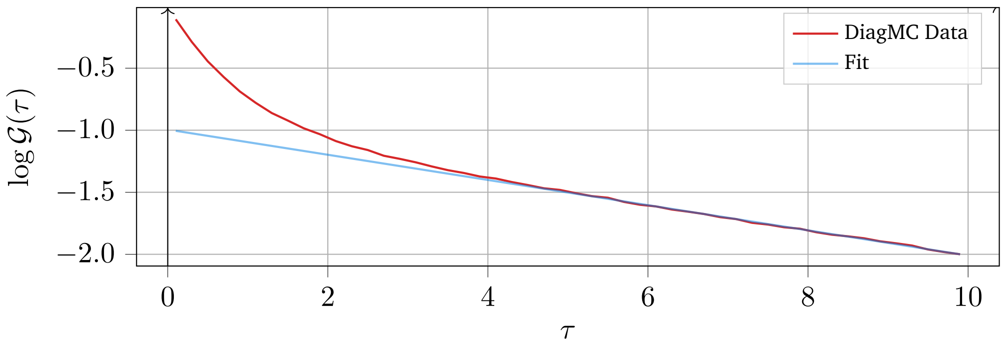

Fig. 5.4: The logarithm of the Green's function for $g = 1$ from the DiagMC sampled data (red) and its linear fit (blue).

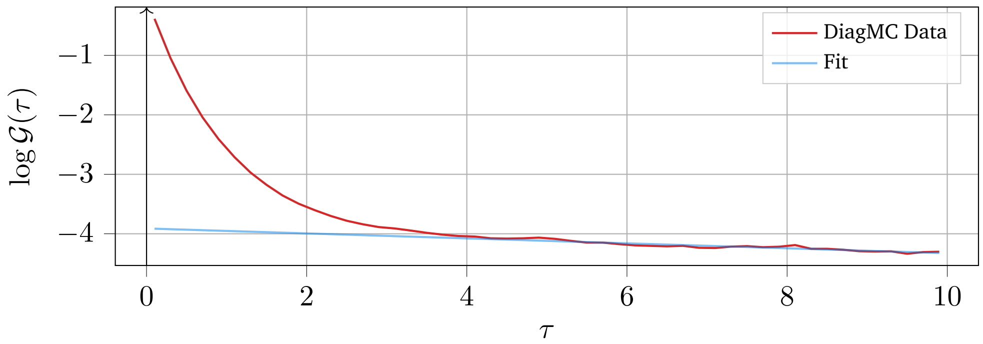

Fig. 5.5: The logarithm of the Green's function for $g = 2$ from the DiagMC sampled data (red) and its linear fit (blue).

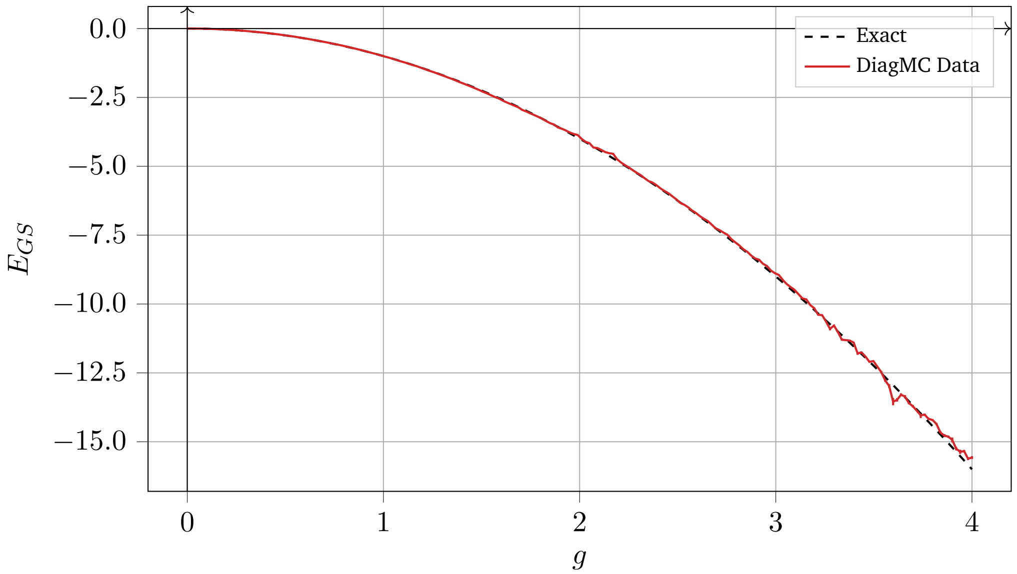

Fig. 5.6: The polaron ground-state energy E_{GS} against the coupling constant g. The exact solution (dashed line) is compared with the DiagMC simulation results (solid line).

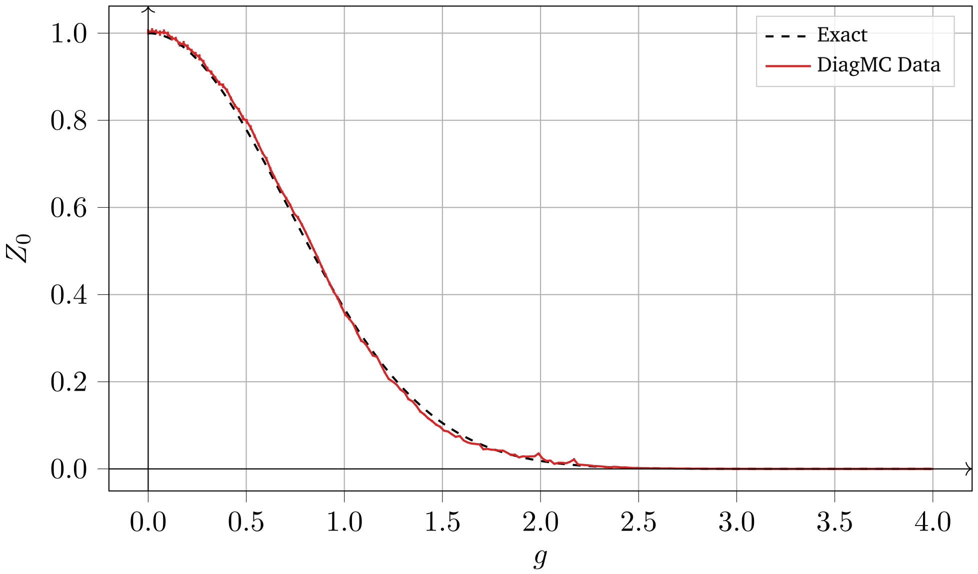

Fig. 5.7: The ground-state quasiparticle weight Z_0 against the coupling constant g. The exact solution (dashed line) is compared with the DiagMC simulation results (solid line).

Conclusions

The first part of this thesis was focused on developing the theoretical knowledge to address the Holstein Hamiltonian and the Diagrammatic Monte Carlo. We started by introducing the fundamentals of second quantisation, with emphasis on the phonons and the electron-phonon interaction, at the heart of the Holstein model. In the following chapter, we introduced the Green's function formalism with particular emphasis on the imaginary-time Green's function, which is the main tool used in this thesis. We then showed how Wick's theorem enables us to expand the electron-phonon interaction in terms of free electron and phonon Green's functions. After achieving a great simplification with the cancellation theorem, we were able to establish the Feynman rules for systematically determining the expansion of the electron Green's function for the electron-phonon interaction.

Later, we introduced the Holstein polaron and wrote the atomic-limit Hamiltonian in second quantisation. An exact solution for the zero-temperature case enabled us to determine the form of two fundamental observables: the ground-state polaron energy and the quasiparticle weight. In the following chapter, we briefly introduced the theoretical framework of the Diagrammatic Monte Carlo and its application to the polaron problem. The Feynman rules allowed us to determine the updates of the Metropolis-Hastings algorithm for the electron-phonon interaction. Finally, we presented an application of the Diagrammatic Monte Carlo for the Holstein Hamiltonian in the atomic limit.

The Monte Carlo simulations enabled us to sample the Green's function, from which we determined the ground-state polaron energy and the quasiparticle weight. Initially, we performed several tests at specific values of the coupling strength and quantitatively compared the results with the exact solution as a reference. Subsequently, the simulations were extended to a broader range of coupling strengths in order to examine the dependence of the ground-state polaron energy and the quasiparticle weight on the coupling parameter. The trends obtained from these simulations were then qualitatively compared with the exact predictions, showing good overall agreement. The consistency of these results with the exact solution allowed us to validate our application of the Diagrammatic Monte Carlo, which was thus deemed correct.

Further improvements of the method could be made by conducting a more precise fine-tuning of the simulation parameters – such as the bare-electron energy and the maximum time τ of the diagram. This would lead to more precise evaluation of the properties for larger values of g. A natural and significant extension would be to implement the full Holstein Hamiltonian beyond the atomic limit. Such a development would require introducing new updates to add and remove external phonon lines.

Bibliography

[1] K. V. Houcke, E. Kozik, N. Prokof'ev, and B. Svistunov. "Diagrammatic Monte Carlo". In: *Physics Procedia* 6 (2010), pp. 95–105. DOI: `10.1016/j.phpro.2010.09.034`. arXiv: `0802.2923 [cond-mat]` (cit. on pp. 1, 63, 67).

[2] N. V. Prokof'ev and B. V. Svistunov. "Polaron Problem by Diagrammatic Quantum Monte Carlo". In: *Physical Review Letters* 81.12 (Sept. 21, 1998), pp. 2514–2517. DOI: `10.1103/PhysRevLett.81.2514`. arXiv: `cond-mat/9804097` (cit. on pp. 1, 63, 68).

[3] L. D. Landau. "Electron Motion in Crystal Lattices". In: *Phys. Z. Sowjetunion* 3 (1933). Ed. by D. ter Haar. DOI: `10.1016/b978-0-08-010586-4.50015-8` (cit. on p. 1).

[4] T. Holstein. "Studies of Polaron Motion: Part I. The Molecular-Crystal Model". In: *Annals of Physics* 8.3 (Nov. 1, 1959), pp. 325–342. DOI: `10.1016/0003-4916(59)90002-8` (cit. on pp. 1, 49).

[5] H. Bruus and K. Flensberg. *ManyBody Quantum Theory in Condensed Matter Physics: An Introduction*. Oxford University PressOxford, Sept. 2, 2004. DOI: `10.1093/oso/9780198566335.001.0001` (cit. on pp. 3, 5, 9, 12, 13, 15, 21, 22).

[6] J. C. Slater. "A Simplification of the Hartree-Fock Method". In: *Physical Review* 81.3 (Feb. 1, 1951), pp. 385–390. DOI: `10.1103/PhysRev.81.385` (cit. on p. 5).

[7] G. D. Mahan. *Many-Particle Physics*. Boston, MA: Springer US, 2000. DOI: `10.1007/978-1-4757-5714-9` (cit. on pp. 6, 27–29, 31, 32, 53).

[8] A. L. Fetter and J. D. Walecka. *Quantum Theory of Many-particle Systems*. Courier Corporation, June 20, 2003. 644 pp. Google Books: `0wekf1s83b0C` (cit. on p. 11).

[9] F. Bloch. "Über die Quantenmechanik der Elektronen in Kristallgittern". In: *Zeitschrift für Physik* 52.7 (July 1, 1929), pp. 555–600. DOI: `10.1007/BF01339455` (cit. on p. 14).

[10] J. C. Slater and G. F. Koster. "Simplified LCAO Method for the Periodic Potential Problem". In: *Physical Review* 94.6 (June 15, 1954), pp. 1498–1524. DOI: `10.1103/PhysRev.94.1498` (cit. on p. 15).

[11] G. H. Wannier. "The Structure of Electronic Excitation Levels in Insulating Crystals". In: *Physical Review* 52.3 (Aug. 1, 1937), pp. 191–197. DOI: `10.1103/PhysRev.52.191` (cit. on p. 16).

[12] A. Altl and S. B. D. er. *Condensed Matter Field Theory, Second Edition*. DOI: `10.1017/CBO9780511789984CBO9780511789984` (cit. on p. 16).

[13] D. Di Sante and C. Franchini. *Interactions and Correlations in Condensed Matter Course Notes, University of Bologna*. 2023 (cit. on p. 18).

[14] R. A. Jishi. *Feynman Diagram Techniques in Condensed Matter Physics*. Cambridge: Cambridge University Press, 2013. DOI: `10.1017/CBO9781139177771` (cit. on pp. 32, 34, 36, 37, 39, 46, 47).

[15] M. Gell-Mann and F. Low. “Bound States in Quantum Field Theory”. In: *Physical Review* 84.2 (Oct. 15, 1951), pp. 350–354. DOI: `10.1103/PhysRev.84.350` (cit. on p. 36).

[16] A. S. Alexandrov and J. T. Devreese. *Advances in Polaron Physics*. Vol. 159. Springer Series in Solid-State Sciences. Berlin, Heidelberg: Springer Berlin Heidelberg, 2010. DOI: `10.1007/978-3-642-01896-1` (cit. on pp. 37, 38).

[17] R. P. Feynman. “Space-Time Approach to Quantum Electrodynamics”. In: *Physical Review* 76.6 (Sept. 15, 1949), pp. 769–789. DOI: `10.1103/PhysRev.76.769` (cit. on p. 39).

[18] G. C. Wick. “The Evaluation of the Collision Matrix”. In: *Physical Review* 80.2 (Oct. 15, 1950), pp. 268–272. DOI: `10.1103/PhysRev.80.268` (cit. on p. 40).

[19] R. P. Feynman. “An Operator Calculus Having Applications in Quantum Electrodynamics”. In: *Physical Review* 84.1 (Oct. 1, 1951), pp. 108–128. DOI: `10.1103/PhysRev.84.108` (cit. on p. 57).

[20] R. Waagepetersen. *A Quick Introduction to Markov Chains and Markov Chain Monte Carlo (Revised Version)* (cit. on p. 63).

[21] J. Gubernatis, N. Kawashima, and P. Werner. *Quantum Monte Carlo Methods: Algorithms for Lattice Models*. 1st ed. Cambridge University Press, Jan. 31, 2016. DOI: `10.1017/CBO9780511902581` (cit. on pp. 66, 70, 72).

[22] T. Hahn. *Simple-MC* (cit. on p. 74).